**Report Title:**
Staged, High-Pressure Oxy-Combustion Technology:
Development and Scale-Up

**Type of Report:** Final Scientific/Technical Report

**Reporting Period Start Date:** 10/01/2012
**Reporting Period End Date**: 09/30/2017


**Principal Authors**

Richard Axelbaum[1] (PI), Benjamin Kumfer[1], Akshay Gopan[1], Zhiwei Yang[1],
Jeff Phillips[2], Bruce Pint[3]


**Report Issued:** 12/29/2017


**DOE** Award Number: DE-FE0009702



**Submitting Organization:**
[1] Washington University in St. Louis
One Brookings Dr.
Saint Louis, MO 63130

**Sub-recipients:**
[2] Electric Power Research Institute, Inc. (EPRI)
3420 Hillview Avenue
Palo Alto, CA 94304

[3] Oak Ridge National Laboratory
1 Bethel Valley Road
Oak Ridge, TN 37830

## DISCLAIMER

## ABSTRACT

The immediate need for a high efficiency, low cost carbon capture process has prompted the recent development of pressurized oxy-combustion. With a greater combustion pressure the dew point of the flue gas is increased, allowing for effective integration of the latent heat of flue gas moisture into the Rankine cycle. This increases the net plant efficiency and reduces costs. A novel, transformational process, named Staged, Pressurized Oxy-Combustion (SPOC), achieves additional step changes in efficiency and cost reduction by significantly reducing the recycle of flue gas. The research and development activities conducted under Phases I and II of this project (FE0009702) include: SPOC power plant cost and performance modeling, CFD-assisted design of pressurized SPOC boilers, theoretical analysis of radiant heat transfer and ash deposition, boiler materials corrosion testing, construction of a 100 $kW_{th}$ POC test facility, and experimental testing. The results of this project have advanced the technology readiness level (TRL) of the SPOC technology from 1 to 5.

**TABLE OF CONTENTS**

## EXECUTIVE SUMMARY

Pressurized oxy-combustion has been identified by DOE as a transformational technology for coal power due to the many advantages obtained when the combustion process is pressurized. The Staged Pressurized Oxy-Combustion (SPOC) process, which has been developed under this program, represents a step change in improving the cost and efficiency for pressurized oxy-combustion. Benefits of the SPOC system include: (1) the latent heat of moisture in the flue gas is recovered (to improve efficiency), while simultaneously removing almost all of the $SO_X$, and much of the $NO_X$ and mercury in the flue gas; (2) minimal flue gas recirculation (FGR), which increases efficiency, nearly eliminates the pumping costs associated with FGR, minimizes flue-gas volume, and reduces component size and costs; (3) a potential modular boiler construction, which will reduce construction time and costs; (4) maximized radiative heat transfer, which improves efficiency and minimizes heat transfer surface requirements and hence cost; and (5) inherent flexibility in operation, resulting from the staged, modular design, allowing for improved plant ramping rates and turndown efficiency.

The following report contains a detailed summary of scientific findings and technical accomplishments resulting from award DE-FE0009702. During Phase I (FY13) of this project, a system performance and techno-economic analysis of the SPOC process was conducted, and this is summarized in Chapter 2. A detailed review can be found in the Phase I Final Technical & Economic Report and Phase I Topical Report [1]. Previous studies conducted by NETL have indicated that the penalty in plant efficiency due to implementation of first-generation (atmospheric pressure) oxy-combustion technology is approximately 10 percentage points. For the SPOC process, the resulting penalty is reduced to approximately 4 percentage points, leading to a sizeable reduction in cost of electricity.

The main objectives of Phase II were to conduct key experiments to develop, test and demonstrate the SPOC process and mitigate the risks and uncertainties identified during Phase I. Specifically, the focused R&D effort was to design and build a laboratory-scale facility, and conduct laboratory-scale experiments and complimentary modeling to prepare the SPOC technology for next-phase pilot-scale testing. A collateral objective was to validate that the staged oxy-combustion process holds promise over alternative approaches to pressurized oxy-combustion which use, for example, flue gas recycle or coal-water slurries to control heat flux.

Using an ASPEN Plus model, a parametric study was conducted to determine the effects of pressure and fuel moisture content on the SPOC system performance (Chapter 3). This study found that combustor pressure has only a minor impact beyond 16 bar since increasing the combustor pressure leads to a negligible increase in the amount of flue gas moisture condensation and a minor increase of the heat available for integration with the Rankine cycle. In the range of pressures considered (10-36 bar), the increase in plant efficiency is quite modest (~ 0.14 percentage points). The efficiency increase is due to the shift of heat integration from the low-pressure region to the high-pressure region of the Rankine cycle, along with a significant increase in the heat available from the compressors within the cryogenic air separation unit.

Fuels with moisture content ranging from 10 – 45% were considered and the results showed that increasing moisture in the fuel reduces the net plant efficiency. When the moisture content is approx. 29%, the amount of latent heat of condensation exceeds that which can be effectively utilized in the steam cycle for low-temperature heating of boiler feedwater, and the plant efficiency

falls rapidly with further increases in fuel moisture content. Therefore, slurry feeding of fuel is not recommended.

A novel burner and boiler was designed via computational fluid dynamics (CFD) modelling to effectively and safely burn coal under elevated pressure and low flue gas recycle (Chapter 4 and Chapter 5). From simulations, with appropriate burner and boiler design a desirable wall heat flux profile can be achieved even when local gas temperatures are extremely high, while minimizing ash deposition. A fundamental study of radiation in high-temperature, high-pressure, particle-laden flows was conducted to provide a more complete understanding of heat transfer in these unusual radiant boilers. At high operating pressures, the combustion flue gas can become optically thick, due to the increase in char and ash particle volume fraction. Under these unique conditions, absorption and emission due to particles is a dominant factor for determining the wall heat flux. A mechanism is found to exist for "trapping" radiant energy within the high-temperature flame region, and tempering the transfer of this heat to the wall. This arises, by design, from the highly non-uniform (non-premixed) combustion characteristics within the boiler, and the resulting gradients in temperature and particle concentration.

A unique 100 $kW_{th}$ test facility was successfully constructed and operated for the study of pulverized coal combustion at elevated pressure (up to 15 bar) and in atmospheres with high overall oxygen concentration (Chapter 6). The combustor geometry parallels the full-scale conceptual design. This facility has a flexible design to experimentally simulate the conditions in each stage of the SPOC process. The small-pilot SPOC facility was successfully operated using pulverized coal at elevated pressure and with varying oxygen concentration, with high-speed video images and system temperatures and pressures collected. The flame images provided validation that the burner provides the flame characteristics predicted by CFD models.

The SPOC process involves the exposure of materials internal to the boiler to unique environments, including potentially high oxygen or sulfur concentrations at elevated pressure. A materials testing program was conducted by Oak Ridge National Laboratory, in consultation with Washington University and the Electric Power Research Institute (EPRI), to experimentally evaluate the potential for enhanced corrosion under conditions of elevated pressure and high oxygen or sulfur concentrations, elucidate the mechanisms of corrosive attack, and to determine suitable materials for the SPOC boiler tubes and other internal components (Appendix A). There was no obvious detrimental effect of the high $O_2$ environment after 500 h exposures. When synthetic ash was added, no particular effect of pressure was observed for short-term testing at 700°C. Higher alloyed steels (e.g. 310HCbN) and/or Ni-base alloys or overlay coatings on steels appear to be possible solutions for high sulfur coals.

This project and subsequent SPOC projects (DE-FE0025193, DE-FE0029087) have advanced the SPOC process towards commercial-scale demonstration. The current Technology Readiness Level (TRL) of SPOC has been evaluated by the Electric Power Research Institute (EPRI) and determined to be TRL-5. EPRI has significant experience in assessing and tracking TRLs for new technologies for the power industry in an unbiased manner. The next step would be to achieve TRL-6 with construction of a 1-10MW prototype pilot plant, and drive the technology towards TRL-7. This will require that the remaining technical uncertainties to be addressed – none of which appear to be insurmountable – and that significant investment from government and private industrial partners be obtained. At the current rate of progress, the commercial readiness of the technology would be validated (TRL-8) in the 2028–2035 timeframe.

# Chapter 1. Introduction to Staged, Pressurized Oxy-Combustion (SPOC)

## 1.1. Pressurized oxy-combustion

The inherent requirement of high pressure carbon dioxide for either enhanced oil recovery (EOR) or sequestration makes it possible to pressurize the oxy-combustion process with no intrinsic added cost or loss in efficiency, since compressing oxygen before combustion requires comparable energy to compressing carbon dioxide after. An important benefit of pressurization is that the dew point of the flue gas moisture increases with pressure, so that at higher pressure, moisture condensation occurs at a higher temperature than at atmospheric pressure [2]. Hence, with pressurized oxy-combustion, a significant portion of the latent heat of condensation can be utilized in the steam cycle, instead of being wasted, as it is in atmospheric pressure oxy-combustion [3, 4]. Thus, pressurized oxy-combustion is well-posed to increase the efficiency of carbon capture.

Previous analyses have indicated that pressurized oxy-combustion can improve overall plant efficiency by approximately 3 percentage points [5-7]. In brief, the primary benefits of pressurized oxy-combustion include the following:

1. The moisture in the flue gas condenses at higher temperature, and thus the latent heat of condensation can be utilized to improve the overall cycle efficiency.
2. The gas volume is greatly reduced; therefore, the size and cost of equipment can be reduced.
3. At higher pressure, the convective heat transfer to boiler tubes is increased for a given mean velocity. This increase is due to the increase in flue gas density with pressure, which in turn produces an increased Reynolds number and convective heat transfer coefficient [6]
4. Air ingress—which normally occurs in atmospheric pressure systems—is avoided, thereby increasing the purity of the $CO_2$ in the combustion products and reducing purification costs. In fact, the elimination of air ingress may remove the need for cryogenic distillation within the $CO_2$ purification process, which would result in a significant cost savings, provided that the oxygen is sufficiently pure and the $CO_2$ purity requirements are not too stringent.

Therefore, pressurized oxy-combustion can make significant progress towards achieving the DOE's goal of at least 90% $CO_2$ removal at no more than a 35% increase in cost of electricity.

While a number of designs for pressurized oxy-combustion have been proposed, they must be carefully analyzed to ensure that they result in significant efficiency gains beyond those of optimizing atmospheric oxy-combustion. While any increase in efficiency is important, there are trade-offs in terms of the process complexity and reliability. Some pressurized oxy-combustion processes have been unable to achieve this step change in efficiency due to the sub-optimal utilization of the advantages provided by pressurizing combustion. For example, the ISOTHERM process of ITEA was one of the first designs for pressurized oxy-combustion [8, 9]. In this process, coal-water slurry (CWS) is fed as fuel into a refractory lined reactor, with a combination of oxygen

and recycled flue gas. The amount of recycled flue gas needed to regulate temperature in the combustor is only approximately 20% because of the water added with the fuel. After combustion in a nearly adiabatic reactor the hot flue gas is mixed with a large amount (~ 60%) of colder downstream recycled flue gas to reduce gas temperature to below 800°C before it enters a convective heat exchanger. This heat recovery steam generator (HRSG), is the primary means of heat transfer to the boiler feed water, and the large amount of recycling is needed to increase the gas volumetric flow rate through the HRSG to improve heat transfer. Nonetheless, one of the greatest drawbacks of this process is the large amount of flue gas recycle required (a total of ~ 80%). An independent analysis by Électricité de France (EDF) [10], the largest French utility, showed that the efficiency of this process is even lower than that of a well-integrated atmospheric pressure oxy-combustion process. Thus, pressurization and extraction of the latent heat of flue gas moisture is not sufficient to provide a significant gain in power plant efficiency with carbon capture. Process innovation is required for the optimal utilization of pressurized oxy-combustion.

## 1.2. Reducing flue gas recycle in oxy-combustion

Since the combustion of coal with pure oxygen could result in adiabatic flame temperatures on the order of 3000 K, most oxy-combustion systems incorporate the concept of flue gas recycle (FGR). From 65-80% of the cooled flue gas is returned back to the boiler to control the flame temperature and thereby the wall heat flux. While reducing flue gas recycle could reduce the cost and energy penalty for oxy-combustion, to do so is challenging. A number of approaches have been proposed to reduce the flue gas recycle without significant negative impact on boiler performance or safety [11, 12]. A few have been tested in demonstration units, but only in industrial furnaces or in boilers operating with low pressure steam, where much harsher conditions can be tolerated compared with utility boilers [11]. Notable among these is the approach of Goanta et al. [12], who used controlled non-stoichiometric burners, placed at several heights, to control the adiabatic flame temperatures of the individual flames. Tests were conducted to try to reduce the FGR to 50%, with three burner levels, each operating at a different stoichiometric ratio. The modeling and experimental results show flame impingement on the wall, which can be a significant problem in terms of heat flux and slagging [12, 13]. The results also showed that even if only the non-impingement side of the furnace was considered, the peak heat flux could be as much as 50% higher than for air-fired combustion [13]. Since the increase in heat flux was high even at 50% FGR, further reduction in recycle was not considered. Chapter 4 contains more discussion on the boiler design challenges posed by low flue gas recycle.

## 1.3. SPOC process description

As discussed earlier the pressurization of oxy-combustion process can provide significant advantages with respect to gain in net plant efficiency. Still, depending on the process configuration a significant loss in efficiency due to FGR and slurry feeding may result. In this work,

a unique pressurized oxy-combustion process is described that aims to further improve the efficiency and costs by reducing the recycling of flue gas to as low as possible. Normally, in the absence of FGR or dilution with another inert gas, combustion of fuel and oxygen results in a dramatic increase in temperature of the combustion products and the rate of radiant heat transfer [11]. The resulting high heat flux to the boiler tubes may result in tube surface temperatures that exceed safe operating limits. In the Staged Pressurized Oxy-Combustion (SPOC) process, this problem is addressed by a combination of staged delivery of the fuel and control of the characteristics of the flame through proper combustor/boiler design.

To reduce the mean combustion product temperature and heat flux associated with burning coal in nearly pure $O_2$, the burner and boiler must be designed specifically to address this. The design must be compatible with the configuration of a pressurized boiler as well. The SPOC approach incorporates a number of different concepts to address this. As with air-firing combustion, non-reacting gases must be present to absorb a portion of the heat released from combustion. With air-firing combustion $N_2$ plays the role of dilution gas, and in first-generation oxy-combustion systems the dilution gases are the cooled combustion products ($CO_2$ and $H_2O$) in the recycled flue gas. In the fuel-staging approach described below both combustion products and excess $O_2$ are utilized for dilution.

As mentioned early, the Technical University of Munich studied one approach to fuel staging to reduce FGR [12-14] under atmospheric pressure conditions. To achieve controlled staging, the concept of utilizing non-stoichiometric burners was investigated. The SPOC approach to fuel staging is somewhat different from this and is conceptually depicted in Figure 1-1. Unlike the staged approach described above, the SPOC process is designed to operate each stage as a separate boiler, with the fuel distributed to the various stages. A large percentage of the total oxygen is supplied to the first stage with a small amount of recycled flue gas, while some oxygen is/could also be supplied to other stages to improve performance and the combustion characteristics. With such a process design, in the first stage there is an over-supply of oxygen, i.e., the stoichiometric ratio, $\lambda$, which is defined as the ratio of the mass of oxygen supplied to the mass of oxygen required for stoichiometric combustion of the fuel, is much greater than unity, $\lambda >> 1$. The excess $O_2$ effectively acts as a diluent, thereby assisting in the control of the well-mixed temperature of the combustion products and downstream heat transfer. The near-burner heat transfer control is more complicated and will be described in Chapters 4-6. In the SPOC process, heat is extracted from the first stage into the Rankine steam cycle. Once the flue gas temperature is sufficiently reduced, the products of combustion from stage 1, including excess $O_2$ are passed to Stage 2 where additional fuel (and oxygen) is injected, and more $O_2$ is consumed. This process continues in multiple stages until all the fuel, and nearly all of the $O_2$ is consumed.

It is important to note that the total gas flow in the SPOC process is equivalent to the case in which coal and nearly pure oxygen are combusted in a single stage, and in nearly stoichiometric proportions. There is no net addition of dilution gases, but through the staging process, dilution is available, in a local sense, from the previous stage. The exact number of stages needed for the process is dependent on the burner and boiler configuration, amount of flue gas recycle, and other constraints discussed in later chapters. With the assumption of a fixed furnace end flue gas

temperature (FEGT), the number of stages will not have a significant effect on the heat and mass balance, or the location for the integration of the heat with the steam Rankine cycle.

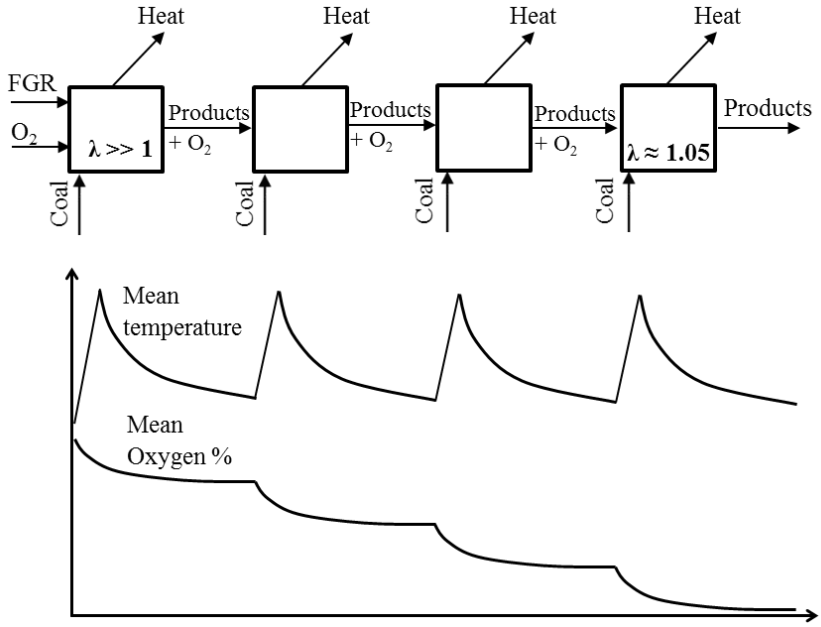


**Figure 1-1. Depiction of the staged combustion concept.**

A process flow diagram for a power plant incorporating the SPOC process is illustrated in Figure 1-2 and Figure 1-3, and is briefly described below. Oxygen is produced via cryogenic separation of air. When feasible, heat generated from the compression of air can be integrated with the steam cycle and utilized for boiler feed water regeneration. Staged combustion of fuel is carried out using three or more combustion vessels or boilers in series. Coal is fed with a pneumatic dry feeder using a small amount of recycled flue gas as motive gas. This feed system is modeled after systems developed by Siemens [15], Shell and Mitsubishi [16] for coal gasification. Other feeding techniques, like dry solids pump, which are capable of delivering dry coal at up to 40 bar without the aid of a motive gas [17, 18] and slurry feed can also be considered, although slurry feeding is detrimental to plant efficiency due to the added water (see Chapter 3).

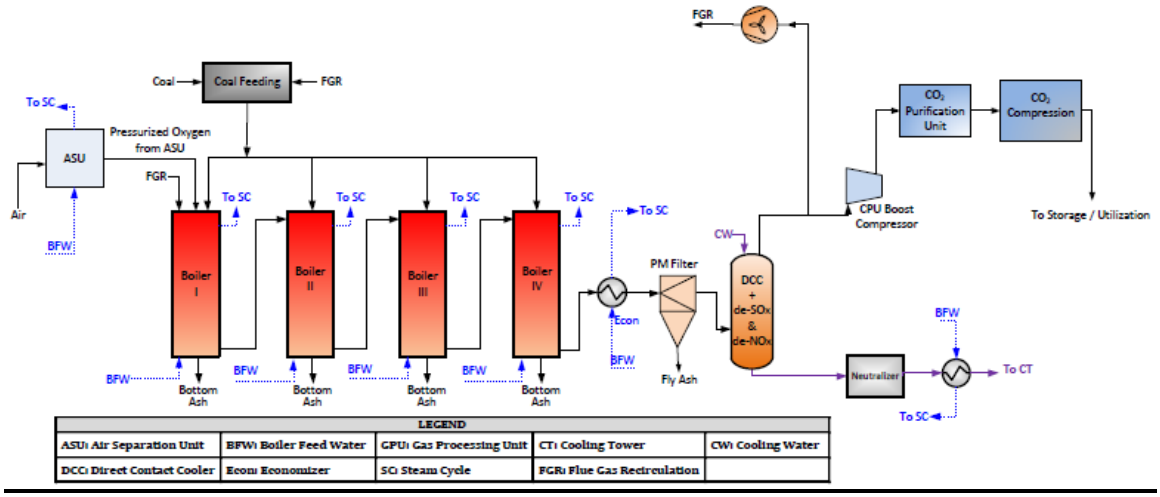


**Figure 1-2 . Gas side process flow diagram for the SPOC process.**

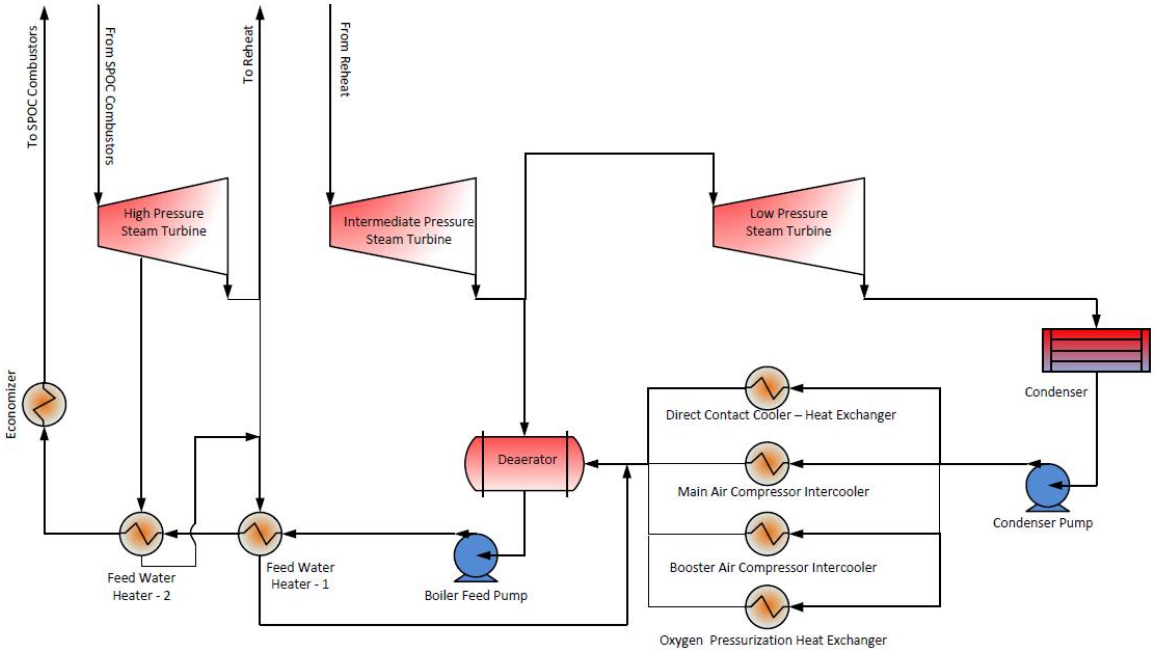


**Figure 1-3. Steam side process flow diagram for the SPOC process.**

In the present analysis for the process model, it is assumed that coal is delivered to each of the boilers in roughly equal amounts, and all the oxygen is delivered to the first stage (Boiler 1). In practice the distribution of the fuel and the oxygen could be different to affect the heat transfer characteristics. Any variation in the distribution of the fuel and oxidizer has no effect on the process modeling results. In the boiler, heat of combustion is transferred to a steam Rankine cycle, primarily by radiation. The products of Boiler 1 are passed to Boiler 2. The oxygen contained in the products of Boiler 1 is available to combust the coal in Boiler 2, along with any extra oxygen

added to Boiler 2. This process continues until nearly all of the oxygen is consumed in the final radiative boiler. The temperature of the products is further reduced in a convective heat exchanger (Economizer) followed by fly ash removal in a candle filter. After the particulates have been removed, the flue gas is further cooled, its moisture condensed, and the pollutants ($SO_2$ and $NO_x$) removed in the Direct Contact Column (DCC). A small fraction of this cooled and dry flue gas is recycled back to the boilers as motive gas, while the majority goes to the CPU where it is further purified to meet the stringent specifications for Enhanced Oil Recovery.

The details of each of these processes and the key assumptions associated with them are given in Section 2.3.

# Chapter 2. Process and Economic Modeling - Summary of Results of Phase I

## 2.1. Modeling approach and key assumptions

For comparison with atmospheric oxy-combustion and air-fired combustion, a process modeling approach that is similar to the National Energy Technology Laboratory (NETL) studies, and NETL guidelines for process modeling, $CO_2$ purity, etc. was used [19-22]. Aspen Plus™ (v7.3.2) software was used for the process modeling. Two cases were modeled, corresponding to two fuel types: bituminous and sub-bituminous coal. The modeled pressurized oxy-combustion (SPOC) power plant has an output of 550 $MW_e$ (net) with a supercritical Rankine cycle – 241 bar/593°C/593°C (3500 psig/1100°F/1100°F), and is located at a generic Midwest ISO location [22]. The process was modeled for 90% carbon capture and Enhanced Oil Recovery grade purity. The site conditions and $CO_2$ purity requirements are detailed in Table 2-1 and Table 2-2 respectively. The design, operating and performance characteristics of the key components of the SPOC models are shown in Table 2-3.The SPOC models were compared to the reference case ("Current Technology" or "Base Case") in the DOE/NETL oxy-combustion R&D guide, which is an ASPEN model of an atmospheric pressure supercritical steam oxy-combustion case [23].

**Table 2-1. Site conditions.**

| Site Conditions | Midwest ISO |
|---|---|
| Elevation, m (ft) | 0 (0) |
| Barometric Pressure, MPa (psia) | 0.101 (14.7) |
| Design Ambient Dry Bulb Temperature, °C (°F) | 15 (59) |
| Design Ambient Wet Bulb Temperature, °C (°F) | 10.8 (51.5) |
| Design Ambient Relative Humidity, % | 60 |
| Cooling Water Temperature, °C (°F) | 15.6 (60) |
| Air Composition, mass% | |
| $H_2O$ | 0.616 |
| Ar | 1.280 |
| $CO_2$ | 0.050 |
| $O_2$ | 22.999 |
| $N_2$ | 75.055 |
| Total | 100.00 |

**Table 2-2. $CO_2$ purity requirement for EOR and $CO_2$ purity achieved with the SPOC process.**

| Component | Enhanced Oil Recovery Target (Max. unless specified) [20] | SPOC Case |
|---|---|---|
| $CO_2$ | 95% (min) | >99.9% |
| $H_2O$ | 300ppmwt | trace |
| $N_2$ | 1% | 11ppb |
| O2 | 100ppm | 10ppm |
| Ar | 1% | 13ppm |
| $H_2$ | 1% | trace |
| CO | 35ppm | trace |
| $SO_2$ | 100ppm | trace |
| NOx | 100ppm | trace |

**Table 2-3. Key components data.**

| Component/ Subsystem | Technology Type, Basis for Design & Performance | Operating Conditions | | | | Performance Characteristics | Notes |
|---|---|---|---|---|---|---|---|
| | | Inlet | | Outlet | | | |
| | | Temp. (°C) | Press. (MPa) | Temp. (°C) | Press. (MPa) | | |
| air separation unit | Cryogenic. vendor data/ commercial design | 15.6 | 0.11 | 20 | 0.11 | 95.9% purity $O_2$. 213kWh/tO2 aux power req. | |
| oxygen compressor | NETL guidelines [22] | 20 | 0.11 | 185 | 1.6 | 84% isentropic efficiency | Multistage compression with intercoolers. |
| coal milling | vendor data/ commercial design | 25 | 0.1 | 49.5 | 0.1 | 15.4kWh/tCoal | typical grind size for PC application |
| coal feeding | Pneumatic dry feed. vendor data/ commercial design | 49.5 | 0.1 | 53 | 1.6 | 15 lbs coal/ lbs feed gas | Proven technology for IGCC applications can be applied |
| radiant boilers I-IV | self-defined | coal: 50 $O_2$: 185 | 1.6 | 700 | 1.6 | approx. 1% heat loss | - Analogous to radiant syngas cooler for IGCC. - Fly ash/bottom ash split equal to other PC systems. |
| economizer | vendor data/ commercial design | 700 | 1.6 | 330 | 1.57 | | |
| particulate filter | Candle filter. vendor data/ commercial design | 330 | 1.57 | 330 | 1.55 | 98% ash | |
| DCC + de-SOx & de-NOx column | Counterflow packed bed. vendor data/ commercial design | 330 | 1.55 | 26.2 | 1.5 | 100% SOx and NOx. | High efficiency conversion into acids will occur at 15 bar, SOx/NOx < 2 . |
| intermediate flue gas compressor | NETL guidelines [22] | 26.2 | 1.5 | 92.3 | 3.5 | 86% polytropic stage efficiency | |
| $CO_2$ cryogenic purification unit | Cryogenic. Vendor data/ commercial design | 21.2 | 3.5 | 44 | 15.3 | 90% $CO_2$ capture. ~45.8 kWh/t$CO_2$ | Includes $CO_2$ auto-refrigeration cycle & cryogenic distillation. Meets EOR purity specs [20]. |
| steam turbine (SC) | NETL guidelines[22] | 593 | 24.2 | 32.2 | 0.005 | single reheat at 4.9MPa to 593 C | |

### 2.1.1 Operating pressure

To determine the appropriate operating pressure for the boilers, three aspects of the process were considered. First, an initial analysis on the flue gas moisture condensation as a function of pressure and temperature was conducted. This study revealed that for pressures higher than 10 bar and flue gas temperatures lower than 50°C, the amount of flue gas moisture condensation did not vary significantly with pressure, with a maximum variation of less than 1% for a pressure variation from 10 bar to 35 bar. Second, the pressure for effective removal of $SO_2$ and $NO_x$ in the integrated removal approach has been reported as approx. 15 bar [24, 25]. Operating the boilers at a slightly higher pressure was considered to be advantageous to avoid additional equipment (*e.g.*, compressors or fans) before the flue gas cleanup, avoiding possible condensation and corrosion in such equipment. Lastly, in order to transfer most of the heat extracted at the direct contact column to the cold boiler feed water for regeneration while maintaining the minimum approach temperature in the regenerator, an additional constraint was imposed on the operating pressure of the process: a pressure high enough to transfer the heat to the boiler feed water without violating the minimum temperature approach was required. For an approach temperature of ~ 9°C, the required operating pressure of the DCC was approx. 15 bar. Based on these three considerations, a pressure of 16 bar was selected to account for pressure losses from the combustors to the DCC as given in Table 2-3. The fluid mechanics was also a consideration in choosing pressure but this will not be discussed here.

### 2.1.2 Radiant and convective heat exchanger

The combustors were modeled as described in the Aspen Plus™ solids modeling guidelines [26] and also by others in literature [27]. The exit temperature of the flue gas from each combustion stage was chosen to be 700°C. Flue gas from the end of the last stage of the process was then sent to an economizer (convective heat exchange). The temperature of the flue gas exiting the economizer was chosen to be 330°C to prevent acid condensation in the heat exchanger. This was based on model prediction of the dew point (~274°C) with a conservative safety factor. Since such predictions based on thermodynamics are not always accurate [28, 29] and experimental data on acid dew point is not available for the conditions of this process, a temperature much higher than that predicted by the model, and also higher than those used by others for pressurized coal combustion [7, 30] was used, as this was deemed to be appropriate, even though this conservative approach will lead to a lower efficiency for the process.

### 2.1.3 Direct contact column (DCC) and integrated pollutant removal

Further cooling and moisture condensation occurs in a contacting column, with cooling water flowing from the top, and flue gas from the bottom. This column has a dual role. The first is to cool and condense the moisture from the flue gas, which occurs in the bottom stages. The second is to remove $SO_x$ and $NO_x$, via conversion to dilute sulfuric and nitric acid, which is performed in the

top stages. The integrated $SO_x$ and $NO_x$ removal from gases at elevated pressure has been studied for power plant applications [31]. Air Products and other gas technology providers have been developing various processes of “sour gas compression” for oxy-combustion applications, in which removal of sulfur and nitrogen containing species in the flue gas is enhanced due to their mutual interaction following flue gas compression.

The integrated $SO_x$ and $NO_x$ removal had been associated with the “lead-chamber” reactions [32, 33]. However, several groups have recently investigated this reaction mechanism in more detail [34-36] and have concluded that the “lead chamber” reactions are not likely to play a critical role in this process due to the requirement of high sulfuric acid concentrations (70-80%) for such reactions to be important. These studies have argued that the conversion of $NO_x$ and $SO_2$ to acids is more likely to occur via some complex liquid-phase reactions between $HNO_2$, $H_2SO_3$ and possibly $H_2SO_4$. Even though the exact reaction mechanism is still under investigation, the experimental results from Air Products have indicated that when the $SO_2/NO_x$ ratio controls the removal efficiency, with a lower $SO_x/NO_x$ ratio resulting in a higher removal efficiency [24, 37, 38]. The SPOC process is expected to remove almost all of the $SO_2$ and $NO_x$ as it can produce higher $NO_x$ than in a typical oxy-combustion system (due to the high local flame temperatures) and hence has a lower $SO_x/NO_x$ ratio. Mercury present in the flue gas can also be removed in the same column either via dissolution or reaction with $HNO_3$ forming $Hg(NO_3)_2$ [32].

In this work, as with others who have modeled such integrated pollutant removal [25, 33, 39], the reactions chosen for modeling were based on the lead-chamber mechanism. As the experimental results from Doosan Babcock and Air Products [24, 25] indicate nearly complete removal of $SO_x$ and $NO_x$ at conditions similar to the SPOC exhaust, and the process modeling results indicate a large enough residence time in the column to completely remove both the gases, modifying the mechanism would not affect the process modeling results. It could however impact the cost of the equipment due to differences in terms of the residence time required in the column. The removal efficiency was also found to be a function of the $SO_x/NO_x$ ratio, and Air Products has suggested the use of an extra column at about 30 bar for a near 100% removal of the $NO_x$ [24]. This has not been considered in the process model presented here. If further polishing of $NO_x$ is found necessary for the SPOC process (based on pilot scale experiments to be conducted at Washington University), an additional efficiency penalty of no more than 0.05 percentage points will be added, since the clean flue gas inherently requires further compression to 35 bar in the CPU for auto-refrigeration requirements [40]. Another factor that enhances the removal efficiency in the SPOC process is that all the cooling water used in the column is fresh water and not recycled with acids [24].

The integrated pollutant removal system has been proposed as either two separate columns [7, 24, 32] or a single column [33]. To minimize equipment exposed to corroding acids (columns and heat exchangers), a single column approach was chosen, and the moisture condensation step was also integrated into the same column. Since rate of the overall rate-limiting reaction ($NO + ½ O_2 = NO_2$) increases with decreasing temperature, the flow rates of the liquid in the column and the column height were adjusted to allow the top stages to be at low temperature, promoting the reactions, while most of the cooling and condensation occurs in the bottom stages. Since the

column is at high pressure, the size of the column would be much smaller than that at atmospheric pressure.

The cooling water used in the direct contact column for cooling and condensation exits the bottom of the column at relatively high temperature (~165°C), with an acid concentration of about 730-4000 ppmv, depending upon the sulfur content of the coal. After neutralization of these dilute acids with caustic, the water is passed through an indirect heat exchanger for regeneration of low temperature boiler feed water (BFW). This heat, in conjunction with the low-grade heat that is available from the ASU, eliminates or nearly eliminates (depending on the fuel) the need for steam extraction from the low-pressure turbine, allowing for higher gross power generation.

### 2.1.4 CO2 purification unit (CPU)

In Chapter 3 the effect of flue gas recycle on efficiency is considered but in this section, the assumption of near zero flue gas is used to evaluate the optimum efficiency of the process. Thus, after removal of the particulates, $SO_x$, and $NO_x$, the flue gas is compressed to a pressure of 35 bar and a small fraction (~3-5%) of this flue gas is recycled back for carrying the coal in a dense phase. The majority (>95 vol%) is sent to the CPU after passing through molecular sieves for further moisture removal, and a bed of an activated carbon for removal of any mercury remaining in the gas.

The CPU uses cryogenic distillation to purify the $CO_2$ to the desired EOR specification. Two designs were initially analyzed – an ammonia chilled CPU (external cooling cycle), and an auto-refrigeration CPU. The auto-refrigeration CPU was found to be significantly more efficient, and the other option was dropped at an early stage in the model optimization.

### 2.1.5 Other considerations

A sub-bituminous Wyoming Powder River Basin coal (Case A), and a bituminous Illinois #6 coal (Case B) were assumed for fuels, and their proximate and ultimate analyses are shown in Table 2-4 [19]. In order to model coal combustion, coal was defined as a non-conventional component and its proximate & ultimate analysis and heating value were provided as user-inputs. The raw coal was dried to the desired level (as-fired moisture: 24% for Case A and 9.75% for Case B) in a dryer block with a hot and dry nitrogen stream from the ASU. The nitrogen from the ASU was heated with a portion of the heat available from air compression. This heat in atmospheric oxy-combustion models can be used for pre-heating oxygen with tight heat-integration. For pressurized combustion, the oxygen compression provides more than the requisite pre-heating (the excess heat being utilized for steam regeneration). The dried coal feed was then split and fed into each of the combustion stages with a small amount of recycled flue gas using a pneumatic dry feed system [15].

Since adsorption and polymeric membrane processes for air separation are economical only when the oxygen requirement is less than 200 tpd and 20 tpd respectively [41], a cryogenic ASU

was chosen for this study. Air separation was performed at low pressure (1-5 bar) in a 3 column cryogenic unit, producing oxygen of 95.9 vol% purity (0.1% $N_2$ and 4% Ar). The specific power consumption for air-separation to atmospheric pressure oxygen was 213 kWh/t $O_2$ [42]. This oxygen stream was then compressed in multiple stages with intercooling to reach the desired combustor operating pressure (16 bar). The intercoolers for both the air and oxygen compressors used boiler feed water (BFW) as the coolant.

**Table 2-4. Properties of Wyodak/Anderson PRB sub-bituminous coal and Illinois #6 bituminous coal on an as-received basis [19]**

| **Proximate Analysis** | PRB | Illinois #6 |
|---|---|---|
| Moisture | 27.42% | 11.12% |
| Volatile Matter | 31.65% | 34.99% |
| Ash | 4.50% | 9.70% |
| Fixed Carbon | 36.43% | 44.19% |
| Total | 100.00% | 100.00% |
| | | |
| **Ultimate Analysis** | | |
| Carbon | 50.23% | 63.75% |
| Hydrogen | 3.41% | 4.50% |
| Nitrogen | 0.65% | 1.25% |
| Sulfur | 0.22% | 2.51% |
| Chlorine | 0.02% | 0.29% |
| Ash | 4.50% | 9.70% |
| Moisture | 27.42% | 11.12% |
| Oxygen | 13.55% | 6.88% |
| Total | 100.00% | 100.00% |
| | | |
| Heating Value | As-Received (Reported) | As-Received (Reported) |
| HHV (kJ/kg) | 20,469 | 27,113 |

The steam turbine, generator and motor efficiencies were obtained from the guidelines issued by the U.S. Department of Energy for process modeling of coal-based power plants (shown in Table 2-5) [21]. The steam side was modeled with a governing stage, high-pressure, intermediate-pressure and low-pressure turbines. For regeneration of boiler feed water, the high-pressure turbine has two steam extractions, the intermediate has one, and the low pressure has none. The condenser pressure is 0.048 bar and operates with a terminal temperature difference of 11.7°C.

For the gas side modeling, the Peng-Robinson equation of state was used. For $SO_x$ and $NO_x$ removal, the ENRTL-RK method (ENRTL activity coefficient method with RK equation of state) was used so as to model the stream of dilute acid formed and the electrolytes present in the unit. For the steam side (Rankine cycle), STEAM-TA (steam tables) was used.

**Table 2-5. Key process parameters [21, 22, 43]**

| Parameter | Value |
|---|---|
| Governing Stage Efficiency | 85% |
| High Pressure Efficiency | 91.5% |
| Intermediate Pressure Efficiency | 94% |
| Low Pressure Efficiency | 89.2% |
| Generator Efficiency | 98.8% |
| Motor Efficiency | 97% |
| Condenser Pressure | 0.048 bar |
| ASU Specific power consumption (at ~ 1 bar) | 213 kWh/tonne$O_2$ |

## 2.2. Process modeling results and discussion

The outlet flow rates and composition from each of the combustor stages for a 550 MWe plant firing PRB coal is shown in Table 2-6 as an example of the conditions. The outlet oxygen concentration at Stage 4 is set to approx. 3% on a dry basis [22], which for the low recycle SPOC case corresponds to 1.7% on a wet basis. In terms of partial pressure of oxygen, this value is equal to 0.26 bar, which is almost an order of magnitude higher than atmospheric pressure combustion in air, with an $O_2$ concentration of 5%. Since the excess oxygen is to ensure complete conversion of char, which is a function of the partial pressure of oxygen in the reactor, the value used in the current modeling of SPOC was deemed sufficient.

**Table 2-6. Flow rates and compositions at the outlet of each stage in the SPOC process firing PRB coal producing 550 $MW_e$ power.**

| V-L Mole Fraction | Stage 1 out | Stage 2 out | Stage 3 out | Stage 4 out |
|---|---|---|---|---|
| Ar | 0.036 | 0.032 | 0.029 | 0.027 |
| $CO_2$ | 0.192 | 0.343 | 0.465 | 0.564 |
| $H_2$ | 0.000 | 0 | 0 | 0.000 |
| $H_2O$ | 0.132 | 0.236 | 0.319 | 0.388 |
| $N_2$ | 0.002 | 0.003 | 0.003 | 0.004 |
| $O_2$ | 0.638 | 0.386 | 0.184 | 0.017 |
| NOx | TBD | TBD | TBD | TBD |
| SOx | 0.00025 | 0.00025 | 0.00025 | 0.00025 |
| Total | 1 | 1 | 1 | 1 |
| | | | | |
| V-L Flowrate (kmol/hr) | 15203 | 17042 | 18877 | 20710 |
| V-L Flowrate (kg/hr) | 497934 | 563864 | 629798 | 695729 |
| Solid Flowrate (kg/hr) | 2436 | 4874 | 7309 | 9745 |
| Temperature (°C) | 700 | 700 | 700 | 700 |
| Pressure (MPa, abs) | 1.6 | 1.6 | 1.6 | 1.6 |

The performance summaries (and comparison with 1 atm oxy-combustion) for the two cases are shown in Table 2-7. The net plant efficiency (HHV) for Case A was found to be 35.7%, while that of Case B was 36.7%, indicating that the process is more efficient when using bituminous coal over lower rank sub-bituminous coal. The Integrated Environmental Control Model (IECM v8.0.2), which is a publicly available modeling tool developed by Carnegie Mellon University [44], was used to obtain a comparison for the decrease in net plant efficiency for a typical, atmospheric pressure oxy-coal power plant operating at the same ambient conditions on fuel switching from a high rank Illinois #6 to a low rank PRB coal. The decrease in efficiency for a typical oxy-coal plant is 7.4%, compared to 2.7% for the SPOC process. The efficiency penalty typically associated with high moisture fuels is not as significant here, as a significant portion of the latent heat of water is captured in the SPOC process. This is another important benefit of pressurized combustion.

**Table 2-7. Performance comparison of SPOC process (Case A and B) with relevant atmospheric pressure reference cases**

| Performance Parameters | Units | PRB SPOC Process (Case A) | Illinois #6 SPOC Process (Case B) | Current Technology Oxy-coal [23] | No Capture, Air-fired [23] |
|---|---|---|---|---|---|
| Gross Power Output (After Generator Loss) | $MW_e$ | 729.2 | 733.1 | 787.8 | 580.4 |
| Total Oxygen Production Load | $MW_e$ | 126.2 | 127.0 | 126.7 | - |
| ASU Main Air Compressors and other auxiliaries | $MW_e$ | *90.1* | *90.6* | *126.7* | - |
| Oxygen Compressors | $MW_e$ | *36.1* | *36.4* | – | - |
| Total Clean-up and CPU load | $MW_e$ | 20.5 | 19.4 | 77.55 | 4.5 |
| Other Auxiliaries and Misc. Balance of Plant | $MW_e$ | 32.8 | 31.6 | 33.53 | 25.9 |
| Total Auxiliary Load | $MW_e$ | 179.5 | 178.0 | 237.8 | 30.4 |
| Net Power Output | $MW_e$ | 549.6 | 555.1 | 550.0 | 550.0 |
| Net Plant Efficiency(HHV) | % | 35.7 | 36.7 | 29.3 | 39.3 |
| Thermal Input (HHV) | $MW_{th}$ | 1,539.3 | 1,511.8 | 1,879.2 | 1,400.2 |

The efficiency penalty for $CO_2$ capture with SPOC is only about 2.6 percentage points as compared to 10 percentage points for the reference atmospheric oxy-combustion case reported by DOE/NETL [41, 45]. The improvement in net plant efficiency over the atmospheric pressure cases is due to several factors. Most of these are related to the SPOC technology and these will be discussed in detail in the following sub-sections. Others are related to differences in the assumed steam turbine efficiencies, condenser operating conditions, etc. These contributions are not intrinsically associated with the SPOC process and will be identified in the comparison.

As shown in Table 2-2, the purity of the $CO_2$ that is captured with the SPOC process meets the purity standards for Enhanced Oil Recovery (EOR) set by DOE/NETL, and even meets the more stringent standards set by Kinder-Morgan and others [20, 46].

### 2.2.1 Auxiliary load comparison

About 28% of the total oxygen production load in the SPOC process is due to oxygen compression to 16 bar, but since the resulting flue gas is at higher pressure, the CPU compression power is equivalently reduced. The power summaries are compared in Table 2-7. Due to the higher efficiency (lower heat rate), the auxiliary load is about 33% lower in the SPOC process than in the atmospheric pressure process (the comparison is based on auxiliary load without feed water pumps as the pumps are turbine driven in the atmospheric pressure report and electric motor

driven for the SPOC cases). This reduction is a sum of reduction due to lower oxygen production, and the reduced gas volume that needs to be purified and compressed for the same power output. The SPOC process minimizes the requirement of recycled flue gas for temperature control and for this analysis, only 3-5% of the total flue gas is assumed to be recycled for the dense-phase coal feeding. Consequently, the fan power requirement for FGR in the SPOC process is small. In other studies, where traditional levels of FGR have been used, the fan loads for recycle have been shown to reduce efficiency by ~0.4-4 percentage points (based on fuel thermal input) at the various combustion pressures analyzed [7, 41].

Another factor that results in a lower auxiliary load for the SPOC process is the lower CPU power load that results from the elimination of air in-leakage at high pressure, and hence a purer $CO_2$ stream entering the CPU.

### 2.2.2 Heat integration and net plant efficiency

The net plant efficiency for the SPOC cases is about 7.4 percentage points higher than for the reference atmospheric pressure oxy-combustion case [41]. This increase in efficiency cannot be attributed to a single aspect of the design but is rather a result of a number of incremental increases in various units of the process. The direct contact cooler/condenser (DCC) is a major contributor towards the increase in efficiency of the SPOC process over atmospheric oxy-combustion, adding about 10% extra heat into the Rankine cycle (~ 0.1 $MW_t$ / $MW_t$ input) in the PRB case. Since not all of the latent heat from the moisture in the flue gas is recoverable, a lower moisture fuel will inherently have lower losses. For example, Illinois #6 coal (Case B) has a lower moisture content and the net plant efficiency is higher than for Case A with PRB coal, as seen in Table 2-7.

As previously stated, pressurization of oxygen to combustor pressure was performed with a multistage compressor with intercooler. The compressed oxygen is at approx. 185°C, eliminating the need for further oxygen pre-heating, which in first generation oxy-combustion processes is done using heat from the Main Air Compressor (MAC) and Booster Air Compressor (BAC) intercoolers. The extra heat thus available in the SPOC process, from the MAC and BAC intercoolers and the oxygen compressor intercooler was also integrated with the Rankine cycle, by utilizing low pressure BFW as the coolant, increasing the net plant efficiency further. This is a conservative approach, and in practice liquid oxygen (LOX) based ASU could be used that would provide a higher overall efficiency, since liquid oxygen compression produces lower energy penalty than gaseous oxygen.

### 2.2.3 Efficiency improvements breakdown

There are a number of reasons for the improved efficiency of SPOC [3] over first-generation oxy-combustion [23], as well as other pressurized oxy-combustion concepts [7]. The benefits primarily arise due to pressurization and staging. As discussed above, with pressurization the latent heat

in the flue gas can be recovered and utilized in the steam Rankine cycle. This adds a large amount of heat into the cycle, but is only one of the reasons for the high efficiency of SPOC. Staging of the fuel (and oxygen) also plays a major role in enhancing the efficiency of the SPOC process by allowing for reduction in flue gas recycle. The impact of reduced recycle on efficiency is not only due to the reduced fan power consumption for recycling, which could be between 0.4–1.2%-pts. [7, 47]. The benefit also arises from the reduced exergy losses due to higher heat transfer in the high temperature region and less heat transfer in the low temperature regions. With higher recycle, the gas volume in the combustor is increased, which pushes more sensible energy to the lower temperature region. Since, the conversion efficiency of thermal energy to electrical energy is a function of the temperature at which it is integrated in the Rankine cycle [48, 49], a lower flue gas recycle leads to a higher power generation, and therefore higher plant efficiency. A brief comparison of the SPOC process with other oxy-combustion processes using exergy analysis is presented by Hagi et al. [10].

## 2.3. Economic analysis

The cost analysis for the SPOC process was performed in collaboration with Burns & McDonnell on the basis of the plant performance and stream tables, by scaling the costs from NETL reports where appropriate and using vendor data otherwise. Process & project contingencies, engineering construction management and home office fees, and owner's cost were included in calculating the total overnight costs. A brief summary of the economic assumptions are provided in Table 2-8. For cost comparison, the reference case was an air-fired, supercritical PC power plant in the Midwest, using PRB coal. The costs for the reference plant were calculated by scaling the costs from the NETL report [50] for Illinois # 6 coal and using the IECM models to obtain scaling factors. The scaling exponents were found from the NETL guidelines [51]. The cost of electricity for the SPOC process was calculated assuming a high-risk finance structure, whereas the baseline was calculated using low risk finance structure (Table 2-9).

**Table 2-8. Global economic assumptions**

| Parameter | Value |
|---|---|
| Income Tax Rate | 38% Effective (34% Federal, 6% State) |
| Capital Depreciation | 20 years, 150% declining balance |
| Repayment Term of Debt | 15 years |
| Capital Expenditure | 5 years |
| Operational Period | 30 years |
| Economic Analysis Period (used for IRROE) | 35 years (capital expenditure period plus operational period) |
| Capital Cost Escalation During Capital Expenditure Period (nominal annual rate) | 3.6% |
| Distribution of Total Overnight Capital over the Capital Expenditure Period (before escalation) | 10%, 30%, 25%, 20%, 15% |
| Working Capital | Zero for all parameters |
| % of Total Overnight Capital that is Depreciated | 100% (*this assumption introduces a very small error even if a substantial amount of TOC is actually non-depreciable)* |
| Escalation of COE (revenue), O&M Costs, Fuel Costs (nominal annual rate) | 3% |

**Table 2-9. Financial structure**

| Type of Security | % of Total | Current (Nominal) Dollar Cost | Weighted Current (Nominal) Cost |
|---|---|---|---|
| LOW RISK (Capital Charge Factor = 0.116) | | | |
| Debt | 50 | 4.5% | 2.25% |
| Equity | 50 | 12% | 6% |
| Total | | | 8.25% |
| Debt | 50 | 4.5% | 2.25% |
| Equity | 50 | 12% | 6% |
| Total | | | 8.25% |
| HIGH RISK (Capital Charge Factor = 0.124) | | | |
| Debt | 45 | 5.5% | 2.475% |
| Equity | 55 | 12% | 6.6% |
| Total | | | 9.075% |

The levelized cost of electricity (LCOE) of the SPOC process with carbon capture was calculated as $98.5/MWh compared to approx. $73.05/MWh for a baseline air-fired plant without carbon capture. Thus, SPOC process captures carbon dioxide for a 34.8% increase in LCOE. In comparison to atmospheric pressure oxy-combustion and post combustion capture processes, this is more than a 40-50% reduction in increase in LCOE [27, 29-31]. This reduction is mainly due to the reduction in efficiency penalty by pressurization and fuel-staging. Furthermore, the use of the integrated pollutant removal column also contributes to the capital cost savings by reducing the cost of gas cleanup.

## 2.4. Conclusions

The Staged, Pressurized Oxy-Combustion process is able to avoid large amounts of flue gas recycle. This, along with the capture of latent heat from the flue gas and other waste heat from the auxiliary systems at high pressure, resulted in a net plant efficiency (HHV) of 35.7% when using subbituminous PRB coal and 36.7% when using bituminous Illinois #6 coal.

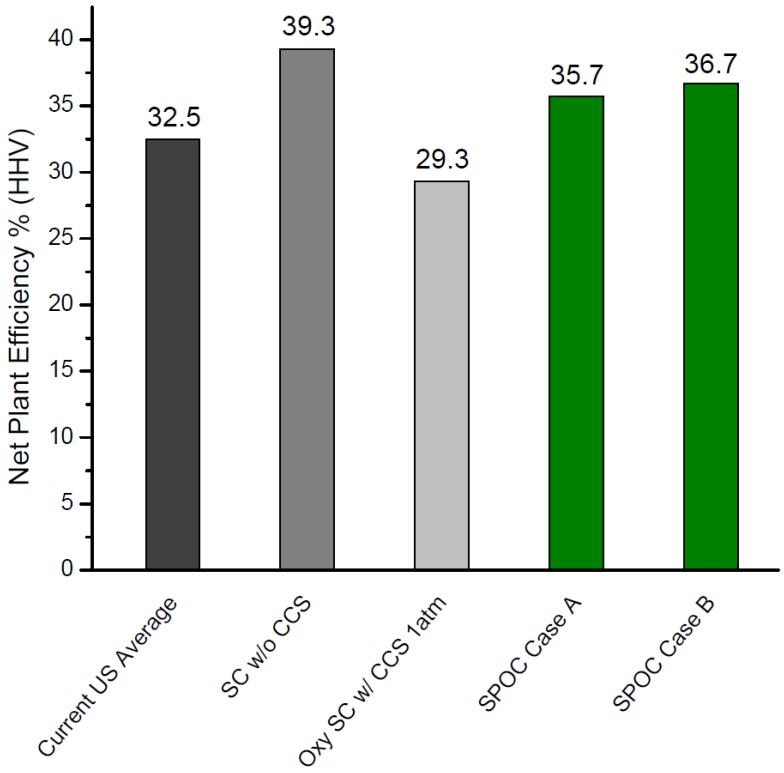


**Figure 2-1. Comparison of net plant efficiencies for various cases (SC: Super Critical. Both SPOC cases are supercritical)**

The penalty in plant efficiency due to carbon capture is reduced from 10 percentage points in the atmospheric pressure oxy-combustion plant (as reported by DOE/NETL) to about 2.6 percentage points due to the SPOC process. The average efficiency for coal-based power production

efficiency in the United States is currently 32.5% (HHV) [33, 52]. This suggests that the SPOC process has a potential to increase the average efficiency of coal-based power generation even with carbon capture, in contrast to the conventional carbon capture processes in the U.S. (Figure 2-1). The significant reduction in efficiency penalty also helps reduce the economic penalty for carbon capture by approximately 50%, making SPOC an attractive process for power generation with minimal $CO_2$ emissions.

# Chapter 3. Parametric Analysis of Staged, Pressurized Oxy-Combustion

## 3.1. Introduction

In Chapter 2, the efficiency and cost of the SPOC process were shown to compare quite favorably to other oxy-combustion approaches for power generation with carbon capture. The analysis of the SPOC process was based on a given operating pressure, fuel-moisture content, and flue gas recycle ratio (~ 5%). From a process perspective, the pressure was chosen to ensure proper operation of the DCC for integrated pollutant removal and flue gas moisture condensation, without the use of any moving parts between the boilers and the DCC. The optimal pressure for pressurized oxy-combustion has been studied for two other systems—one developed by Babcock Power and Thermo-Energy [53], and the other, a flameless combustion system, developed by ITEA and ENEL [41]. Pressures ranging from 6 bar to 80 bar have been considered, and the optimal pressure has been found to be system dependent [39, 41, 53, 54]. The optimal pressure for processes that involve a high level of FGR is strongly dependent on the need to maintain sufficient velocity for heat transfer while minimizing pressure drop [41]. This is primarily because with increased FGR the proportion of radiative relative to convective heat transfer to the steam tubes decreases. With an increased dependence on convective heat transfer—which inherently has a lower heat flux—the gas-side velocity in the heat recovery steam generator must be high to obtain a high convective heat flux. But, this leads to increased pressure drop, and hence auxiliary power requirement, reducing the efficiency. With a high pressure, the density is high, but that leads to a reduced volumetric flow rate, and thereby velocity. The competing effects of increasing velocity by shrinking the size of the heaters, leads to an optimal pressure that is around 6–8 bar.

The SPOC process, on the other hand, is based on minimizing FGR, with the primary mode of heat transfer being radiative, rather than convective. Thus, the pressure drop in the SPOC system is much lower than that of other processes. Since the optimal operating pressures are system dependent, it is necessary to understand the best operating conditions to maximize the efficiency gain. Furthermore, understanding the effect of as-fired fuel moisture is also seen as crucial, not only for this process, but for other pressurized oxy-combustion processes as well, as some have proposed coal-water slurry feeding for pressurized oxy-combustion processes [5, 7, 53]. In this chapter, the motivation for the selection of 16 bar pressure and surface-dried fuel will be provided.

Another key feature of the low flue gas recycle in SPOC is investigated in this chapter, that is, to understand how plant efficiency varies with the amount of FGR. Since the SPOC process models developed in the previous chapter showed excellent efficiency with 5% flue gas recycle (sufficient for dense-phase transport of coal), the first SPOC boiler was developed to operate with nearly-pure oxygen. Though it appears possible to control the heat flux in SPOC boilers even with pure oxygen [55], other considerations detailed in Chapter 4 could potentially limit the immediate acceptance of such a configuration in utility boilers. Thus, an understanding of the effect of the amount of FGR on net plant efficiency will provide insights for better process and boiler design.

Finally, some potential areas for process intensification, such as the direct contact column and the steam Rankine cycle operating conditions, are explored to increase the plant efficiency.

The key assumptions and modeling approach used is similar to that described in Chapter 1, and hence is not repeated here. In this chapter, and henceforth, only the sub-bituminous PRB coal (proximate and ultimate analysis provided in Chapter 2) will be used, unless otherwise specified. The choice of PRB coal is due to the low cost and high availability of this coal in the US—accounting for more than 40% of the coal consumed in the US for power generation.

## 3.2. Operating pressure

Operating pressure analyses are divided into two different studies – the first analyzes the effect of direct contact column (DCC) operating pressure on moisture condensation and lays the groundwork for the next part, which is to analyze the effect of combustor operating pressure on the net plant efficiency. For the operating pressure analyses, the coal is surface-dried to 24% as-fired moisture.

*Direct contact column (DCC) pressure:*

For moisture condensation in the DCC, six different flue gases and DCC pressures are analyzed over the range of 10 to 35 bar. All pressures are in units of bar absolute. Based on equilibrium flash calculations, Figure 3-1 shows the effect of operating pressure on the gas exit temperature of the DCC. The greatest difference is seen between 10 bar and 15 bar, while at higher pressures almost no difference in moisture condensation is observed, especially at lower exit temperatures. It can be seen that for temperatures less than 50°C, the moisture condensation and heat in the DCC increases by less than 1% when the pressure is more than doubled, beyond 15 bar. At any given exit temperature, the effect of pressure on moisture condensation yields diminishing returns with increasing pressure.

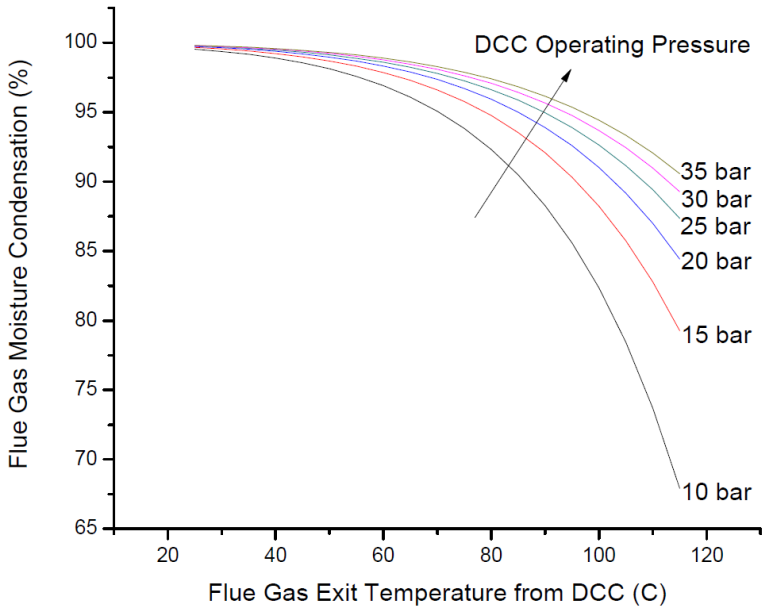


**Figure 3-1. Percentage of flue gas moisture condensation at various DCC operating pressures and flue gas exit temperatures from the DCC**

*Radiant boiler operating pressure:*

Since the analysis of the DCC indicates that 15 bar is sufficient to capture a large majority of the latent heat, the minimum operating pressure of the radiant boilers considered in this study is slightly higher, 16 bar, to allow for pressure losses between the boilers and the DCC. This will be called Case P1. Two higher pressures—30 bar (Case P2) and 36 bar (Case P3)—will also be considered. Pressures higher than 36 bar were not considered, even though they were analyzed by others [53], due to the limitation of coal feeding by solid pumps at higher pressures.

Case P1 is the same case as analyzed in Chapter 1, and the results of the process model have been discussed in detail. Case P1 is the base case for this study, and the corresponding net plant efficiency is 35.7% (HHV). Cases P2 and P3 only differ in the combustion pressure. An increase in combustion pressure above 16 bar increases the net plant efficiency only slightly, and with diminishing returns, as can be seen in Figure 3-2. The difference in net plant efficiency between 16 bar and 36 bar cases is less than 0.14 percentage points. The different contributors to this trend are discussed below.

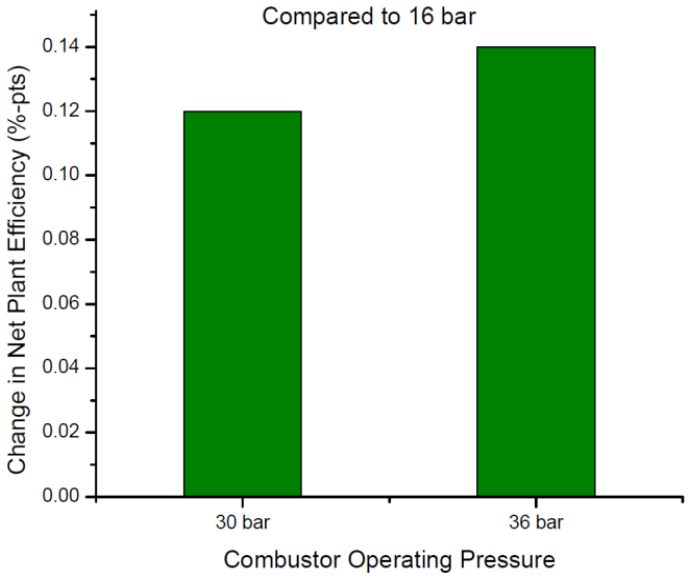


**Figure 3-2. Increase in net plant efficiency (HHV) as a function of pressure over Case P1 (16 bar).**

The power requirement for oxygen production increases with combustion pressure. Since this increase in power demand is only for increased compression, and since the final flue gas is required to be compressed up to 153 bar, the CPU power load is reduced. The sum of ASU and CPU power demand, on the other hand, remains relatively constant, between 142–145 $MW_e$ ($\approx$ 0.09$MW_e$/$MW_{th}$ fuel input), for all three pressures cases.

In SPOC, heat from either flue gas moisture condensation or “waste heat” from auxiliary systems can be integrated into the steam cycle, thereby reducing the steam extraction requirement for regeneration of BFW. As is well known, steam extraction for feedwater heating (regeneration) is used to increase plant efficiency of the Rankine cycle, but utilizing the heat from the DCC and the auxiliary systems instead of from the boiler increases the overall (net) plant efficiency.

The bottoms product (subsequently referred to as “bottoms”) of the DCC is hot water along with some (dilute) acids. The temperature of the bottoms of the column is a function of the operating pressure of the column, and increases with operating pressure. This hot water can be used to exchange heat with the Rankine cycle either upstream or downstream of the de-aerator (see Figure 1-3), replacing some of the extraction steam from such locations. As the de-aerator pressure is set at 8 bar, which corresponds to a saturation temperature (and hence BFW exit temperature) of 170°C, the DCC bottoms water temperature is not high enough in Case P1 to allow integration into the Rankine cycle downstream (high-temperature side) of the de-aerator. In contradistinction, for both the higher pressure cases—Cases P2 and P3—the exit water temperature is high enough (193°C and 200°C respectively) to allow for partial integration downstream of the de-aerator. As already stated, higher pressure (higher than Case P1) does not increase the amount of moisture condensation significantly (difference between Case P1 and P3

= 0.16 percentage points), but integrating into the high-pressure region allows heat transfer from the DCC bottoms water to the Rankine cycle in a larger temperature range. This also reduces the amount of cooling water required in the DCC, from 864 tonnes/h (16 bar) to 690 tonnes/h (36 bar) and hence reduces the rejected heat after heat transfer to the boiler feed water. In other words, with increasing pressure the amount of heat addition from the DCC increases by approx. 8 $MW_{th}$ (5.3%) from 16 bar to 36 bar (Figure 3-3a). And more importantly, the amount of heat shifted from the LP to the HP region for the 30 bar and 36 bar cases are, respectively, 6.5 $MW_{th}$ and 11.5 $MW_{th}$.

In this work, the only other auxiliary heat integrated into the Rankine cycle is the heat from oxygen production. As the operating pressure of the combustor increases, the oxygen compression requirement increases. This compression is accomplished with multistage compressors and intercoolers that use low-pressure boiler feed water (LP BFW) for cooling. As the compression requirement increases, the oxygen temperature at the intercooling heat exchangers increases. Thus, more heat can be transferred at higher temperature. As the compression requirement increases further, the stage pressure ratio in the multistage compressor increases significantly, requiring the addition of another stage to keep the compression process efficient. For both 30 bar and 36 bar cases, three stages were required, while only two were required in the 16 bar case. Addition of an extra stage reduces the maximum temperature and the temperature range in which heat is available from the oxygen compressors. Thus, the heat from the ASU is restricted in the temperature range suitable for integration with the low pressure BFW only.

Figure 3-3b shows that with increasing pressure, more heat is available from the ASU. The partial shift of DCC heat into the HP region allows the increased heat transfer from the ASU into the steam cycle, thus increasing the net plant efficiency (Figure 3-2). Still, since the temperature at which heat is available from oxygen compression is restricted, the benefit from increasing pressure is quite modest.

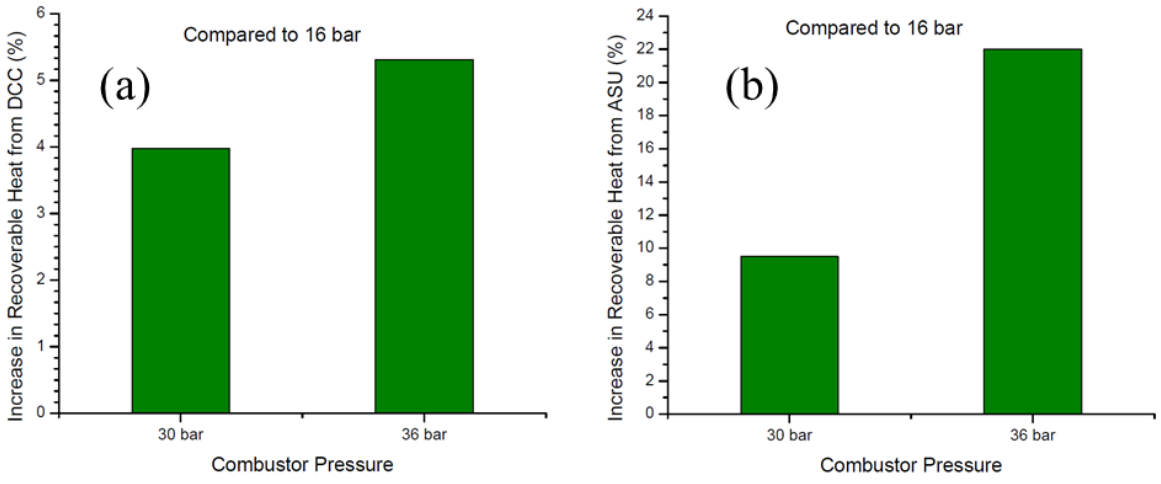


**Figure 3-3. Increase in recoverable heat (integration into Rankine cycle) from (a) DCC, (b) oxygen production.**

Increasing system pressure has two benefits—first is in increasing the efficiency of the process, and the second is in reducing the size of various units. The first effect has been quantified and discussed above. For the second effect, a brief and qualitative discussion is provided here. Since, the change in efficiency is small with increasing pressure above 16 bar, we will, for ease of discussion, neglect the effect of reduced thermal input for the same power output on size and only concentrate on the reduced gas volumes due to compression. The various units in the SPOC process are the ASU, $O_2$ compressors, radiant boilers, DCC, $CO_2$ boost compressor (which pressurizes the clean flue gas to about 36 bar) and the CPU. Of these, the ASU and CPU sizes remain the same since they always operate between the same states: ASU produces 1 bar $O_2$ from 1 bar air, while the CPU purifies the clean and dry $CO_2$ and compresses it from 36 bar to 153 bar. The combination of the $O_2$ compressors and the CPU boost compressor would have similar overall size, since they compress from atmospheric pressure to about 36 bar in all cases. In the higher pressure cases since the number of compressors increases, and more oxygen compressors are required, the capital cost may increase with increasing pressure. The radiant boilers, on the other hand, are not sized based only on the gas volumes. The primary purpose of the radiant boilers is to transfer heat to the steam cycle, and their size is dependent on heat transfer surface area requirements, and this size does not reduce proportionally with increasing pressure. On the other hand, the material of construction required will increase with pressure due to an increase in wall thickness of the boilers, even though the overall size may be reduced slightly due to reduced thermal input (higher net plant efficiency). It is important to note, however, that the material of construction only forms a small part of the boiler cost, which is mainly governed by boiler tube costs. The effect of pressure on the design of the DCC is not obvious, though there is potential for size reduction with increasing pressure, both due to the potential increase in performance of the integrated pollutant removal reactions at higher pressure [24, 56, 57] and reduced gas volumes.

## 3.3. Fuel moisture content

In order to feed the coal into the boilers at elevated pressure, a high pressure, dense-phase feeding system (pneumatic dry feeding) has been considered in the process analysis. This process requires, at a minimum, that the surface moisture of the pulverized coal be removed for optimal feeding. Further drying to remove some inherent moisture may also be considered, and may be required, to allow for effective coal delivery. An alternative method to feed coal is to use a coal water slurry, which can be readily pumped to deliver the coal at elevated pressure.

For a typical 1 atm coal-fired power plant, it is well understood that increasing moisture content decreases plant efficiency, since the added flue gas volume from moisture results in additional stack loss. However, in pressurized systems, the impact on moisture content is not obvious since a portion of the latent heat associated with flue gas moisture may be recovered. Thus, a systematic study on the effect of as-fired moisture on net plant efficiency was performed for 6 different cases, for a constant thermal input of 1539 $MW_{th}$, matching the work in Chapter 2. The as-received coal moisture is 27.42%. Coal drying was considered in three cases: drying to 9.7%,

17% and 24% moisture. The three other cases represent moisture addition (30%, 35% and 45% moisture). All other parameters of the process were kept constant. The drying of the coal was modeled as being accomplished with the dry nitrogen gas from the ASU. The heat for drying was partly derived from ASU and partly from previously unutilized low temperature heat from CPU boost compressors.

As can be seen from Figure 3-4, the net plant efficiency monotonically decreases with increasing moisture content, but the slope of the curve changes dramatically between the low moisture and high moisture cases. In the low moisture cases, low pressure BFW is heated with a combination of auxiliary heat and steam extraction. With increasing amounts of moisture in the fuel, the high temperature sensible heat available from the combustion gas in the radiant boilers and the economizer reduces, whereas the amount of low temperature latent heat available in the DCC increases. Overall, this shift of heat from the higher grade to the lower grade reduces the amount of steam extraction for BFW regeneration. The sum of the heat available from the boilers, economizer and the DCC is constant at low moistures, and so is the heat available from other auxiliary systems like the ASU and CPU for a given fuel input. Since the net heat supplied to the steam cycle is constant, but the steam extraction is reduced, the cycle efficiency reduces, as does the plant efficiency. Nonetheless, the reduction in plant efficiency is only slight when the amount of fuel moisture is low.

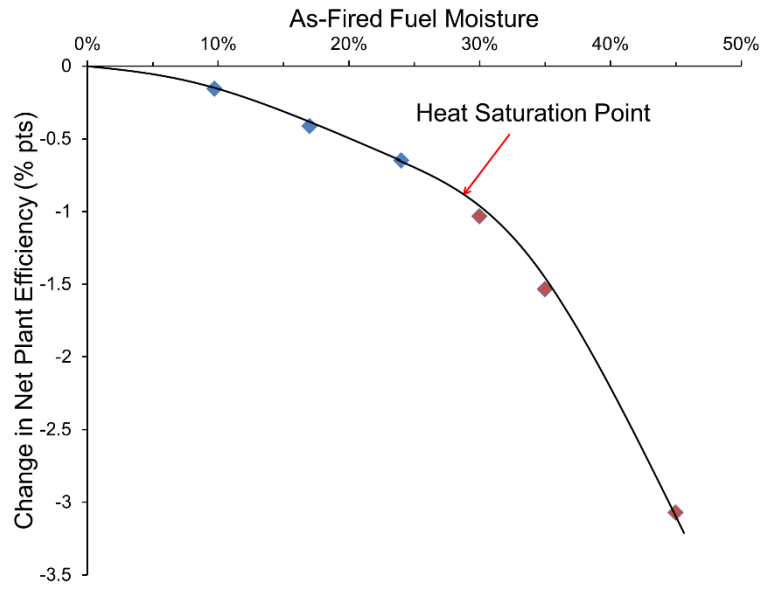


**Figure 3-4. Change in net plant efficiency (HHV) as a function of as-fired fuel moisture. Reference is a fully dry fuel.**

As the fuel moisture increases further, more heat is available from the DCC for integration and steam extraction from the LP steam turbine is completely eliminated. This is considered the point of *heat saturation* of the LP BFW. This heat saturation point is around 29% as-fired moisture for the system modeled in this paper. Beyond the point of heat saturation, increasing fuel moisture does not lead to additional heat integration into the Rankine cycle and hence does not affect the cycle efficiency, so the net plant efficiency decreases. This is because at the point of heat saturation, the maximum possible heat is integrated in the low pressure region of the BFW. Even if more heat is made available from the DCC, it cannot be integrated into the steam cycle. The excess heat from the DCC condensate needs to be cooled using cooling water and discarded.

In most conceptual pressurized systems modeled, coal water slurry (CWS) feeding is considered as the standard approach for fuel feeding due to experience and expertise in such feeding for other purposes, such as coal gasifiers. Furthermore, the pressurized oxy-combustion systems are considered to be more beneficial for low rank coals, as the hitherto unrecovered heat of moisture condensation at lower pressure, can be recovered, potentially making them more efficient. However, as seen above, increasing the moisture content beyond what would lead to LP BFW heat saturation is detrimental to plant efficiency. The challenges of feeding low rank coal as a slurry are discussed in [58]. In order to pump slurry, the maximum apparent viscosity accepted in the industry is about 1000 mPa-s at $100s^{-1}$ [59, 60]. The viscosity of the CWS increases with the hydrophilicity of the coal. Therefore, a hydrophobic coal can more easily be used to form low viscosity slurry at high solids loadings. Normally, high-rank coals are hydrophobic, while low-rank coals are hydrophilic [37]. For high pressure operations, like coal gasification, coal water slurry feeding works well for bituminous coals but not for lower grade coals [61]. Delivering a coal water slurry using PRB coal requires water content as high as 65 wt% in order to make it pumpable [58], which corresponds to more than 3%-pts. loss in net plant efficiency.

In summary, a steep decrease in plant efficiency occurs when the low-grade heat available through flue gas moisture condensation is sufficiently high such that there is excess latent heat that cannot be integrated into the steam cycle. Thus, slurry feeding of fuel even with high-pressure combustion is not recommended since the as-fired moisture in slurries exceeds this limit for heat saturation in the Rankine cycle. On the other hand, drying the fuel (beyond the minimum requirement for dry feeding) does not increase the efficiency significantly. This result is true for other pressurized processes as well, though the point of heat saturation in the Rankine cycle may occur at different fuel moisture contents.

## 3.4. Flue gas recycle ratio

Two main configurations for flue gas recycle are considered in oxy-combustion systems—warm gas recycle, and cold gas recycle. For warm-gas recycle, the flue gas is recycled prior to the gas clean-up equipment (in some cases after the filter, but still before the FGD). This increases the sulfur content in the boilers, and is only considered for operation with low sulfur coals. This

configuration has a slightly higher efficiency at atmospheric pressure. The cold-gas recycle entails complete gas cleanup, moisture condensation, and then recycling back the flue gas to the boiler.

For the SPOC process, due to high pressure in the boilers, warm-gas recycling could lead to high $SO_2$ and $SO_3$ concentrations, and this configuration is not considered here. In the cold-gas recycle configuration on the other hand, the flue gas passes through the DCC before being recycled back. As the DCC is a direct contact heat exchanger, the heat transfer is not efficient from an exergic perspective. The temperature of the flue gas for recycling is reduced to about 38°C. Flue gas recycling also increases the volumetric flow in the combustor and pushes a significant amount of sensible energy downstream to lower temperature regions. The conversion of thermal energy to electrical energy from the lower temperature regions (DCC) is much less efficient compared to what could be achieved from the high temperature regions (combustor/economizer). Therefore, during recycling, a lot of energy is wasted leading to reduced efficiency. Figure 3-5 shows the net plant efficiency as a function of flue gas recycle ratio.

As can be expected, increasing flue gas recycle increases the efficiency penalty, with 70% recycle (conventional flue gas recycle ratio) resulting in an efficiency penalty of almost 4 percentage points. However, the relation of flue gas recycle with efficiency is not linear, and most of the efficiency is penalized in the flue gas recycle ratio range above 33%. Below 33%, the efficiency loss is less than 1 percentage point.

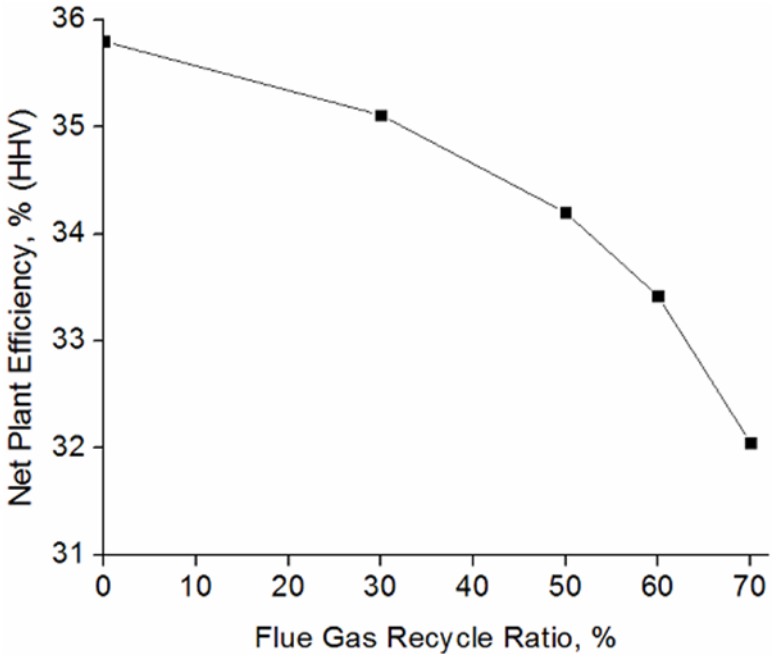


**Figure 3-5. Effect of flue gas recycle ratio on the net plant efficiency (HHV) in the SPOC process**

## 3.5. Process intensification and advanced Rankine cycles

Process intensification in staged, pressurized oxy-combustion can be achieved by the modification of the flue gas condensing heat exchanger from a low efficiency direct contact column, to a more efficient indirect contact heat exchanger. Modifications to the Rankine cycle, in line with the latest industrial advancements, such as a double reheat steam cycle or advanced ultra-supercritical Rankine cycle would also help increase the plant efficiency. In this section, the results from such intensification or cycle modification are presented.

### *Indirect contact heat exchanger for flue gas moisture condensation:*

The direct contact column used in the SPOC process provides a practical means of condensing the flue gas moisture, while minimizing the impact of the acids that would condense along with the moisture. In the DCC, due to the very large amount of water added for cooling, the acids are diluted. Furthermore, since the heat exchange is not through the surface of the contacting column, the material of construction can be made acid resistant at low cost. However, the process is highly inefficient in terms of heat transfer. The raw hot flue gas enters the DCC at approximately 330°C, and the maximum temperature of the hot water from the DCC used for heat exchange with the boiler feed water is at 165°C. This represents a significant loss in availability (exergy). An indirect contacting heat exchanger could be used instead of the direct contact column to capture this availability. The flue gas at the outlet of this indirect heat exchanger can be designed to enter the DCC at a low temperature for an efficient integrated pollutant removal (~ 46°C). The indirect heat exchanger would be exposed to very high acids concentration (acid dew point is higher than moisture dew point), and hence would require expensive materials of construction. For the SPOC process, the gain in net plant efficiency when using an indirect heat exchanger is approximately 0.55 %-pts. This analysis provides a basis for cost-benefit analysis for the utilization of such a heat exchanger.

### *Advanced Rankine cycles:*

Advances in the development of materials and turbo-machinery have allowed two primary modifications in the design of Rankine cycle to further increase efficiency—double reheat of steam, and higher steam temperature and pressures (USC and AUSC cycles). Similar to the indirect heat exchanger for flue gas moisture condensation, the implementation, or lack thereof, of these process intensification measures is dictated by the economics. However, in this section, only the performance improvements through such process intensification are discussed. The cycle conditions for the different configurations studied are presented in Table 3-1. In the cases of double reheat, the steam temperature at the outlet of the second reheat is maintained the same as in the first reheat. In all the cases, a direct contact column is considered for flue gas latent heat recovery. Only the cycle conditions are changed, while the coal properties, site conditions, etc. are maintained the same as described in Chapter 2.

**Table 3-1. Steam conditions for the various Rankine cycles considered**

| Condition | Main Steam Pressure (bara) | Main Steam Temperature (°C) | Reheat Steam Temperature (°C) |
|---|---|---|---|
| SC | 242 | 593 | 593 |
| Ultra-Supercritical (USC) | 277 | 690 | 690 |
| Advanced USC (AUSC) | 277 | 732 | 732 |

The results for the sub-bituminous PRB coal are shown in Figure 3-6. For the steam conditions shown in Table 3-1, adding a second reheat leads to approximately 1.5 %-pts. increase in net plant efficiency. Whereas, increasing the steam temperature and pressure from that for SC to AUSC can increase the efficiency by almost 3 %-pts. Overall, the highest efficiency of 40.64% is obtained by using an AUSC steam cycle with double reheat. If a higher rank coal, such as the Illinois #6 coal described in Chapter 2 is considered, the net plant efficiency is approximately 41.4%. These efficiencies are 25–30% higher than the current U.S. average.

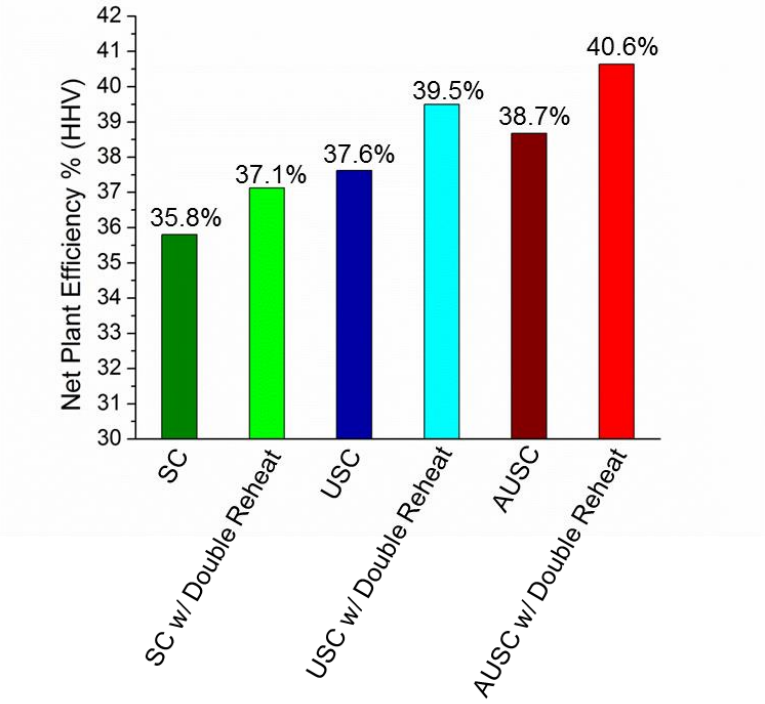


**Figure 3-6. Net plant efficiencies when using different steam temperatures and pressures, and number of reheats in the Rankine cycle of the SPOC process.**

## 3.6. Conclusions

In this chapter, parametric analyses on the effects of combustor operating pressure and fuel moisture were performed for a fuel staged, pressurized oxy-combustion power plant. It was found that combustor pressure has only a minor impact beyond 16 bar. At higher pressures, the increase in pressure leads to a negligible increase on the amount of flue gas moisture condensation and only a small increase on the heat available for integration with the Rankine cycle. But, its ability to partially shift the location of the heat integration to the HP region of the Rankine cycle from the LP region, along with a small increase in the heat available from the ASU, results in an increase in the net plant efficiency. In the range of pressures considered, although the net plant efficiency increases, the increase is quite modest (~ 0.14 percentage points) for the significant increase in combustor operating pressure (pressure is more than doubled in the range considered). Overall, the economic gain or loss due to further pressurization will be case dependent. The fuel cost, fuel moisture, sulfur and nitrogen in fuel, etc. will play a role in determining the optimal pressure. Based on this analysis, though, it is expected that the optimum would be around 16 bar.

When compared to an atmospheric pressure oxy-combustion system the plant efficiency increases for the high-pressure combustion systems for all moisture contents. But, if the as-fired moisture content of the fuel is increased, the gain in efficiency will reduce. This is an important observation, especially when slurry feeding is considered for high pressure operation, and when working with low rank coals or lignites, which require a large amount of water for slurry feeding. Operating with as-fired moisture lower than what would cause heat saturation in the low pressure regenerators is recommended. In almost all cases, this translates to dry or surface-dry feeding of coal.

Similarly, the non-linear dependence of net plant efficiency on the flue gas recycle ratio provides some room for recycle without significant loss in efficiency. Flue gas recycle up to a recycle ratio of 33% results in an efficiency penalty of less than 1%-pts. This has implications in addressing other burner design constraints, as will be highlighted in Chapter 4 and Chapter 5.

Finally, process intensification through indirect heat exchangers, instead of a direct contact column for flue gas moisture latent heat recovery, and advanced steam Rankine cycle can increase the plant efficiency. The indirect heat exchanger can increase the efficiency by 0.55%-pts., whereas the advanced ultra-supercritical Rankine cycle with double reheat will result in about 4.5%-pts. higher efficiency than the supercritical, single reheat Rankine cycle considered in Chapter 2.

# Chapter 4. Introduction to Burner and Boiler Design for Low-recycle Pressurized Oxy-Combustion

## 4.1. Introduction

In the previous two chapters, the process design and parametric analysis of the SPOC power plant were discussed, with an emphasis on the net plant efficiency. It was assumed that such a low FGR oxy-combustion boiler could be designed and operated at high pressure. This chapter presents a brief discussion on the primary design considerations for such a boiler, and the burner therein.

Boiler walls are made up of tubes carrying water/steam at very high pressures (up to 250 bar). In a supercritical steam cycle, the high pressure water/steam is heated in the boiler to become a supercritical fluid at high temperature and pressure, and is then expanded in a turbine to produce electricity. Since the boiler tubes are under high pressure, significant care is required to not exceed their temperature constraints. A very high wall heat flux could lead to a boiler tube temperature that is above its limit, resulting in tube failure. In air-fired conditions, the heat flux is below the maximum permissible value, due to the low flame temperature caused by the large amount of inert ($N_2$) in air. On the other hand, the combustion of coal with pure oxygen could result in an adiabatic flame temperature as high as 3000 K, leading to excessively high heat flux. The primary method of controlling wall heat flux in first generation oxy-combustion is through the control of flame temperature by recycling a large quantity of flue gas [62, 63]. Reducing flue gas recycle has, therefore, traditionally been considered to pose risks and has been avoided.

Nonetheless, as shown in Chapter 3, reducing FGR leads to an increase in plant efficiency. Furthermore, reducing FGR increases the portion of heat transfer to the furnace wall that is due to radiation, as opposed to convection [13]. Since radiative heat flux from a flame is usually higher than convective heat flux in power plants, reducing FGR can reduce the amount of boiler tube materials required, thereby reducing capital costs. A few combustor designs have been proposed for reduced recycle [11-13, 64], however, as Kobayashi and Bool [11] have noted, these were only demonstrated for industrial furnaces or for boilers with low thermal input and low temperature and pressure steam, where much higher heat fluxes can be handled than in a typical utility-scale boiler. None of these designs have been demonstrated for utility-scale boilers, due to the inability to control wall heat flux within manageable levels.

## 4.2. Boiler design considerations

In most traditional boilers, the fuel and oxidizer are supplied at the bottom of a large rectangular boiler and are rapidly mixed, usually by generating a swirling flow, to react the two streams and release heat. This configuration has many disadvantages for pressurized, low recycle combustion and the subsequent discussion will address why a radical departure from traditional

combustor/boiler design is required for SPOC. For example, swirling motion has many disadvantages when designing a low recycle boiler where the flame temperature is higher than typical. First, the swirling motion invariably pushes the flame towards the wall—potentially leading to flame impingement. Swirling also throws large particles to the wall, and for a boiler with a very high temperature flame, the particles can be molten, and swirling would invariably lead to a high level of slagging on the boiler tubes. Finally, rapid mixing could lead to an excessively high heat flux in the near-burner region because of the high flame temperature. These issues, and others, will be addressed in the SPOC design.

Another important difference for the design of a pressurized combustion system is that the standard design for a pressure vessel is a cylindrical shape and, thus, the aspect ratio is considerably larger in a pressurized boiler compared with the typical rectangular shape of an atmospheric-pressure boiler. This high aspect ratio will be an important factor in all of the subsequent design considerations.

As noted in Chapter 2, the plant efficiency of SPOC is very high due to pressurized combustion and minimal recycle, but the flame temperatures for the initial stages can be very high. The high flame temperature presents a number of challenges, such as excessive wall heat flux and slagging, which will be addressed in the SPOC design. To avoid flame impingement and slagging on the walls requires that swirl be minimized, and a high level of symmetry be maintained throughout the pressure vessel. To maintain axisymmetric flow, buoyancy dictates that the pressure vessel and burner be oriented vertically. This is very different from the traditional atmospheric-pressure boilers, which are typically up-fired, with the burners placed horizontally on vertical walls. For SPOC, the axisymmetric burner arrangement is preferred, with the burner down-fired from the top of the cylindrical pressure vessel. Down-firing from the top (as opposed to up-firing from the bottom) avoids the possibility that ash/slag build-up will fall on the burner.

A number of factors must be considered to avoid excessive heat flux, but a more fundamental question with respect to heat flux in the pressurized system is how to ensure high, but not excessive heat flux throughout the length of the long, narrow (high aspect ratio) pressurized boiler. A high average heat flux over the length of the boiler will minimize boiler tube surface area, and lead to a reduction in capital costs for the plant. As will be shown, with proper design for SPOC, a high radiative heat flux can be maintained throughout the boiler. This is assisted by ensuring slow mixing between the fuel and the oxidizer, so that the heat release can be distributed over a longer length of the boiler. Once again, this shows a fundamental difference between pressurized combustion and traditional boiler combustion, where rapid combustion and heat release are required. In Figure 4-1 [65] the heat flux profile for coal burning in pure oxygen in a swirl-stabilized, rapidly mixed combustor is compared with that of an axial jet flame with the same coal and oxygen feed rate. The swirl-stabilized flame leads to rapid mixing and heat release, which leads to a sharp peak in heat flux as well as flame impingement, whereas the axial jet flame has a more distributed heat release and no flame impingement, leading to a more distributed wall heat flux.

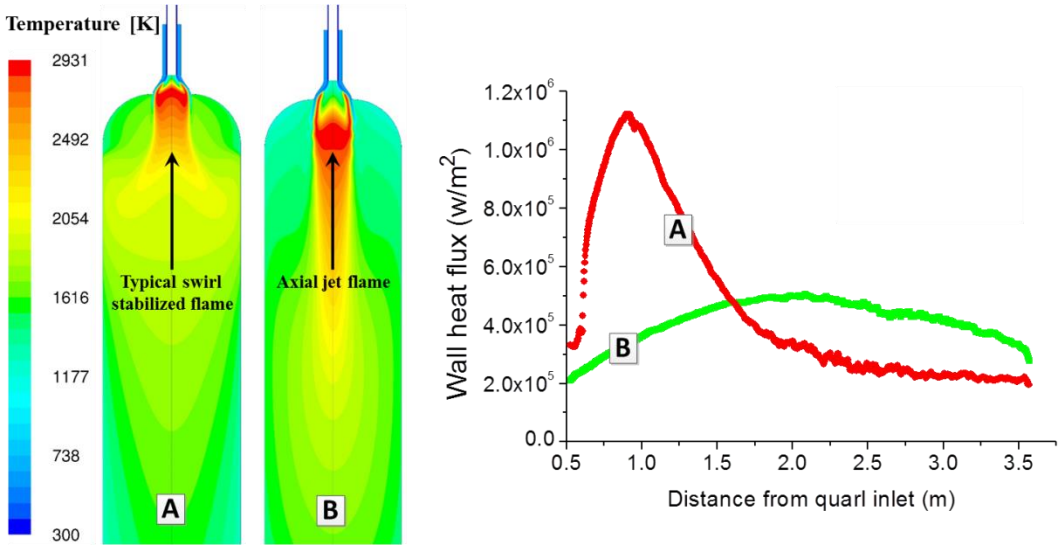


**Figure 4-1. A comparison of a swirl-stabilized and an axial jet flame of coal combusting in pure oxygen. Temperature contours in false colors are shown on the left, and the corresponding wall heat flux profiles are shown on the right. Figure reproduced from Xia et al. [80].**

While the axial jet flame has a lower mixing rate than the swirl-stabilized flame, it does not intrinsically represent a low-mixing system. To minimize mixing, a low relative velocity between the fuel and the oxidizer is needed because in an axial flow system, near-burner mixing is controlled by the relative velocity between the streams. Furthermore, if such a system can be designed, while at the same time avoiding recirculation, there would be no mean velocity towards the wall. The lack of mean radial velocity would reduce the rate of deposition on the wall by an order of magnitude, due to the elimination of inertial impaction [66]. Fuel-staging, as discussed in Chapter 1, leads to a higher gas flow than the stoichiometric amount required by the fuel in that stage. This larger gas flow can also act as a shroud to reduce particle deposition on the walls. However, for the small number of particles that still penetrate the boundary layer and reach the wall, due to eddy-impaction or thermophoresis, the shroud gas can be used to cool them enough to avoid slagging [66].

External recirculation can be avoided by controlling the Thring-Newby parameter [55, 67]. Still, in a high-temperature down-fired flame, buoyancy could lead to internal recirculation. Depending on the size and location of the internal recirculation, the volatile flame shape could significantly be altered. A much shorter and bulkier volatile flame could result, leading to flame impingement and therefore a very high heat flux. For illustration, a false-color temperature contour from simulation of a case with buoyancy is compared to a case without buoyancy (body-force set to zero) in Figure 4-2.

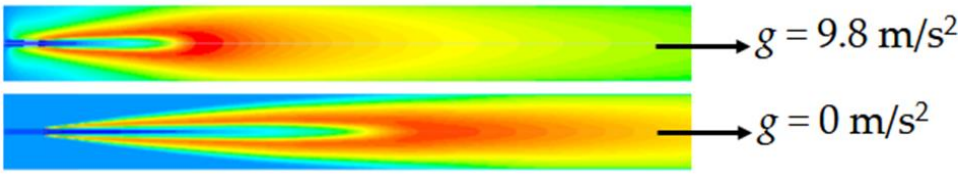


**Figure 4-2. Temperature contours for a case with buoyancy (top) and a case without buoyancy (bottom).**

Finally, even if flame-impingement could be avoided and a distributed heat release achieved, since the adiabatic flame temperature in this system will be very high, the wall heat flux could also be very high. To control the wall heat flux in such low-recycle systems, the burner and boiler can potentially be designed to utilize radiative trapping. Detailed discussions on the fundamentals and the potential applications of radiative trapping are presented in [68].

## 4.3. Burner and boiler constraints

Xia et al. [55], using computational fluid dynamics (CFD) simulations, showed a concept design for the SPOC boilers where, even at very low flue gas recycle, the wall heat fluxes for all stages were controlled to manageable levels for utility-scale applications. In the design, the fuel was staged into four boilers, while all the oxygen was supplied to the first stage, creating highly over-ventilated initial stages. After combustion of the fuel in the first stage and sufficient cooling by heat transfer to the boiler tubes, the exhaust gas—which still contained a high oxygen concentration—was fed to the next stage where more fuel was injected and some of the oxygen was consumed. This process was repeated until almost all the oxygen and all the fuel was consumed. In this system, the flue gas recycle was only about 5% of the total exhaust gas, and was required only for the dense-phase transportation of the fuel [3].

Though conceptually the design of Xia et al. [55] shows that the wall heat flux can be controlled even for negligible flue gas recycle, certain practical constraints might limit the use of such a design. Primary among them is the high oxygen concentration next to the boiler tubes. For example, in Stage 1 of the design, the oxygen concentration next to the boiler tubes could be as high as 100%, creating a risk of metal fires if an ignition source—such as an impacting ash particle—is present. Thus, to provide a safe operating condition, the oxygen concentration next to the wall must be constrained to a pre-defined maximum, dictated by the application—utility boiler or industrial furnace. A new burner design will be presented in Chapter 5, which satisfies the constraints presented herein.

# Chapter 5. Burner Design and the Effect of Mixing

## 5.1. Introduction

As discussed in the previous chapter, the concept boiler described in [55] had a very high oxygen concentration next to the boiler walls in the initial stages. The current chapter will discuss a new burner that can reduce the maximum oxygen concentration next to the boiler walls, while still maintaining a low flue gas recycle. Certain modifications to the process will also be discussed, where with little loss of efficiency, the complexity of the process can be further reduced.

## 5.2. Process modification – reduction in the number of stages

As discussed in Chapter 4, the oxygen concentration next to the boiler tubes might need to be controlled to a pre-defined maximum from a safety perspective due to the high temperature environment in the boiler. To control the near-wall oxygen concentration, some amount of flue gas recycle would be required. The objective is to keep the amount of flue gas recycle sufficiently low, such that the loss in efficiency associated with the recycling of flue gas is not large. In Chapter 3, the effect of cold recycle of flue gas on the net plant efficiency was presented. It was seen that the efficiency penalty for recycling flue gas is very small for recycle ratios less than 33%.

If some flue gas recycle is used in the process, further simplification of the process may be possible by, for example, reducing the number of stages from four to, say, three. A simplified process flow diagram for this is shown in Figure 5-1. In this process, flue gas recycle would only be required in stage 1 to control the oxygen concentration next to the wall. The near-wall oxygen concentration of the other stages would be controlled using the products of combustion from the previous stage. The smaller number of stages, and the burner modifications presented in this paper, significantly reduce the complexity of the process and provide additional control on the amount of oxygen and its inlet concentration for each stage. Furthermore, with the new burner design, each stage can be supplied with some amount of pure oxygen through a central tube to enhance the combustion characteristics, such as ignition and flame stabilization, as well as reaction rates due to multiple flame fronts, as discussed in Section 5.5. Using computational fluid dynamics (CFD) simulations, the effects of various design parameters on the fluid dynamics, and thereby the wall heat flux in a pressurized boiler are investigated. The principles developed here can then be utilized to design low recycle, pressurized oxy-combustion burner/boilers, where wall heat flux is controlled without large amounts of recycled flue gas.

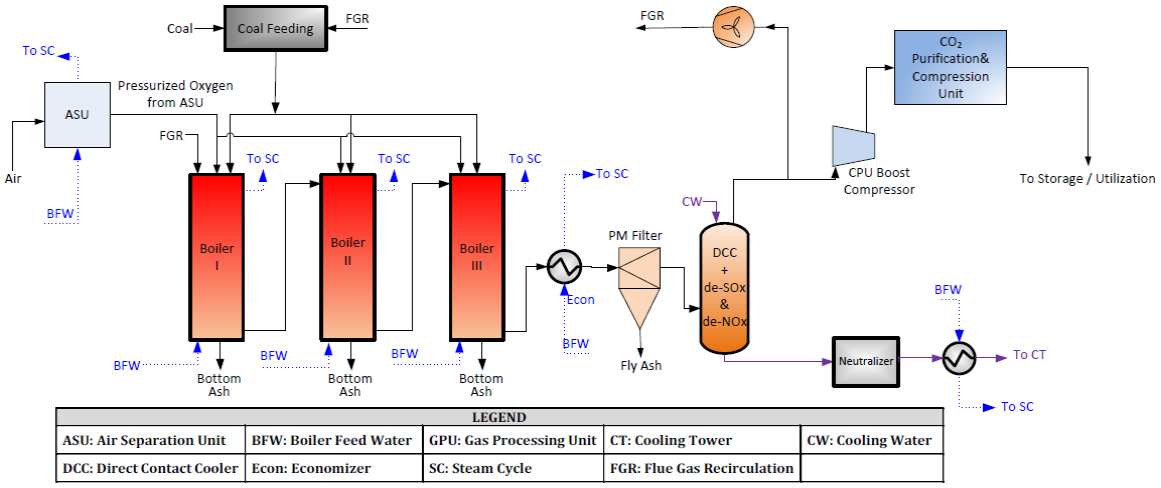


**Figure 5-1. Simplified process flow diagram for a three-stage SPOC power plant.**

## 5.3. Burner design

In these high temperature, vertical, pressurized boilers, to minimize the effect of buoyancy, which could negatively impact flame shape and wall heat flux, the initial section of the boiler is designed as the frustum of a cone, as shown in Figure 5-2. This helps in maintaining a low Richardson number (i.e., low natural convection relative to forced convection) throughout the flame region. The effectiveness of such a cone-shaped boiler in avoiding buoyancy-induced recirculation has been demonstrated in Xia et al. [55] and Gopan et al. [69]. The Richardson number is low at the burner head because the small cross-sectional area of the conical design yields a high velocity. As the flow moves downstream, the cross-sectional area increases, but the volumetric flow rate of the gas also increases, because as the coal devolatilizes and combusts, both the moles of gas and the gas temperature increase. The cone angle of the boiler is designed by matching the increasing volumetric flow rate of the gas with the increasing cross-sectional area. The axial profile of the mass-averaged mean velocity for the base case (discussed later) is shown Figure 5-3 to demonstrate the effectiveness of the conical design in maintaining a relatively uniform, high velocity throughout the flame region.

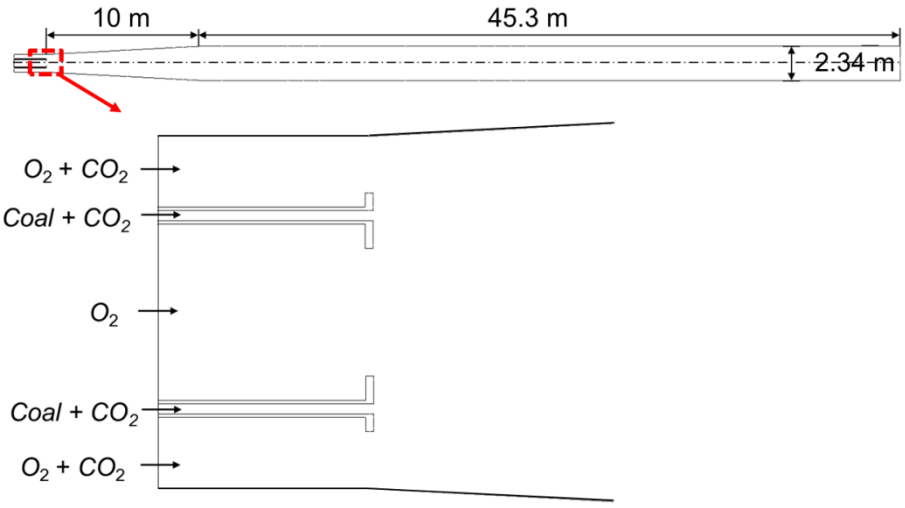


**Figure 5-2. Geometry of the burner and the boiler.**

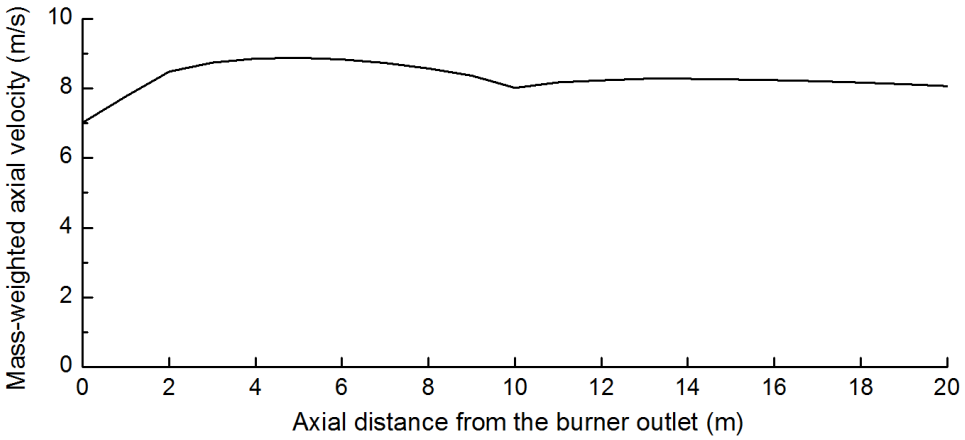


**Figure 5-3. First 20-meter axial profile of the mass-averaged mean velocity in the boiler.**

To provide a safe operating condition, with the oxygen concentration next to the wall constrained to a pre-defined maximum, while still maintaining a low flue gas recycle, the burner design, shown in Figure 5-2, incorporates a central pure oxygen stream surrounded by fuel in an annulus, which is further surrounded by a secondary oxidizer (SO) with an oxygen concentration that can be varied. In this study, as an example, the SO oxygen concentration is held constant at 35 vol.%, which is similar to the SO oxygen concentration in first generation oxy-combustion. Circular rings are included on the nozzle ends on both the surrounding oxidizer side and the central oxygen side of the fuel annulus to assist with flame holding. These rings trip both oxidizer flows at the burner exit and cause small localized recirculation zones at the burner, which enhances flame stability, resulting in predicted flame attachment for a wide range of flows, including all flow

conditions modeled in this study. The first 2 m of the boiler wall is refractory and is modeled as adiabatic.

It is important to note that this design with inner oxygen is quite different in both intent and implementation from the oxygen lance used in some other atmospheric pressure oxy-combustions burners. In the atmospheric pressure systems, an oxygen lance stabilizes the flame at the burner tip and incrementally improves boiler efficiency. In such systems, the amount of oxygen used is less than 5% of the total oxygen required for the fuel [70]. In contrast, the amount of oxygen supplied from the inner tube in the SPOC burner is substantial and can even be more than the oxygen required for stoichiometric combustion of fuel in that stage. Furthermore, since the pure oxygen stream in the center is surrounded by a large number density of fuel particles, the radiation from the flame is trapped and only a portion reaches the wall, thereby controlling wall heat flux even with reduced recycle.

There are any number of ways in which the flows of fuel and oxidizer in the three stages can be distributed. To maintain a relatively low oxygen concentration near the boiler walls, some flue gas recycle is required in the first stage, with the later stages using the exhaust gases from the previous stage to maintain a relatively low near-wall oxygen concentration. The flue gas recycle ratio is thus inherently a function of the oxygen concentration in the SO flow in the first stage. For a given SO oxygen concentration and total fuel amount, assigning less fuel in the first stage would lead to a smaller flue gas recycle ratio. For a SO oxygen concentration of 35%, even with an equal distribution of fuel between the stages, the amount of flue gas recycle required is only 33%. This SO oxygen concentration is similar to the oxygen concentration in first generation oxy-combustion processes which utilize about 70% of flue gas recycle. Thus, the same near-wall oxygen concentration can be maintained with less than half the amount of recycle incorporated in first generation approaches. Process calculations show that under these conditions the effect on net plant efficiency is small (less than 1 %-pt.). In practice, the process configuration could utilize a deeper staging, resulting in a still smaller flue gas recycle.

PRB coal is assumed for this study, with the proximate and ultimate analyses provided in Table 5-1. The coal thermal input to the stage is 385 MWth, and is carried by a 1.2 kg/s stream of $CO_2$. The inner oxidizer is pure oxygen with a flow rate of 21.7 kg/s for the base case, corresponding to 78% of the total oxygen required for the fuel in this stage. The flow rate of the surrounding oxidizer for the base case is 69.44 kg/s.

**Table 5-1. Properties of Powder River Basin (PRB) coal**

| Proximate analysis (%wet) | | | | Ultimate analysis (%daf) | | | | | HHV |
|---|---|---|---|---|---|---|---|---|---|
| Moisture | VM | FC | Ash | C | H | O | N | S | (MJ/kg) |
| 27.42 | 31.65 | 36.43 | 4.5 | 73.81 | 5.01 | 19.91 | 0.95 | 0.32 | 20.47 |

Critical design parameters are studied to determine their impacts on wall heat flux. These can broadly be broken down into two categories: 1) the effect of buoyancy-induced internal recirculation, and 2) the effect of fluid dynamic mixing between the fuel and the two oxidizer streams. Finally, the effect of scaling on wall heat flux will be discussed briefly.

## 5.4. CFD methods

ANSYS FLUENT version 13.0 was used to simulate different burner designs. The flow field was modeled using the Reynolds-Averaged Navier-Stokes (RANS) equations with the Semi-Implicit Method for Pressure Linked Equations (SIMPLE). Particle trajectories were computed in the Lagrangian frame and were coupled to the gas phase. The sub-models used in this study are presented in Table 5-2, together with the particle and wall properties. Further details on the selection criteria for the sub-models and the sensitivity studies of the particle and wall properties are discussed in Appendix A. Mesh insensitivity studies, including comparison with a 3D mesh consisting of 10 million cells, showed that a 2D axisymmetric mesh with 230,000 cells was sufficient to model the system.

**Table 5-2. CFD sub-models and some input parameters**

| | **Sub-models and parameters** | **Source** |
|---|---|---|
| Turbulence | shear stress transport k-ω | [71] |
| Turbulence-chemistry interaction | Finite rate/eddy dissipation model | [72] |
| Particles turbulent dispersion | Discrete random walk model | [72] |
| Coal devolatilization | Chemical percolation devolatilization model | [73] |
| Char oxidation | Kinetics/diffusion-limited model | [72] |
| Radiation | Discrete ordinates model | [74, 75] |
| Gas absorption coefficient | Weighted sum of gray gases model | [76] |
| Coal size distribution | Rosin-rammler distribution, $d_{mean}$ = 65 μm,$d_{min}$ = 10 μm, $d_{max}$ = 200 μm, $s$ =3.5 | [55] |
| Particle emissivity | 0.6 | [77] |
| Particle scattering factor | 0.6 | [78] |
| Wall emissivity | 0.8 | [79] |
| Wall temperature | 700 K | [80] |

## 5.5. Results and discussion

### 5.5.1 Low-recycle SPOC boiler – base design

The use of two separate oxidizer streams produces a flame structure with two volatile flame fronts, as shown schematically in Figure 5-4. The inner flame front (closer to the axis) results from the reaction between the fuel and pure oxygen (inner oxygen), and the corresponding local flame temperature is very high (~2800 K). The outer flame front results from the reaction between the fuel and the secondary oxidizer (SO), which has a lower oxygen concentration, and thus the corresponding flame temperature is lower.

When over-ventilated (i.e., excess oxygen is delivered for that boiler stage relative to the stoichiometric requirement for complete consumption of the fuel delivered to that stage), three main flame types can result, as shown in Figure 5-4. The type of flame formed would depend on the amount of oxygen supplied through each oxidizer tube, relative to the stoichiometric amount required by the fuel in the stage. The following discussion on the flame types assumes that the total oxygen supplied is the same (same stoichiometric ratio), though its placement through the inner and surrounding oxidizer tubes could be different. The Type I structure occurs when the oxygen supplied through the SO is much lower than the stoichiometrically required amount, resulting in a short outer flame, while the inner oxygen (IO) flame expands to the wall. This configuration leads to flame impingement, and hence is not an acceptable configuration. The Type II structure occurs when the SO oxygen supply is sufficiently high to prevent flame impingement, but the inner oxygen supply is much lower than the stoichiometric requirement. Due to a small oxygen supply from the central tube, the inner flame is small. This configuration is acceptable from a flame impingement perspective. But, for a given stoichiometric ratio in the stage, this structure would result in a relatively high flue gas recycle requirement since much of the required oxygen is supplied from the SO ([$O_2$] = 35%, [recycled flue gas] = 65%). The Type III structure occurs when the SO flow is just sufficient to prevent flame impingement, while most of the oxygen is supplied as inner oxygen. Since most of the oxygen required for the combustion of the fuel in the stage is supplied through the inner tube, this configuration utilizes the full advantage of pure oxygen, and allows the requirements for flue-gas recycle to be minimized. This is, thus, the preferred configuration.

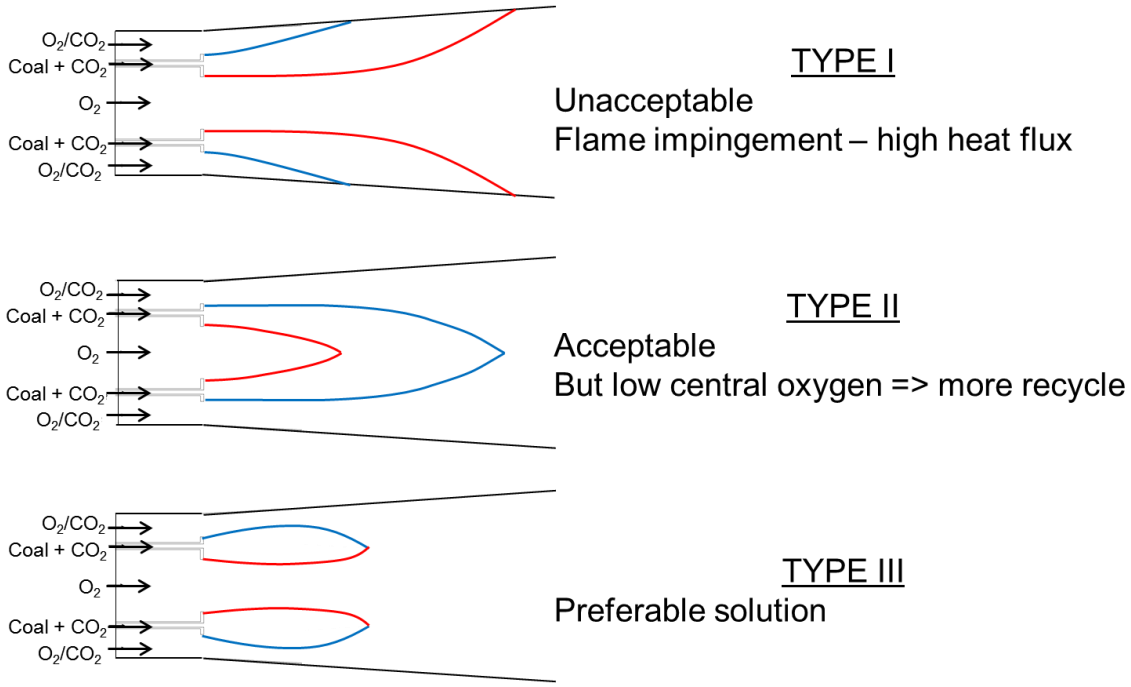


**Figure 5-4. Possible flame shapes for a triaxial system with fuel in the annulus, and two oxidizer streams. Dark blue represents the flame resulting from the SO and red represents the flame resulting from the IO.**

Under the conditions discussed for the base case in Section 5.3, a Type III flame structure is formed, as can be observed from the volatile reaction rate contours shown in Figure 5-5.

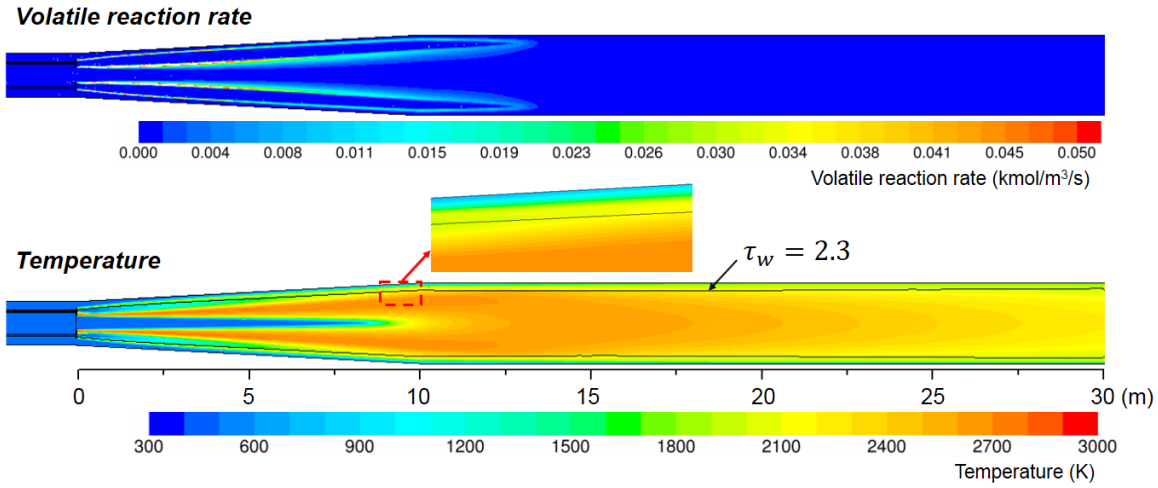


**Figure 5-5. Volatile reaction rate and temperature contours for the base case. Note: Only the first 30 m of the boiler shown.**

The radiative and total (radiative plus convective) heat flux profiles are shown in Figure 5-6. It is clear, that in the initial region, the radiative heat flux is much lower than what might be expected from such a high flame temperature (up to 2800 K) if trapping of radiation had not been effectively implemented. The boiler design ensures that the radiative heat flux is not excessive even further downstream. The peak radiative heat flux is comparable to that observed in air-fired boilers, even though the temperature in the core of the boiler is much higher.

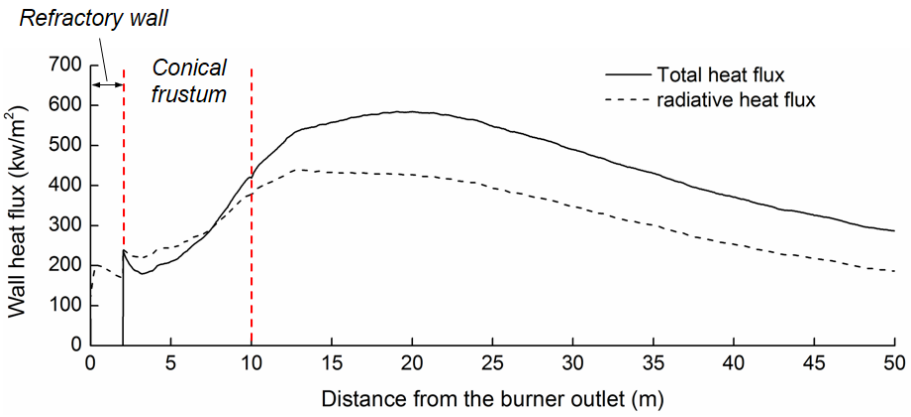


**Figure 5-6. Radiative and total heat flux profile for the base case.**

### 5.5.2 Effect of buoyancy-induced internal recirculation

As described in Section 5.3 the cone angle is designed to result in a uniform axial velocity profile (Figure 5-3) to minimize the impact of buoyancy. The impact of buoyancy-induced internal recirculation on the wall heat flux of such an optically dense boiler is studied here by changing the conical frustum length to induce recirculation. For a given cone angle, a longer frustum length leads to a larger boiler diameter and lower velocity, which could lead to buoyancy-induced internal recirculation.

Figure 5-7 shows the axial velocity and temperature contours for two cases, the base design with no recirculation (10 m cone length), and another design with internal recirculation (20 m cone length and same cone angle). In the latter case, the internal recirculation zone is formed at around 18 m. While this is downstream of the peak temperature region, the recirculation slows the fluid flow upstream, causing the peak temperature region to broaden. This pushes the high temperature gases closer to the wall and results in higher heat transfer.

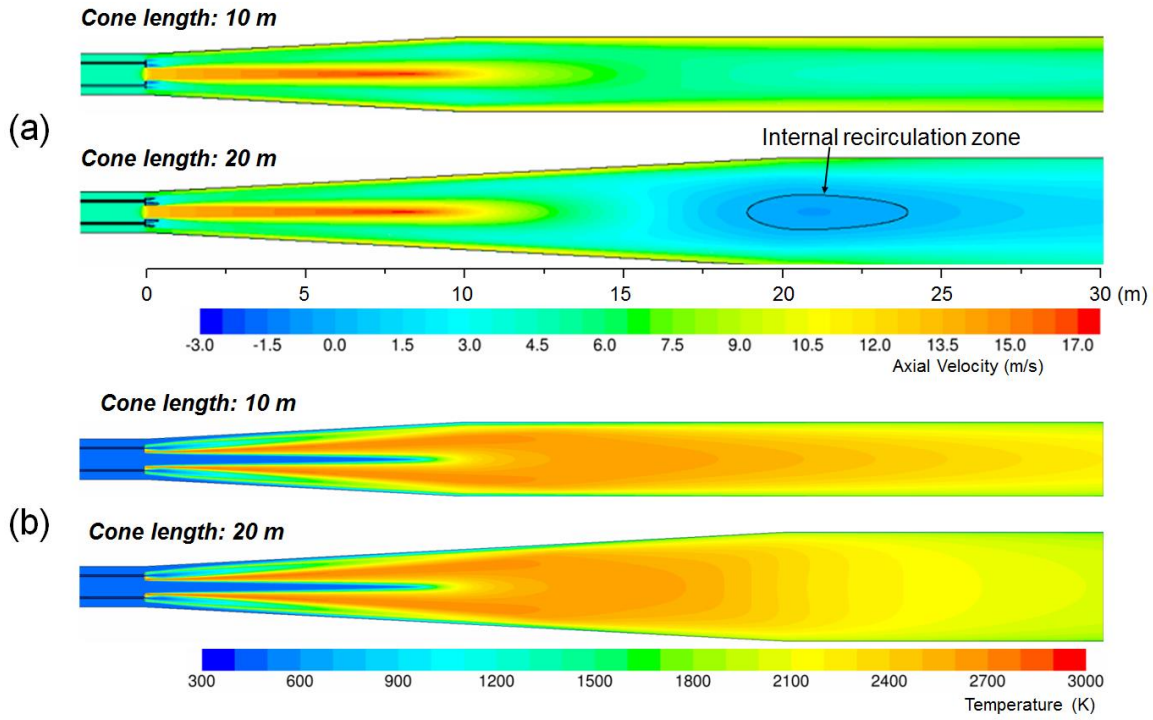


**Figure 5-7. First 30 m of (a) axial velocity and (b) temperature contours for two lengths of the conical frustum (10m and 20m).**

## 5.6. Ash deposition characteristics

Figure 5-8 shows the temperature contour and velocity vectors of the boiler used as one stage of the SPOC process. This boiler design is completely different from the conventional coal-fired boiler design, which features a swirl- or recirculation-based enhanced-mixing flow, as shown in Figure 5-8b. The difference in flow field leads to significantly different ash deposition mechanisms. While inertial impaction is the dominant ash deposition mechanism in conventional boilers, in a parallel flow system, inertial impaction is negligible, because the mean flow velocity towards the wall is zero. The dominant mechanisms of ash deposition will then become eddy impaction (i.e., impaction caused by eddy diffusion) and thermophoresis. Although there have been extensive studies on particle deposition behaviors in iso-thermal, turbulent parallel flows (i.e., there is *no* thermophoresis) in the aerosol research community [81-83], few studies have examined particle deposition in non-isothermal, turbulent parallel flow systems, especially in reacting, turbulent parallel flow systems.

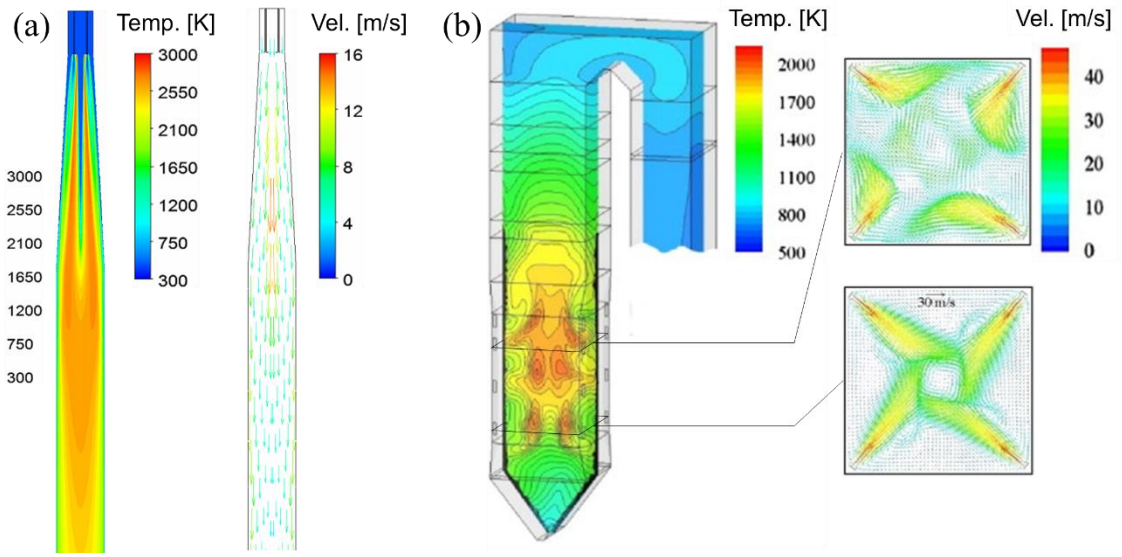


**Figure 5-8. Temperature contours and velocity vectors of (a) a boiler designed for one stage of the SPOC process and (b) a typical tangentially-fired coal combustion boiler [84]. Note: due to a large aspect ratio of the SPOC boiler, only the first 25 meters of the furnace is shown in Figure 1a. The total furnace length of the boiler is about 65 meters.**

Understanding the ash deposition behaviors in the SPOC boiler is important to the success of the technology. In the early stages of SPOC, ash droplets can potentially form in the flame region, due to the high flame temperature. If all these ash droplets reach the wall before they re-solidify,

severe slagging can occur. In this work, the slagging tendency in the first-stage boiler (i.e., the boiler that has the highest flame temperature) of a utility-scale SPOC process is examined. Two critical parameters in determining the slagging tendency are investigated: maximum particle deposition rate (i.e., the deposition rate when all particles hitting the wall become deposits) and particle deposition temperature (i.e., the temperature of a particle when it hits the wall). The former parameter determines how many particles can reach the wall, while the latter determines whether the particles are molten and sticky when they hit the wall.

The total ash deposition rate and deposition temperature for each particle along the length of the SPOC boiler is shown in Figure 5-9. Note that, in the present work, all particles hitting the wall are assumed to become deposits. Therefore, the ash deposition rate in Figure 5-9(a) is also equivalent to the ash particle impact rate. The dashed line in Figure 5-9(a) represents the average ash particle impact rate on the vertical walls of a conventional coal-fired boiler predicted by a CFD model [85]. The ash impact rate in the SPOC boiler is one order of magnitude lower than that in a conventional coal-fired boiler. This lower ash impact rate is expected because there is no inertial impaction in the SPOC boiler. Also, Figure 5-9b shows that the deposition temperatures of all ash particles are lower than 1260 K, which is much lower than the fusion temperature of most coal ash. Therefore, slagging is unlikely to occur in the SPOC boiler.

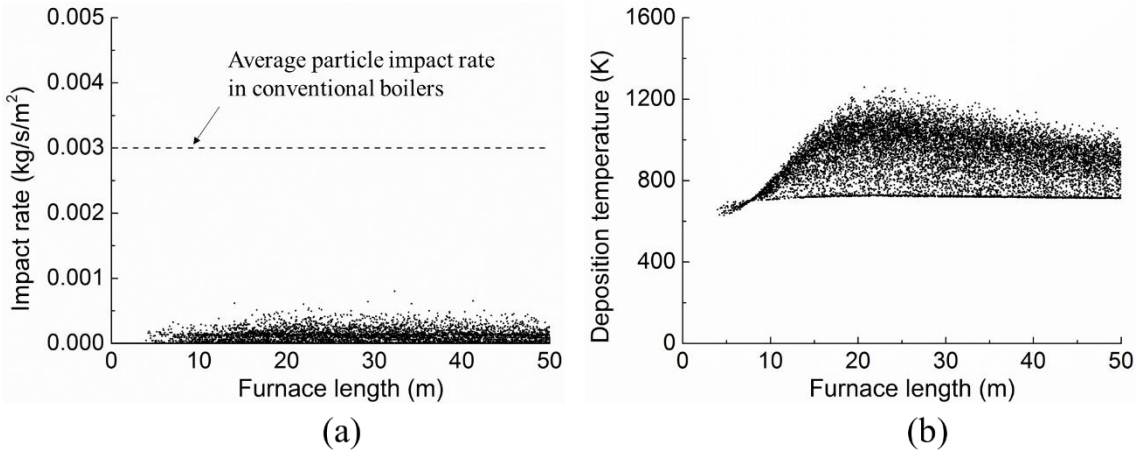


**Figure 5-9. (a) Ash deposition rate along the length of the SPOC boiler. The dashed line represents the average particle deposition rate on the vertical walls of a conventional coal-fired boiler predicted a CFD model [85]. (b) Predicted deposition temperatures of all ash particles in the SPOC boiler.**

## 5.7. Conclusions

A new and flexible, staged, pressurized oxy-combustion (SPOC) boiler design is presented for carbon capture with low flue-gas recycle. The burner and boiler design is based on the goal of ensuring a relatively smooth and high wall heat flux profile over the length of the boiler, with a manageable level of peak heat flux. Inner oxygen injection is utilized to supply most of the required oxygen, thus minimizing flue gas recycle, while still maintaining a low oxygen concentration next to the boiler tubes, with the use of a surrounding oxidizer outside of the fuel annulus. With the fuel being supplied in the annulus, a significant portion of the radiation from the inner-oxygen flame is trapped, thus effectively limiting wall radiation even though the inner-oxygen flame is at a very high temperature. The surrounding oxidizer serves to keep the flame away from the wall. It also serves an additional purpose of providing a cold buffer gas layer next to the wall as a means to control wall heat flux. Furthermore, flexible operation is possible by the ability to control the amount and concentration of oxygen supplied to each stage in this multi-stage process. Lastly, modeling of ash deposition has indicated that the deposition rate in the SPOC boiler is predicted to be far below that of conventional pulverized coal boilers, and that the potential for slagging is minimal since particles are sufficiently cooled prior to contact with the wall.

# Chapter 6. Development of 100kWth POC Test Facility and Test Results

## 6.1. Introduction to the 100 kWth POC test facility

A 100 $kW_{th}$ pressurized oxy-combustion facility was designed and constructed to demonstrate the SPOC boiler design concepts discussed above, and to study the fundamental characteristics of coal combustion under SPOC conditions. The 1800 $ft^2$ research facility, located at Washington University in St. Louis, was designed to study pressurized oxy-combustion for a wide range of fuels and at pressures up to 20 bar. The facility can accommodate a variety of gas inlet conditions and can simulate the different stages of the SPOC process.

Figure 6-1 shows a schematic of the research facility, and a photograph of the reactor section. The facility includes bulk liquid storage and gas delivery systems for $O_2$ and $CO_2$ for pressurized oxy-combustion research. The coal feeder pressure vessel is suspended above the reactor vessel, and the coal is fed from a hopper using a gravimetric twin screw feeder to allow for gravity feeding of coal to the burner. Coal is then transferred to the burner inlet via a horizontal vibrating linear feeder to maintain a uniform feed rate. A high-voltage spark ignition system is used for ignition at pressures up to 8.5 bar.

An industry-standard Allen Bradley safety and control system with Rockwell Automation software is used for automated operation of the facility. Automated flow control valves, pressure control valves and quench water feeding allow for easy control of various operating parameters, including inlet concentration, stoichiometric ratios, inlet gas flowing rates, coal feeding rates and pressures to allow for a systematic study of a range of parameters. In addition, a Labview-based system is used for high-resolution experimental data acquisition and storage.

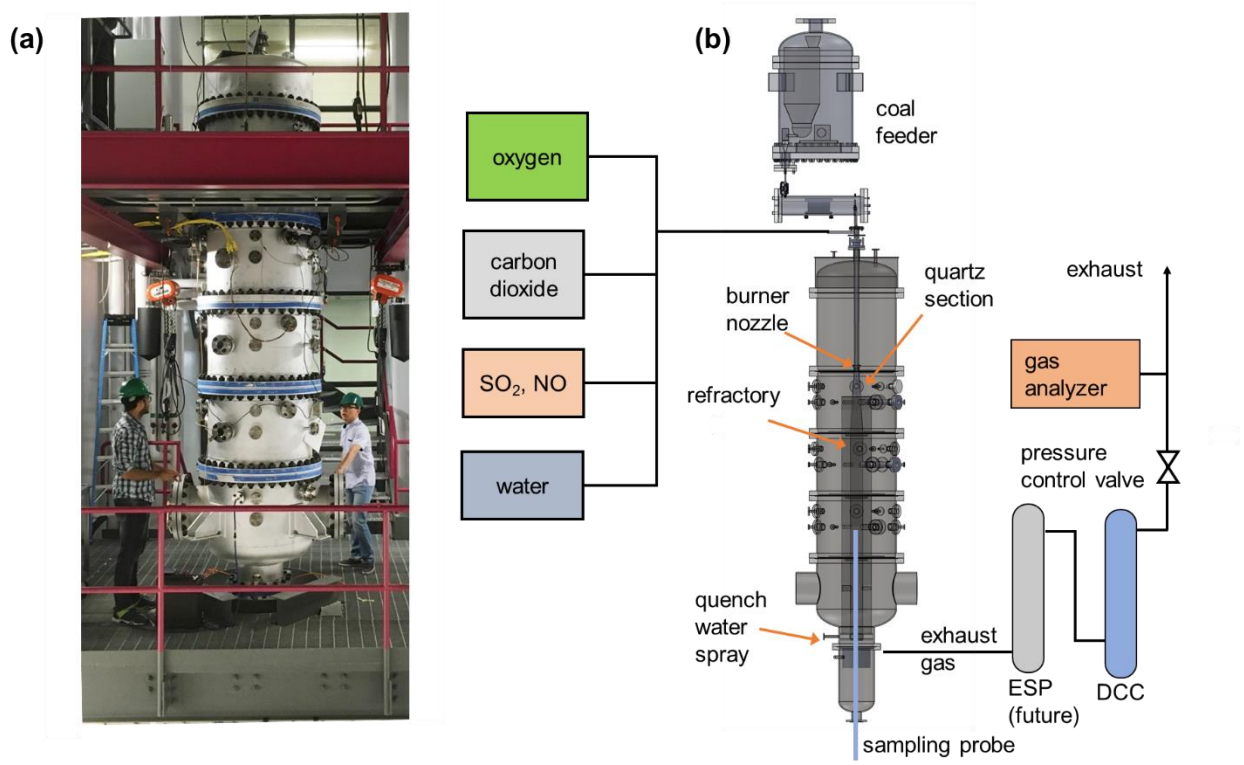


**Figure 6-1 The 100 kWth pressurized facility: (a) photograph and (b) schematic.**

Figure 6-2 shows an inside view of the top reactor section of the facility. Features include:

- A conical-shaped quartz reactor tube to allow for visual access to the flame and for optical diagnostics. The reactor tube has ignition and sampling ports as shown
- Six air-cooled HD webcams installed inside the pressurized chamber to observe the flame from multiple angles and provide a complete view of the quartz reactor section, covering the majority of the flame.
- Several optical ports on the pressure vessel's side wall, which are used for high-speed flame videography. Through high-speed videography detailed information on the flame structure can be readily observed, including the flow field, particle motion, and particle transformation (i.e. particle ignition, volatile release and combustion, and char combustion).
- Type K thermocouples installed along the length of the reactor to remotely monitor the temperature distribution along the reactor wall.
- A laser diagnostic system, including an RGB three-color laser and fiber optic system, to provide information on particle volume fraction. The fiber-optic system is mounted on a multi-axis translation stage which allows for two-dimensional scanning of the flame through the quartz tube.

- Two Medtherm Schmidt-Boelter heat flux sensors (model 64-30SB-18/SW-1C-150 and 64-100SB-18/SW-1C-150) which can measure up to 300 and 1000 kW/m$^2$, respectively and can be positioned in different segments of the combustor.

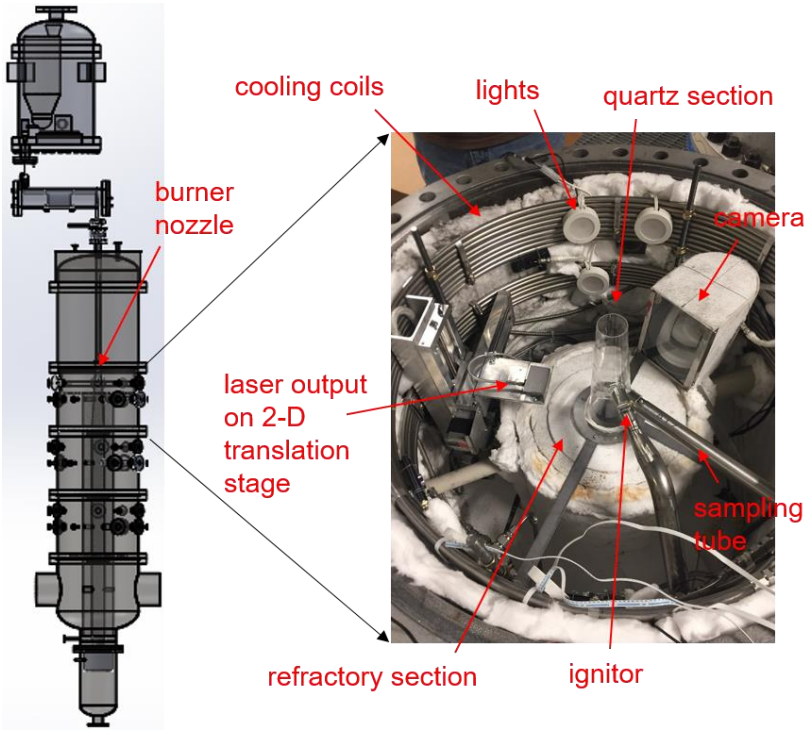


**Figure 6-2 Photograph of SPOC reactor section, featuring quartz section and diagnostics for flame visualization**

Two types of pressurized sampling probes are used for sampling particles and gases: a water-cooled sampling probe inserted through the base of the pressure vessel, and a two-stage dilution sampling probe inserted into the reactor through the side ports of the pressure vessel. The two probes can be used to sample gas and particles from different axial and radial locations, providing a full map of gas composition and particle size and compostion distribution inside the reactor.

A pulverized coal conveying system for charging the coal feeder hopper was installed. Designed and constructed by Flexicon Corp the equipment includes a bulk bag discharge system and a flexible auger-type conveying system which transports pulverized coal directly from the bottom floor storage to the pressurized coal feeder vessel. The system provides for dust-free transfer of coal from the bulk storage bags to the feed vessel and allows quick charging of the feed vessel between expeririments.

A concise summary of the diagnosing capabilities is given in Table 6-1.

**Table 6-1. Measurements and the devices used in the SPOC facility.**

| Measurement | Device |
|---|---|
| Wall heat flux (both convective and radiative at port locations) | Medtherm Schmidt-Boelter heat flux sensor |
| Flue gas composition | Flue gas sampler, HORIBA Multi-gas analyzer |
| Centerline profiles of gas composition (i.e., $CO_2$, $O_2$, CO, $H_2O$, NOx, $SO_2$) | Pressurized gas & particle sampler, HORIBA Multi-gas analyzer |
| Centerline particle size distribution | Pressurized gas & particle sampler, DEKATI Electrical Low-Pressure Impactor (ELPI) |
| Centerline temperature | Thermocouple |
| Visual observation of flames | HS camera and HD webcam |
| Flue gas CO and soot concentration | Flue gas sampler, Horiba Multi-gas analyzer, Optical Particle Sizer (OPS) |
| Ash carbon concentration | Flue gas sampler, Cyclone, Thermogravimetric Analyzer |

## 6.2. Experimental campaign and results

The 100 KW pressurized test facility was operated for over 200 hours to improve system reliability, and evaluate burner design and performance over a wide range of operating conditions. The initial experiments in the pressurized facility utilized a burner design in which coal and a small amount of carrier gas ($CO_2$) are fed to the combustor via a central tube and the oxygen is fed through a sheath tube in a $O_2/CO_2$ mix (Burner 1 in Figure 6-3). A summary of experimentation during the first campaign is listed in Table 6-2.

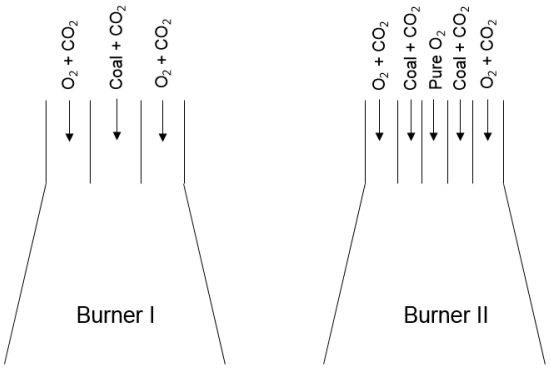


**Figure 6-3 Two types of burner configurations considered to-date**

**Table 6-2. Experimentation campaign with Burner I**

| Objective | Conditions | Conclusions |
|---|---|---|
| Ignition Study | • Fuel: mixture of $CH_4$ and $CO_2$<br>• Oxidizer: Air<br>• $CH_4$ concentration in fuel: 50~100%<br>• Thermal input 1~3 $kW_{th}$<br>• S.R. 0.5~2.0<br>• Pressure 1~3 bara | • Robust approach to ignition identified<br>• Repeatable ignition achieved<br>• By adding $CO_2$ dilution in the fuel, ignition with a non-sooting blue flame can be achieved<br>• Stable flame achieved with a co-axial flow burner configuration |
| Gaseous flame Study | • Fuel: mixture of $CH_4$ and $CO_2$<br>• Oxidizer: Air<br>• $CH_4$ concentration in fuel: 50~100%<br>• Thermal input: 3~30 $kW_{th}$<br>• S.R. 1.1~3.0<br>• Pressure: 1~4 bara | • When pressure and thermal input are increase proportionally, the flame size remains similar but turbulent intensity increases<br>• As S.R. increases, the flame length first increases, then decreases. The flame is the longest when the oxidizer flow velocity is similar to the fuel flow velocity<br>• The flame shape and size were in qualitative agreement with CFD predictions, see Figure 6-5<br>• No flame impingement on the reactor walls was observed.<br>• Increased pressure resulted in increased soot formation.<br>• At low stoichiometric ratio and elevated pressure, a “smoking” flame was produced, in which soot particles were emitted from the flame |
| Coal Study | • Fuel: Pulverized Coal and $CH_4$<br>• Oxidizer: Air<br>• Thermal input: 3~30 $kW_{th}$<br>• Fraction of coal thermal input in the total thermal input: 0%~85%<br>• S.R. 1.1~3.0<br>• Pressure: 1~4 bara | • No particle deposition on the quartz walls<br>• No slagging or ash deposition on reactor walls after ~30 hrs of coal tests<br>• Flame becomes unstable when the thermal input of coal is more than 85% of the total thermal input |

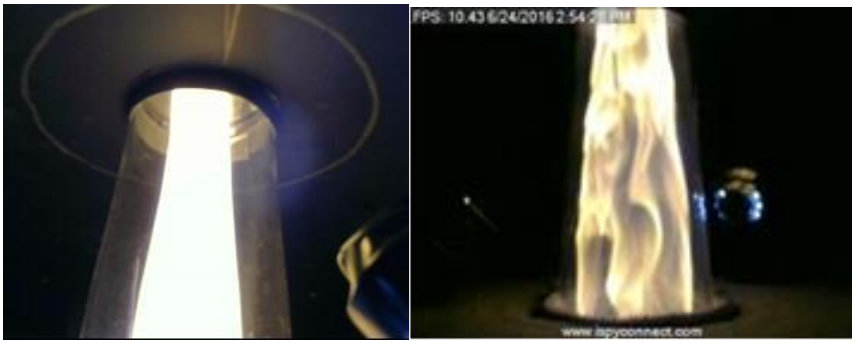

**(a)** **(b)**

**Figure 6-4. Photographs from initial firing tests in the 100kW POC facility.(a) laminar and (b) turbulent methane/air flames. The quartz reactor wall can be easily observed in (a).**

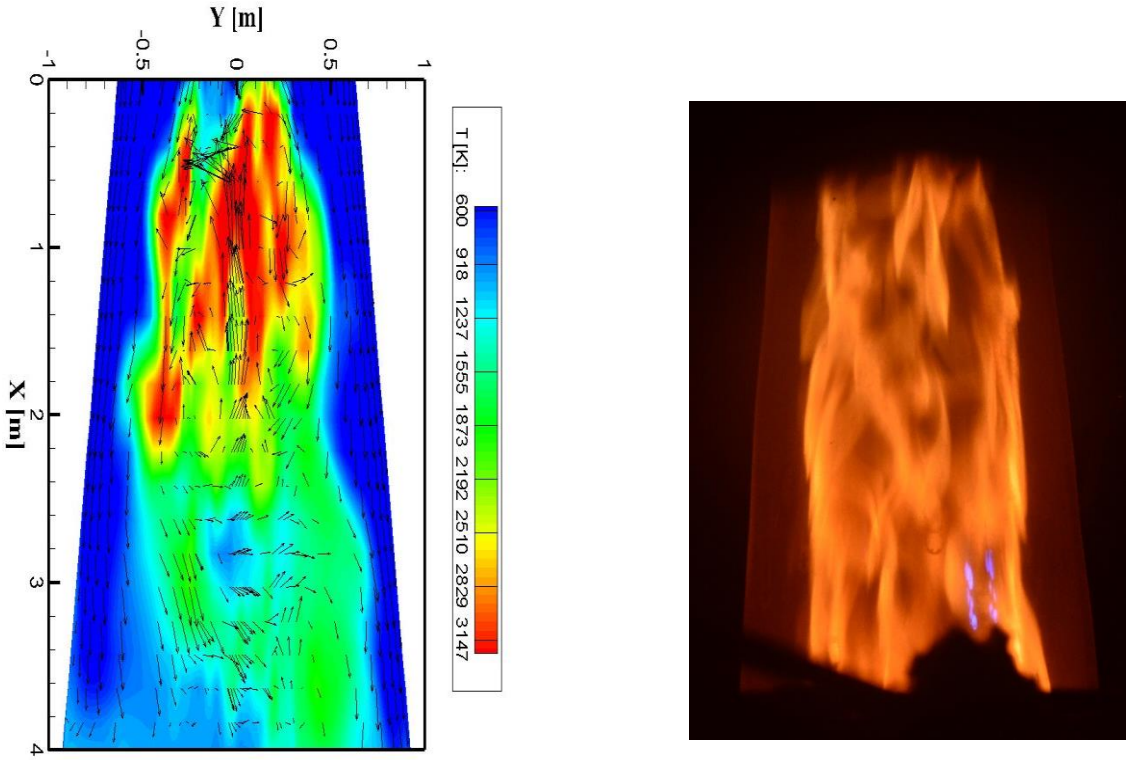


**(a)** **(b)**

**Figure 6-5. Comparison of (a) LES and (b) experimentally-observed pressurized methane-air flames.**

This results from the first campaign with Burner I indicate that the experimental facility is capable of yielding stable combustion under pressure and that the conical chamber configuration, described in Section 5.3, is effective at minimizing the effects of buoyancy, leading to an inverted flame configuration without wall impingement (Figure 6-4 and Figure 6-5). Furthermore, no

particle deposition was observed on the walls of the quartz chamber after 30 hours of operation with coal, again reinforcing that the combustor design is operating as intended. A comparison of the basic flame structure from LES measurements (Figure 6-5a) and experiment (Figure 6-5b) shows consistent results and the effectiveness of the design [86].

After the first set of experiments, a new burner nozzle (Burner II in Figure 6-3) was designed and installed to improve flame stability, allow for high overall oxygen concentration and reduce soot formation. The new burner design is based on the concepts described in Chapter 5. The burner operates in a non-premixed combustion mode and incorporates three reactant streams (fuel plus two separate oxidizer streams) to provide enhanced operating flexibility, in contrast to the previous burner which only included two streams (fuel and oxidizer).

A summary of the experimental campaign performed with Burner II is listed in Table 6-3 with reference to Figure 6-6 and Figure 6-8. Important results from this campaign are that the new burner has successfully improved flame stabilization and reduced soot formation. The burner can operate stably with only coal (Figure 6-8a) and has been operated at up to 80 $kW_{th}$. The operating conditions tested have been conducted at high SR (SR=2, Stage 1) as well as low SR (SR=1.1, Stage 3). Under all conditions the flames are stable, particle deposition is negligible and the CO ratio in the flue gas was undetectable. While additional tests are needed, the conclusions of this campaign are that the experimental findings support the CFD results and indicate that the SPOC process holds promise as a low cost, high efficiency process for generating electricity from coal with carbon capture.

**Table 6-3. Experimentation campaign with Burner II.**

| Objective | Conditions | Conclusions |
|---|---|---|
| Ignition Study | • Fuel: mixture of $CH_4$ and $CO_2$<br>• Oxidizer: Air<br>• $CH_4$ concentration in fuel: 50~100%<br>• Thermal input 1~3 $kW_{th}$<br>• S.R. 0.5~2.0<br>• Pressure 1~3 bara | • Approach to robust ignition identified<br>• After ignition, soot formation can be significantly reduced by adding oxygen in the central tube |
| Gas flame study | • Fuel: mixture of $CH_4$ and $CO_2$<br>• Surrounding oxidizer: $O_2$ and $N_2$<br>• Central oxidizer: $O_2$<br>• $CH_4$ concentration in fuel: 50~100%<br>• Thermal input: 3~30 $kW_{th}$<br>• S.R. 1.1~2.5<br>• C.S.R. 0~0.7<br>• Pressure: 1~4 bara | • The injection of oxygen in the central tube improves soot burnout, as indicated by the absence of scattered green light in the post-flame region (Figure 6-5)<br>• Increase in the oxygen flow rate results in a shorter flame with no soot emissions. |
| Coal Experiments | • Fuel: Pulverized Coal and $CH_4$<br>• Surrounding oxidizer: $O_2$ and $N_2$<br>• Central oxidizer: $O_2$<br>• Thermal input: 3~30 $kW_{th}$<br>• Fraction of coal thermal input in the total thermal input: 0%~100%<br>• S.R. 1.1~2.5<br>• C.S.R. 0~0.7<br>• Pressure: 1~4 bara | • The flame size can be maintained by increasing thermal input proportionally with operating pressure.<br>• Steady operating conditions were found at all pressures.<br>• At all conditions, the flame stays at the center of the reactor (Figure 6-6), and no flame impingement or ash deposition were observed<br>• In Figure 6-7, stable 20 kW-coal flames at 3 bar without methane pilot were obtained, which shows the robustness of SPOC burners. The central oxygen flow helps stabilize the flame in a co-flow burner configuration<br>• 80 $kW_{th}$ coal flame was tested for more than 30 min. No flame impingement or ash deposition were observed (See Figure 6-8). |

| | | |
|---|---|---|
| | | • With the central oxygen flow, zero CO concentration in the exhaust gas was achieved when S.R. is as low as 1.1. |

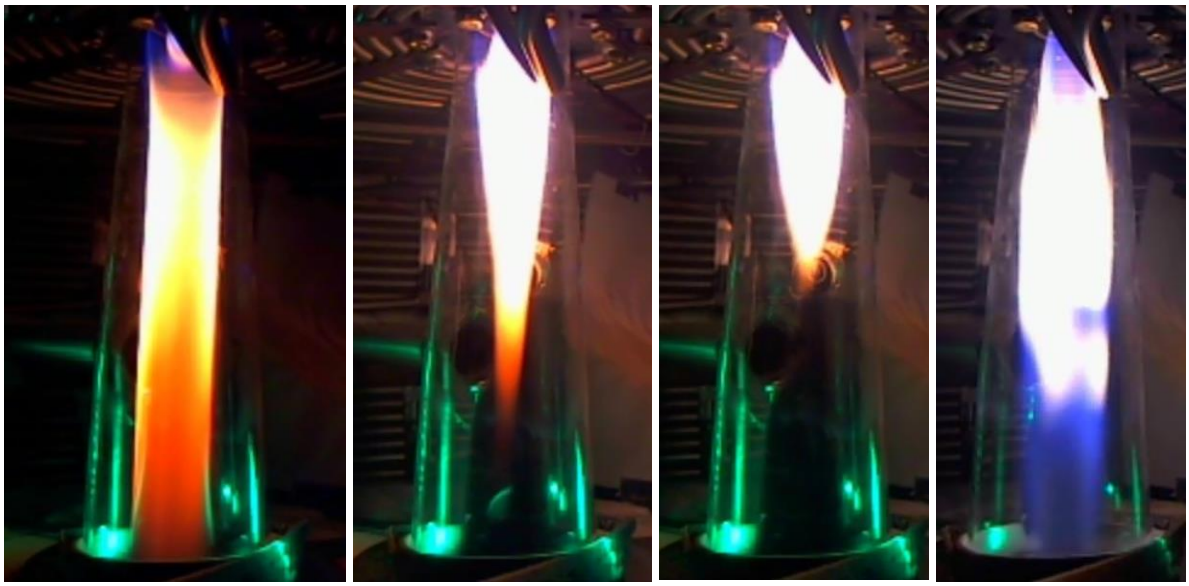

(a) (b) (c) (d)

**Figure 6-6. Photographs of methane combustion in SPOC test facility. (a) Methane-air combustion at ignition conditions. (b) Flame after starting flow of oxygen. (c) Flame after further increase in oxygen flow, reaching conditions similar to Stage 1 of the SPOC process (d) Flame after increasing thermal input to final condition.**

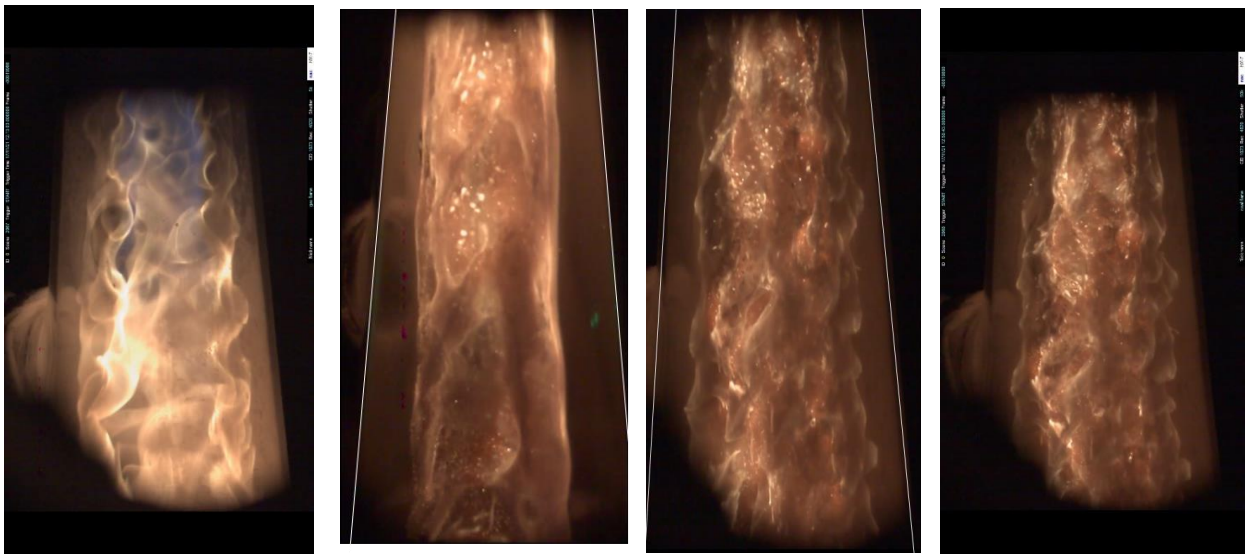

(a) (b) (c) (d)

**Figure 6-7. Photographs of coal-methane combustion taken from high-speed camera. (a) 20 kWth methane, S.R.= 2, 3 bar; (b) 5 kWth methane- 2 kWth coal at atmospheric pressure; (c) 20 kWth methane - 2 kWth coal at 3 bar and (d) 20 kWth coal-2 kWth methane, SR 2, 3 bar**

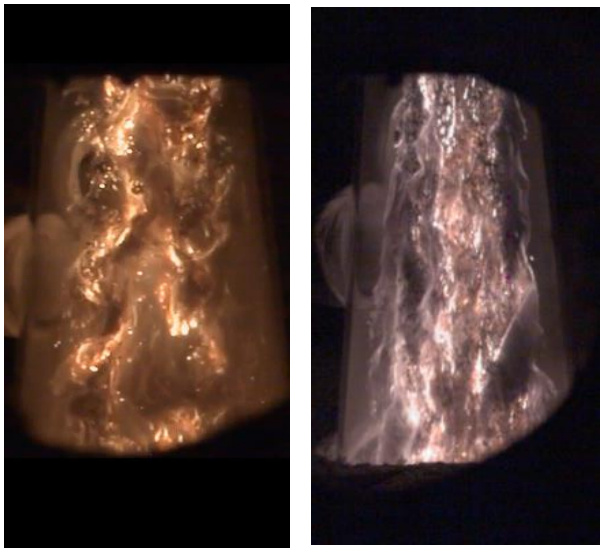

**(a)** **(b)**

**Figure 6-8. Photographs taken from high-speed camera. (a) 20 kWth coal without methane pilot, S.R.= 2, 3 bar; (b) 80 kWth coal-6 kWth methane, S.R.= 2, 3 bar**

## Chapter 7. Final Conclusions and Recommendations

The future of coal as a source of stable, reliable energy is being questioned as international demand to reduce emissions grows and other forms of lower-emitting generation continue to become more competitive. Existing, first-generation technologies for carbon capture and storage (CCS) are expensive and energy intensive. To ensure that coal can supply clean, low-cost, stable, and reliable energy for the future energy mix, second-generation CCS technologies that can reduce all emissions to near-zero values with lower cost and energy penalty are needed. The Staged, Pressurized Oxy-Combustion (SPOC) technology, developed at WUSTL, is an ideal candidate technology for this purpose, showing significant gains in overall efficiency and economic performance over today's state-of-the art technology.

This project and subsequent SPOC projects have successfully advanced the SPOC process towards commercial-scale demonstration. The current TRL of SPOC has been evaluated as TRL-5 by EPRI, which has significant experience in assessing and tracking technology TRLs across the power industry in an unbiased manner. A summary of the TRL progression is provided below in Table 7-1. Major accomplishments to date under this award include: 1) optimization of the SPOC plant configuration and parametric study of factors affecting plant efficiency via process modeling, 2) improved design of SPOC burner and combustor via CFD modelling, 3) detailed study of ash deposition and radiant heat transfer in SPOC boilers, 4) construction and operation of a small-pilot SPOC test facility to validate burner design performance, 5) Potential for corrosion of boiler materials under SPOC conditions has been experimentally evaluated, and recommendations for suitable materials have been made.

**Table 7-1. TRL Assessment for the SPOC Process.**

| TRL | Description | Summary of Work Done | Comments |
|---|---|---|---|
| **1** | Basic principles observed and reported | An idea to utilize fuel staging as a means to reduce FGR and apply this approach to pressurized oxy-combustion was conceived in 2012 and proposed to DOE. A techno-economic assessment was completed in 2013, which demonstrated potential to meet DOE cost and performance targets. | Process modeling [48, 87-89] demonstrated that SPOC leads to superior efficiency due to reduced FGR and greater utilization of radiation heat transfer. |
| **2** | Technology concept and/or application formulated | A conceptual design of a boiler for SPOC was developed during Phase I of a DOE project. This design yielded approximate vessel size, burner arrangement, and boiler tube surface arrangement for a 550-MWe plant. A patent for the SPOC boiler was published in 2014 [90]. | The boiler concept design has, to date, not yet been evaluated and/or validated (focus of ongoing project). |
| **3** | Analytical and experimental critical function and/or characteristic proof-of-concept validated | The full-scale boiler has been simulated using modeling tools [55]. Atmospheric pressure combustion tests were performed at a scale of 300 $kW_{th}$ with oxygen enrichment up to 50%. Results showed that post-flame temperature can be controlled under conditions of high oxygen concentration by using fuel staging This understanding provided valuable guidance for the design of SPOC boilers. | Drastically reduced FGR can only be achieved when the combustor is pressurized, which allows for the “radiative trapping” phenomenon to occur [68]. |
| **4** | Basic technology components integrated and validated in a laboratory environment | A lab-scale, 1-atm (~30 kW) prototype was constructed with the same geometry as the simulated full-scale boiler. Combustion testing using coal was done to demonstrate that desired flame shape and fluid flow could be obtained. The results confirmed the design, which was incorporated into the pressurized test facility. | The 1-atm system was safely and repeatedly operated under conditions of coal combustion in 100% oxygen. |
| **5** | Basic technology components integrated and validated in a relevant environment | A pressurized test facility (100 $kW_{th}$, 20 bar) has been constructed and achieved stable combustion at a pressure of 5 bar. Data regarding burner flexibility, heat flux, gas composition, and ash properties will be collected and used to validate models. | Other work relating to capture of particulates and $SO_X/NO_X$ is concurrently ongoing. |

To successfully design future larger-scale SPOC boilers, additional experimental data is needed to validate CFD sub-models, which have not been before applied to conditions of elevated pressure or high oxygen concentration. These include models of gas and particle radiation, coal combustion and gasification, and ash formation and fragmentation. Experiments in the 100 kW small-pilot facility are continuing in order to collect this key data.

The co-capture of $SO_X$ and $NO_X$ and flue gas latent heat in a direct-contact cooler is being addressed in a separate project sponsored by the DOE (DE-FE0025193). Determination of the optimal operating parameters and capture efficiencies will further enhance the commercial readiness of SPOC. Under DOE's joint US-China Clean Energy Research Center (DE-PI0000017), the SPOC technology is being readied for up to 250-$kW_{th}$ scale through modifications to the existing test facility. A new project was recently initiated with EPRI (DE-FE0029087), which aims to further advance the technology by seeking input from an OEM boiler manufacturer (Doosan Babock) and will result in further definition of the SPOC boiler design with considerations made for steam cycle integration, boiler tube surface arrangement, and operational flexibility. Combined, these projects have advanced the SPOC process and readied it for a large-scale pilot. The next step would be to achieve TRL-6 with construction of a 1-10MW prototype pilot plant, and drive towards TRL-7. This will require any remaining technical uncertainties to be addressed – none of which appear to be insurmountable – and significant investment from government and private industrial partners. At the current rate of progress, the commercial readiness of the technology would be validated (TRL-8) in the 2028–2035 timeframe.

## GRAPHICAL MATERIALS LIST

## TABLES

## REFERENCES


1. Axelbaum, R., F. Xia, A. Gopan and B. Kumfer, *Staged, High-Pressure Oxy-Combustion Technology: Development and Scale-Up, Phase I Topical Report*. 2014.
2. Gopan, A., B.M. Kumfer and R.L. Axelbaum, *Effect of Operating Pressure and Fuel Moisture on Net Plant Efficiency of a Staged, Pressurized Oxy-Combustion Power Plant.* International Journal of Greenhouse Gas Control, 2015.
3. Gopan, A., B.M. Kumfer, J. Phillips, D. Thimsen, R. Smith and R.L. Axelbaum, *Process design and performance analysis of a Staged, Pressurized Oxy-Combustion (SPOC) power plant for carbon capture.* Applied Energy, 2014. **125**(0): p. 179-188.
4. *Cost and Performance for Low-Rank Pulverized Coal Oxycombustion Energy Plants; Report DOE/NETL - 401/093010.* 2010, U.S. Department of Energy National Energy Technology Laboratory.
5. Deng, S.M. and R. Hynes, *Thermodynamic Analysis and Comparison on Oxy-Fuel Power Generation Process.* Journal of Engineering for Gas Turbines and Power-Transactions of the Asme, 2009. **131**(5).
6. Hong, J., R. Field, M. Gazzino and A. Ghoniem. *Performance of the pressurized oxy-fuel combustion power cycle with increasing operating pressures* in *The 34th International Technical Conference on Clean Coal & Fuel Systems*. 2009. Clearwater, FL.
7. Hong, J.S., G. Chaudhry, J.G. Brisson, R. Field, M. Gazzino and A.F. Ghoniem, *Analysis of oxy-fuel combustion power cycle utilizing a pressurized coal combustor.* Energy, 2009. **34**(9): p. 1332-1340.
8. Gazzino, M. and G. Benelli. *Pressurised Oxy-Coal Combustion Rankine-Cycle for Future Zero Emission Power Plants: Process Design and Energy Analysis*. in *ASME Conference Proceedings*. 2008.
9. Benelli, G., G. Girardi, M. Malavasi and A. Saponaro. *ISOTHERM®: a new oxy-combustion process to match the zero emission challenge in power generation*. in *The 7 th High Temperature Air Combustion and Gasification International Symposium, Phuket, Thailand*. 2008.
10. Hagi, H., M. Nemer, Y.L. Moullec and C. Bouallou. *Towards Second Generation Oxy-Pulverized Coal Power Plants: Energy Penalty Reduction Potential of Pressurized Oxy-Combustion Systems*. in *International Conference on Greenhouse Gas Technologies (GHGT)*. 2014. Austin, TX: Energy Procedia.
11. Kobayashi, S. and L.E. Bool, *Direct oxy-coal combustion with minimum or no flue gas recycle*, in *Oxy-fuel combustion for power generation and carbon dioxide capture*, L. Zheng, Editor. 2011, Woodhead Publishing.
12. Goanta, A., V. Becher, J.-P. Bohn, S. Gleis and H. Spliethoff. *Controlled Staging with Non-Stoichiometric Burners for Oxy-fuel Processes - Numerical Validation*. in *33rd International Technical Conference on Coal Utilization & Fuel Systems*. 2008.
13. Becher, V., J.P. Bohn, A. Goanta and H. Spliethoff, *A combustion concept for oxyfuel processes with low recirculation rate - Experimental validation.* Combustion and Flame, 2011. **158**(8): p. 1542-1552.
14. Bohn, J.P., M. Blume, A. Goanta and H. Spliethoff, *Flame temperatures and species concentrations in non-stoichiometric oxycoal flames.* Fuel, 2011. **90**(10): p. 3109-3117.
15. Morehead, H., *Siemens Global Gasification Update*, in *Designing & Operating US Substiutue Natural Gas Plants*. 2008: Houston, TX.
16. Maroto-Valer, M.M., ed. *Developments and innovation in carbon dioxide ($CO_2$) capture and storage technology*. Vol. Volume 1: Carbon dioxide ($CO_2$) capture, transport and industrial applications. 2010, Woodhead Publishing Limited.

17. Sprouse, K.M. and D.R. Matthews, *Topical Report, Linear Extrusion 400 Tons/Day Dry Solids Pump*. 2008.
18. Aldred, D.L., *Final Report, Proof of principal test to feed and meter granular coal into 450 psig gas pressure*. 2000.
19. *Quality Guidelines for Energy System Studies: Specifications for Selected Feedstocks; Report DOE/NETL - 341/081911.* 2012, U.S. Department of Energy National Energy Technology Laboratory.
20. *Quality Guidelines for Energy System Studies: $CO_2$ Impurity Design Parameters; Report DOE/NETL - 341/081911.* 2012, U.S. Department of Energy National Energy Technology Laboratory.
21. *Quality Guidelines for Energy System Studies: Process Modeling Design Parameters; Report DOE/NETL - 341/042613.* 2013, U.S. Department of Energy National Energy Technology Laboratory.
22. *Quality Guidelines for Energy System Studies: Process Modeling Design Parameters, rev. 2; Report DOE/NETL - 341/081911.* 2012, U.S. Department of Energy National Energy Technology Lab.
23. *U.S. Department of Energy National Energy Technology Laboratory, (U.S. DOE NETL). Current and Future Technologies for Power Generation with Post-Combustion Carbon Capture*. 2012.
24. White, V., A. Wright, S. Tappe and J. Yan, *The Air Products Vattenfall Oxyfuel CO2 Compression and Purification Pilot Plant at Schwarze Pumpe.* Energy Procedia, 2013. **37**: p. 1490-1499.
25. White, V., L. Torrente-Murciano, D. Sturgeon and D. Chadwick, *Purification of oxyfuel-derived CO2.* International Journal of Greenhouse Gas Control, 2010. **4**(2): p. 137-142.
26. Bell, D.A., B.F. Towler and M. Fan, *Coal gasification and its applications*. 2010: William Andrew.
27. Xiong, J., H. Zhao, M. Chen and C. Zheng, *Simulation Study of an 800 MWe Oxy-combustion Pulverized-Coal-Fired Power Plant.* Energy & Fuels, 2011. **25**(5): p. 2405-2415.
28. Verhoff, F. and J. Banchero, *Predicting dew points of flue gases.* Chem. Eng. Prog, 1974. **70**(8): p. 71-72.
29. Okkes, A.G., *Get acid dew point of flue gas.* Journal Name: Hydrocarbon Process.; (United States); Journal Volume: 66:7, 1987: p. Medium: X; Size: Pages: 53-56.
30. Zheng, L., R. Pomalis and B. Clements. *Technical Feasibility Study of TIPS Process and Comparison with other CO2 Capture Power Generation Processes*. in *The 32nd International Technical Conference on Coal Utilization and Fuel Systems*. 2007. Clearwater, FL.
31. Ellison, T.K. and C.A. Eckert, *The oxidation of aqueous sulfur dioxide. 4. The influence of nitrogen dioxide at low pH.* J. Phys. Chem., 1984. **88**(11): p. 2335-9.
32. White, V., R. Allam and E. Miller. *Purification of Oxyfuel-Derived CO2 for Sequestration or EOR*. in *Technical paper, 8th International Conference on Greenhouse Gas Control Technologies*. 2006. Trondheim, Norway.
33. Iloeje, C., R. Field, M. Gazzino and A. Ghoniem. *Process modeling and analysis of CO2 purification for oxy-coal combustion*. in *The 35th International Technical Conference on Clean Coal & Fuel Systems*. 2010. Clearwater, FL.
34. Liémans, I., B. Alban, J.-P. Tranier and D. Thomas, *SOx and NOx absorption based removal into acidic conditions for the flue gas treatment in oxy-fuel combustion.* Energy Procedia, 2011. **4**(0): p. 2847-2854.
35. Normann, F., E. Jansson, T. Petersson and K. Andersson, *Nitrogen and sulphur chemistry in pressurised flue gas systems: A comparison of modelling and experiments.* International Journal of Greenhouse Gas Control, 2013. **12**: p. 26-34.

36. Pétrissans, S.M., A. Pétrissans and A. Zoulalian, *Experimental study and modelling of mass transfer during simultaneous absorption of SO2 and NO2 with chemical reaction.* Chemical Engineering and Processing: Process Intensification, 2005. **44**(10): p. 1075-1081.
37. Lee, S., J.G. Speight and S.K. Loyalka, *Handbook of alternative fuel technologies*. 2007: crc Press.
38. Salvador, C. *Modeling, design, and pilot-scale experiments of CANMET's advanced oxy-fuel/steam burner*. in *2nd Workshop of the IEA GHG International Oxy-Combustion Research Network*. 2007. Wndsor, CT.
39. Zebian, H., N. Rossi, M. Gazzino, D. Cumbo and A. Mitsos, *Optimal design and operation of pressurized oxy-coal combustion with a direct contact separation column.* Energy, 2012.
40. Shah, M.M., *Carbon dioxide compression and purification technology*, in *Oxy-fuel combustion for power generation and carbon dioxide (CO2) capture*, L. Zheng, Editor. 2011, Woodhead Publishing, Limited.
41. Zebian, H., M. Gazzino and A. Mitsos, *Multi-variable optimization of pressurized oxy-coal combustion.* Energy, 2012. **38**(1): p. 37-57.
42. *Engineering and Economic Evaluation of 1300°F (700°C) Series Oxy-PC Power Plant: Interim Report #1023870*. 2012, EPRI: Palo Alto, CA.
43. Gao, X., Y. Li, M. Garcia-Perez and H. Wu, *Roles of Inherent Fine Included Mineral Particles in the Emission of PM10 during Pulverized Coal Combustion.* Energy & Fuels, 2012. **26**(11): p. 6783-6791.
44. Karabulut, H. and Ö.E. Ataer, *Numerical solution of boundary layer equations in compressible cross-flow to a cylinder.* International journal of heat and mass transfer, 1998. **41**(17): p. 2677-2685.
45. *Current and Future Technologies for Power Generation with Post-Combustion Carbon Capture; Report DOE/NETL - 2012/1557.* 2012, U.S. Department of Energy National Energy Technology Laboratory.
46. de Visser, E., C. Hendriks, M. Barrio, M.J. Mølnvik, G. de Koeijer, S. Liljemark and Y. Le Gallo, *Dynamis CO2 quality recommendations.* International Journal of Greenhouse Gas Control, 2008. **2**(4): p. 478-484.
47. *Pulverized Coal Oxycombustion Power Plants. Vol. 1: Bituminous Coal to Electricity, rev. 2; Report DOE/NETL-2007/1291.* 2008, U.S. Department of Energy National Energy Technology Laboratory.
48. Hagi, H., M. Nemer, Y. Le Moullec and C. Bouallou, *Optimal Integration of the Flue Gas Heat for the Minimization of the Energy Penalty of Oxy-fired Power Plants.* Energy Procedia, 2014. **63**: p. 7359-7366.
49. Hagi, H., T. Neveux and Y. Le Moullec, *Efficiency evaluation procedure of coal-fired power plants with CO2 capture, cogeneration and hybridization.* Energy, 2015. **91**: p. 306-323.
50. *Updated Costs (June 2011 Basis) for Selected Bituminous Baseline Cases; Report DOE/NETL - 341/082312.* 2012, U.S. Department of Energy National Energy Technology Laboratory.
51. *Quality Guidelines for Energy System Studies: Capital Cost Scaling Methodology; Report DOE/NETL - 341/013113.* 2013, U.S. Department of Energy National Energy Technology Laboratory.
52. *Improving the Efficiency of Coal-Fired Power Plants for Near Term Greenhouse Gas Emissions Reductions; Report DOE/NETL - 2010/1411.* 2010, U.S. Department of Energy National Energy Technology Laboratory.
53. Zheng, L., R. Pomalis, B. Clements and T. Herage. *Optimization of a high pressure oxy-fuel combustion process for power generation and CO2 capture* in *International*

*Technical Conference on Coal Utilization & Fuel Systems*. 2010. Clearwater, Florida, USA.
54. Hong, J., R. Field, M. Gazzino and A.F. Ghoniem, *Operating Pressure dependence of the pressurized oxy-fuel combustion power cycle.* Energy, 2010. **35**: p. 9.
55. Xia, F., Z. Yang, A. Adeosun, A. Gopan, B.M. Kumfer and R.L. Axelbaum, *Pressurized oxy-combustion with low flue gas recycle: Computational fluid dynamic simulations of radiant boilers.* Fuel, 2016. **181**: p. 1170-1178.
56. Murciano, L.T., V. White, F. Petrocelli and D. Chadwick, *Sour compression process for the removal of SOx and NOx from oxyfuel-derived CO2.* Energy Procedia, 2011. **4**(0): p. 908-916.
57. Ajdari, S., F. Normann, K. Andersson and F. Johnsson, *On the liquid phase chemistry in pressurized flue gas cleaning systems: the effect of process design parameters*, in *The 39th International Technical Conference on Clean Coal & Fuel Systems*. 2014: Clearwater, FL.
58. Yi, F., A. Gopan and R.L. Axelbaum, *Characterization of coal water slurry prepared for PRB coal.* Journal of Fuel Chemistry and Technology, 2014. **42**(10).
59. Wibberley, L., D. Palfreyman and P. Scaife, *Efficient Use of Coal Water Fuels Technology Assessment Report 74*. 2008, CSIRO Energy Technology.
60. Wang, R.K., J.Z. Liu, Y.J. Yu, Y.X. Hu, J.H. Zhou and K.F. Cen, *The Slurrying Properties of Coal Water Slurries Containing Raw Sewage Sludge.* Energy & Fuels, 2011. **25**: p. 747-752.
61. Laskowski, J.S., *Chapter 3 Coal surface properties*, in *Developments in Mineral Processing*. 2001, Elsevier. p. 31-94.
62. Stanger, R., T. Wall, R. Spörl, M. Paneru, S. Grathwohl, M. Weidmann, G. Scheffknecht, D. McDonald, K. Myöhänen, J. Ritvanen, S. Rahiala, T. Hyppänen, J. Mletzko, A. Kather, and S. Santos, *Oxyfuel combustion for CO2 capture in power plants.* International Journal of Greenhouse Gas Control, 2015.
63. Toftegaard, M.B., J. Brix, P.A. Jensen, P. Glarborg and A.D. Jensen, *Oxy-fuel combustion of solid fuels.* Progress in Energy and Combustion Science, 2010. **36**(5): p. 581-625.
64. Nikzat, H., H. Pak, T. Fuse, Y. Hu, K. Ogyu, N. Kobayashi and M. Hasatani, *Characteristics of Pulverized Coal Burner Using a High-Oxygen Partial Pressure.* Chemical Engineering Research and Design, 2004. **82**(1): p. 99-104.
65. Xia, F., B.M. Kumfer, B. Dhungel and R.L. Axelbaum, *Staged, pressurized oxy-combustion: computational fluid dynamics simulations of a novel burner design*, in *Eastern States Section of the Combustion Institute*. 2013: Clemson, SC.
66. Yang, Z., A. Gopan and R.L. Axelbaum. *Predicting ash deposition from non-isothermal, turbulent parallel flows*. in *10th US National Combustion Meeting*. 2017. College Park, Maryland.
67. Mullinger, P. and B. Jenkins, *Industrial and process furnaces : principles, design and operation*. Butterworth-Heinemann/IChemE series. 2008, Amsterdam: Elsevier/Butterworth-Heinemann. 524.
68. Xia, F., Z. Yang, A. Adeosun, B.M. Kumfer and R.L. Axelbaum, *Control of radiative heat transfer in high-temperature environments via radiative trapping—Part I: Theoretical analysis applied to pressurized oxy-combustion.* Fuel, 2016. **172**: p. 81-88.
69. Gopan, A., Z. Yang, A. Adeosun, B.M. Kumfer and R.L. Axelbaum. *Effect of stoichiometric ratio and oxygen concentration on heat flux profiles in oxy-coal combustion*. in *9th U.S. National Combustion Meeting*. 2015. Cincinnati, Ohio.
70. Baumgartner, A., M. Blume, C. Wolf and H. Spliethoff. *Impact of direct oxygen injection on flame stability and overall burnout during oxyfuel combustion*. in *18th IFRF Members' Conference: Flexible and clean fuel conversion in industry*. 2015. Freising, Germany.

71. Menter, F.R., *Two-equation eddy-viscosity turbulence models for engineering applications.* AIAA journal, 1994. **32**(8): p. 1598-1605.
72. Fluent, A., *12.0 Theory Guide.* Ansys Inc, 2009. **5**.
73. Fletcher, T.H., A.R. Kerstein, R.J. Pugmire and D.M. Grant, *Chemical percolation model for devolatilization. 2. Temperature and heating rate effects on product yields.* Energy & Fuels, 1990. **4**(1): p. 54-60.
74. Chui, E. and G. Raithby, *Computation of radiant heat transfer on a nonorthogonal mesh using the finite-volume method.* Numerical Heat Transfer, 1993. **23**(3): p. 269-288.
75. Raithby, G. and E. Chui, *A finite-volume method for predicting a radiant heat transfer in enclosures with participating media.* ASME, Transactions, Journal of Heat Transfer, 1990. **112**: p. 415-423.
76. Shen, Z. and J. Friedman, *Evaluation of Coefficients for the Weighted Sum of Gray Gases Model.* 1982.
77. Yin, C., *On gas and particle radiation in pulverized fuel combustion furnaces.* Applied Energy, 2015.
78. Backreedy, R., L. Fletcher, L. Ma, M. Pourkashanian and A. Williams, *Modelling pulverised coal combustion using a detailed coal combustion model.* Combustion science and technology, 2006. **178**(4): p. 763-787.
79. Wall, T., S. Bhattacharya, D. Zhang, R. Gupta and X. He, *The properties and thermal effects of ash deposits in coal-fired furnaces.* Progress in Energy and Combustion Science, 1993. **19**(6): p. 487-504.
80. Basu, P., C. Kefa and L. Jestin, *Boilers and burners: design and theory*. 2012: Springer Science & Business Media.
81. Papavergos, P. and A. Hedley, *Particle deposition behaviour from turbulent flows.* Chemical engineering research & design, 1984. **62**(5): p. 275-295.
82. Sippola, M.R. and W.W. Nazaroff, *Particle deposition from turbulent flow: Review of published research and its applicability to ventilation ducts in commercial buildings.* Lawrence Berkeley National Laboratory, 2002.
83. Sheldon, K.F., *Smoke, Dust, and Haze: Fundamentals of Aerosol Dynamics*. 2000, Oxford Univ. Press, New York.
84. Choi, C.R. and C.N. Kim, *Numerical investigation on the flow, combustion and NOx emission characteristics in a 500MW e tangentially fired pulverized-coal boiler.* Fuel, 2009. **88**(9): p. 1720-1731.
85. Wang, H. and J.N. Harb, *Modeling of ash deposition in large-scale combustion facilities burning pulverized coal.* Progress in Energy and Combustion Science, 1997. **23**(3): p. 267-282.
86. Guda, S.S., I.B. Celik, Z. Yang, A. Gopan, R.L. Axelbaum, F.N. Karaismail and V. Akkerman, *Comparison of Large Eddy Simulations for a Lab Scale and Pilot Scale Pressurized Oxy-Coal Combustor.* In Prep.
87. Gopan, A., B.M. Kumfer, J. Phillips, D. Thimsen, R. Smith and R.L. Axelbaum, *Process design and performance analysis of a Staged, Pressurized Oxy-Combustion (SPOC) power plant for carbon capture.* Applied Energy, 2014. **125**: p. 179-188.
88. Hagi, H., M. Nemer, Y. Le Moullec and C. Bouallou, *Towards Second Generation Oxy-pulverized Coal Power Plants: Energy Penalty Reduction Potential of Pressurized Oxy-combustion Systems.* Energy Procedia, 2014. **63**: p. 431-439.
89. Gopan, A., B.M. Kumfer and R.L. Axelbaum, *Effect of operating pressure and fuel moisture on net plant efficiency of a staged, pressurized oxy-combustion power plant.* International Journal of Greenhouse Gas Control, 2015. **39**: p. 390-396.
90. Axelbaum, R.L., B.M. Kumfer, F. Xia, A. Gopan and B. Dhungel, *Method and apparatus for capturing carbon dioxide during combustion of carbon containing fuel*. 2014, Google Patents.

## LIST OF RESULTING PUBLICATIONS AND PRODUCTS

### Peer-Reviewed Publications:

Gopan A, Kumfer B, Phillips J, Thimsen D, Smith R, Axelbaum RL. (2014) Process design and performance analysis of a staged, pressurized oxy-combustion (SPOC) power plant for carbon capture. *Applied Energy*, 125:179-188.

Gopan A, Kumfer B, Axelbaum, RL. (2015) Effect of operating pressure and fuel moisture on net plant efficiency of a staged, pressurized oxy-combustion power plant. *International Journal of Greenhouse Gas Control*, 39:390-396.

Xia, F., Yang, Z., Adeosun, A., Kumfer, B.M., Axelbaum, R.L. (2016) Control of radiative heat transfer in high-temperature environments via radiative trapping—Part I: Theoretical analysis applied to pressurized oxy-combustion. *Fuel*, 172:81-88.

Xia, F., Yang, Z., Adeosun, A., Kumfer, B.M., Axelbaum, R.L. (2016) Pressurized oxy-combustion with low flue gas recycle: computational fluid dynamic simulations of radiant boilers. *Fuel*, 181:1170-1178.

Yang Z*, Xia F*, Adeosun A, Kumfer BM, Axelbaum RL. (2017) Control of radiative heat transfer in high-temperature environments via radiative trapping—Part II: Application in pressurized oxy-combustion. *Fuel*, submitted. (*Co-first Author)

Yang Z, Adeosun A, Kumfer BM, Axelbaum RL. (2017) An approach to estimating flame radiation in combustion chambers containing suspended-particles. *Fuel*, 199: 420-429.

Gopan, A., Yang, Z., Kumfer, B. M. and Axelbaum, R. L. (2017). The effects of inert-placement (Zst) on soot and radiative heat flux in turbulent diffusion flames. *Energy & Fuels* 31(7), 7617–7623.

### Conference Presentations & Proceedings:

R.L. Axelbaum, Staged, High Pressure Oxy-combustion Technology: Development and Scale-Up, Phase 2. NETL CO2 Capture Technology Project Review Meeting, Pittsburgh, PA, Aug. 25, 2017. (presented by Rich Axelbaum)

Yang Z, Gopan A, Axelbaum RL. Predicting ash deposition from non-isothermal, turbulent parallel flows: application to staged, pressurized oxy-combustion. The 42nd International Technical Conference on Clean Energy. Clearwater, Florida, USA. Jun. 11-15, 2017.

Yang Z, Adeosun A, Khatri D, Li T, Kumfer BM, Axelbaum RL. Design and commissioning of the staged, pressurized oxy-combustion experiment. The 42nd International Technical Conference on Clean Energy. Clearwater, Florida, USA. Jun. 11-15, 2017.

Gopan A, Yang Z, Adeosun A, Kumfer BM, Axelbaum RL. Burner and Boiler Design Concepts for a Low Recycle, Staged, Pressurized Oxy-Combustion Power Plant. The 42nd International Technical Conference on Clean Energy. Clearwater, Florida, USA. Jun. 11-15, 2017.

Wang, X., Adeosun, A., Yang, Z., Sun, Y., Axelbaum, R. L., Yablonsky, G., and Tan, H. The Synergetic Promotion of SO3 and NO2 Formation in the Post-flame Region of Pressurized Oxycombustion The 42nd International Technical Conference On Clean Energy, Clearwater, Fl, June 11-15, 2017.

Adeosun A, Huang Q, Li T, Wang X, Gopan A, Yang Z, Li S, Axelbaum RL. Ignition of a dispersed coal particle stream and measurement of ultrafine particle size distributions. 10th U. S. National Combustion Meeting. College Park, Maryland. April 23-26, 2017.

Adeosun A, Huang Q, Li T, Li S, Axelbaum RL. Design and characterization of a two-stage Hencken burner for combustion of solid fuels. 10th U. S. National Combustion Meeting. College Park, Maryland. April 23-26, 2017.

Wang X, Liu Z, Adeosun A, Sun Y, Yablonsky G, Tan H, Axelbaum RL. A kinetic evaluation on $NO_2$ formation in the post-flame region of pressurized oxy-combustion process. 10th U. S. National Combustion Meeting. College Park, Maryland. April 23-26, 2017.

Yang Z, Gopan A, Axelbaum RL. Predicting ash deposition from non-isothermal, turbulent parallel flows: application to staged, pressurized oxy-combustion. 10th U. S. National Combustion Meeting. College Park, Maryland. April 23-26, 2017.

Gopan A, Yang Z, Adeosun A, Kumfer BM, Axelbaum RL. Scaling and burner design concepts of a staged-pressurized oxy-combustion boiler. 10th U. S. National Combustion Meeting. College Park, Maryland. April 23-26, 2017.

Gopan A, Yang Z, Kumfer BM, Axelbaum RL. Effect of Stoichiometric Mixture Fraction (Zst) on Soot and Radiative Heat Flux in a Turbulent Diffusion Flame. 10th U. S. National Combustion Meeting. College Park, Maryland. April 23-26, 2017.

R.L. Axelbaum, Staged, High Pressure Oxy-combustion Technology: Development and Scale-Up, Phase 2. NETL CO2 Capture Technology Project Review Meeting, Pittsburgh, PA, Aug. 12, 2016. (presented by Ben Kumfer)

Yang Z, Kumfer BM, Axelbaum RL, Effects of particle radiative properties on radiative heat transfer in pressurized coal-fired systems. 2016 Spring Technical Meeting of the Central States Section of the Combustion Institute, Knoxville, Tennessee, May. 15-17, 2016.

Yang Z, Adeosun A, Kumfer BM, Axelbaum RL, Estimation of flame radiation in a confined combustion chamber: theoretical analysis and validation. 2016 Spring Technical Meeting of the Central States Section of the Combustion Institute, Knoxville, Tennessee, May. 15-17, 2016.

Gopan, A. Z. Yang, A. Adeosun, B.M. Kumfer, R.L. Axelbaum, J. Philips, D. Thimsen Development of staged pressurized oxy-combustion. 5th Oxyfuel Combustion Research Network Meeting. Wuhan, China. Oct. 27-30, 2015.

Adeosun, A., Xia, F., Yang, Z., Gopan, A., Kumfer, B.M., Axelbaum, R.L. Advanced Pressurized Oxy-Combustion: Towards Higher Plant Efficiency through Near-Zero Flue Gas Recycle and Boiler Designs. 32nd International Pittsburgh Coal Conference, Pittsburgh, PA, Oct. 5-8, 2015.

Kumfer, B. Advances in Carbon Capture Technology. 5th International Advanced Coal Technologies Conference, Jackson, WY, Oct. 6-7, 2015.

Kumfer, B. M. Evaluation of Staged Oxyfuel Combustion for CO2 Capture. 2015 Clean Coal Technology Research Symposium, Laramie, WY, Aug 20, 2015.

Xia, F., Yang, Z., Adeosun, A., Kumfer, B., Axelbaum, R.L. Numerical Study of Staged, Pressurized Oxy-Coal Combustion with Near-Zero Flue Gas Recycle. 8th International Symposium on Coal Combustion. , Beijing, China, July 19-22, 2015.

Axelbaum, R. L. Staged, Pressurized Oxy-Combustion for Carbon Capture. NETL CO2 Capture Meeting, Pittsburgh, PA, Jun 23 – 26, 2015.

Yang, Z., Xia, F., Adeosun, A., Kumfer, B.M., Axelbaum, R.L. Control of radiative heat transfer in pressurized, high temperature combustion applications. 9th U.S. National Combustion Meeting, Cincinnati, OH, May 17-20, 2015.

Adeosun, A., Xia, F., Yang, Z., Gopan, A., Kumfer, B.M., Axelbaum, R.L. A design and numerical study of a staged, pressurized oxy-coal combustion furnace with near-zero recirculation. 9th U.S. National Combustion Meeting, Cincinnati, OH, May 17-20, 2015.

Gopan, A., Yang, Z., Adeosun, A., Kumfer, B.M., Axelbaum, R.L. Effect of stoichiometric ratio and oxygen concentration on heat flux profiles in oxy-coal combustion. 9th U.S. National Combustion Meeting, Cincinnati, OH, May 17-20, 2015.

Gopan, A., Kumfer, B. M., Axelbaum, R. L., Phillips, J. and Thimsen, D. Process design and parametric analysis of a staged, pressurized oxy-combustion power plant, 31st International Pittsburgh Coal Conference, Pittsburgh, PA, Oct 6-9, 2014.

Adeosun, A., Gopan, A., Xia, F., Dhungel, B., Kumfer, B. and Axelbaum, R. An experimental investigation of heat transfer behavior in oxygen-enriched coal combustion, 31st International Pittsburgh Coal Conference, Pittsburgh, PA, Oct 6-9, 2014.

Gopan A, Kumfer B, Phillips J, Thimsen D, Axelbaum RL. Cost and performance of fuel-staged, pressurized oxy-combustion power plant. The 12th Greenhouse Gas Control Technologies (GHGT-12) conference, Austin, TX, Oct. 5-9, 2014.

Axelbaum, R. L. Staged, Pressurized Oxy-Combustion for Carbon Capture. NETL CO2 Capture Meeting, Pittsburgh, PA, Jul. 29 – Aug. 1, 2014.

Gopan A, Kumfer B, Phillips J, Thimsen D, Axelbaum RL. Techno-economic study of fuel-staged, pressurized oxy-combustion power plant. The 39th International Technical Conference on Clean Coal & Fuel Systems, Clearwater, FL, Jun. 1-5, 2014.

Dhungel, B, Xia F, Kumfer BM, Axelbaum RL. Investigation of oxygen enriched combustion for application to a novel fuel-staged pressurized oxy-combustion (SPOC) process. The 39th International Technical Conference on Clean Coal & Fuel Systems, Clearwater, FL, Jun. 1-5, 2014.

Gopan A, Kumfer B, Phillips J, Thimsen D, Axelbaum RL. Performance analysis of a staged pressurized oxfuel combustion (SPOC) power plant with minimal flue gas recycle. 2013 AIChE Annual Meeting, San Francisco, CA, Nov. 3-8, 2013.

Xia F, Kumfer B, Dhungel B, Axelbaum RL, Staged, pressurized oxy-combustion: computational fluid dynamics simulations of a novel burner design. Proceedings, 2013 Fall Technical Meeting of the Eastern States Section of the Combustion Institute, Clemsen University, SC, October 13-16, 2013.

Kumfer B, Dhungel B, Gopan A, Xia F, Holtmeyer ML, Phillips J, Thimsen D, Axelbaum RL. A Staged, Pressurized Oxy-Combustion System for Carbon Capture, 3rd Oxyfuel Combustion Conference, Ponferrada, Spain, Sept. 9-13, 2013.

Kumfer B, Xia F, Dhungel B, Axelbaum RL, CFD Simulation of Staged Oxyfuel Combustion, 2012 AIChE Annual Meeting, Pittsburgh, PA, Oct. 28 – Nov. 2, 2012.

**Ph.D. Dissertations**

Gopan, Akshay. *Studies in Pressurized Oxy-Combustion: Process Development and Control of Radiative Heat Transfer*. PhD Dissertation. Washington University in St. Louis, Dept. Energy, Environmental and Chemical Engineering. Aug 2017.

Xia, Fei. *Studies in Advanced Oxy-combustion Technologies*. PhD Dissertation. Washington University in St. Louis, Dept. Mechanical Engineering & Materials Science. Dec 2014.

**Patent Applications:**

Fuel-Staged Oxy-Combustion Process and Apparatus. (Provisional) (2013).

Method and apparatus for capturing carbon dioxide during combustion of carbon containing fuel (2014).

Method of radiant trapping to control heat flux in high temperature particle-laden flows at elevated pressure (Provisional) (2014).

**Other**

R.L. Axelbaum, B. Kumfer, X. Wang, Advances in pressurized oxy-combustion for carbon capture. *Cornerstone* 4(2):52-56 (2016).

**Appendix A. Materials Evaluations for Staged Pressurized Oxy-Combustion: Final Report of Work Performed at Oak Ridge National Labs Under Agreement DE-FEAA120**

# FINAL REPORT

Materials Evaluations for Staged Pressurized Oxy-Combustion

December 2017

**WORK PERFORMED UNDER AGREEMENT**

DE-FEAA120
in support of award to Washington University in St. Louis

**SUBMITTED BY**

Oak Ridge National Laboratory
P.O. Box 2008
Oak Ridge, TN 37831-6156

**PRINCIPAL INVESTIGATOR**

Dr. B. A. Pint
(865) 576-2897
pintba@ornl.gov

**SUBMITTED TO**

U. S. Department of Energy
National Energy Technology Laboratory

A. C. Bose

# Materials Evaluations for Staged Pressurized Oxy-Combustion

B. A. Pint and E. K. Hess

Corrosion Science and Technology Group, Materials Science and Technology Division
Oak Ridge National Laboratory, Oak Ridge TN 37831-6156

## Executive Summary

The purpose of this research was to determine the feasibility of current commercial alloys with staged pressurized oxy-combustion (SPOC) technology. Corrosion studies are rarely performed above ambient pressure and there was a significant concern about the effect of pressure on the proposed conditions. In Phase 1, gas only studies were carried out on Fe-based alloy coupons at 600°C and Ni-based alloys at 800°C in $O_2$-10%$H_2O$±0.1%$SO_2$ for 500 h at 1 and 17 bar. In Phase 2, coupons with and without synthetic ash were exposed at 700°C in two simulated gas compositions with 0.1% and 0.5% $SO_2$ at 1 and 17 bar. Without $SO_2$ and ash, the oxidation behavior in $O_2$-10%$H_2O$ was similar to prior observations in steam or wet air and there was no obvious detrimental effect of the high $O_2$ environment. The addition of $SO_2$ was detrimental, as expected, especially at 17 bar. When synthetic ash was added, no particular effect of pressure was observed. Higher alloyed steels (e.g. 310HCbN) and/or Ni-base alloys or overlay coatings on steels appear to be possible solutions for a high S coal SPOC environment. If additional experiments are conducted, particularly at higher pressure, the focus should be on a narrower selection of candidates for longer times. In general, there is limited understanding of the effect of pressure on high temperature oxidation/corrosion and more work is needed in this area.

## Introduction

This project was initiated due to concerns with materials compatibility in the environments associated with staged pressurized oxy-combustion (SPOC) technology [1] and the expertise and equipment available at Oak Ridge National Laboratory. In particular, there was concern about oxidation behavior in high $O_2$ contents and increased pressure (~1-20 bar, 0.1-2 MPa) found in SPOC. A series of screening experiments were conducted to determine if there were commercial materials solutions compatible with SPOC environments. In Phase 1, gas only experiments were conducted at 600°C primarily for Fe-based alloys and at 800°C for Ni-based alloys. In Phase 2, the effect of a synthetic ash deposit was evaluated at 700°C in two different gas mixtures representing a medium and a high S coal composition, based on input from EPRI and a prior DOE-funded study [2].

## Experimental Procedure

Alloy coupons (typically 1.5 x 10 x 19mm) were machined and then hand polished to a 600 grit finish. The exposures were conducted in a test rig with parallel alloy 230 (Ni-22Cr-14W) containment tubes and the specimens held on a vertical alumina tube using Pt-10Rh wire [3]. The specimens were slowly heated to temperature in argon and then exposed to the same gas

with one tube at 1 bar and the second at 17 bar (500 psig). In Phase 1, gas only studies were carried out on Fe-based alloy coupons at 600°C and Ni-based alloys at 800°C in $O_2$-10%$H_2O$±0.1%$SO_2$ for 500 h at 1 and 17 bar. Without $SO_2$, distilled deionized water was atomized into the $O_2$ carrier gas. For the second experiment, $O_2$-0.1%$SO_2$ was used as the carrier gas with the same 10%$H_2O$ addition. Prior to exposure, all specimens were ultrasonically cleaned in acetone and ethanol and specimen mass was measured using a Mettler Toledo model XP205† balance (±0.04mg or ~0.01mg/cm$^2$ accuracy). In Phase 2, coupons with and without synthetic ash were exposed at 700°C in two simulated gas compositions at 1 and 17 bar, (a) 63.4%$CO_2$-5%$N_2$-1.5%$O_2$-30%$H_2O$-0.1%$SO_2$ and (b) 63%$CO_2$-5%$N_2$-1.5%$O_2$-30%$H_2O$-0.5%$SO_2$. The composition of the synthetic ash is given in Table 1. A slurry was prepared to coat the specimens after each cycle. The goal of Phase 2 testing was to operate for five 100-h cycles. However, these conditions resulted in significant corrosion to the gas train of the test rig. As a result, only four 100-h cycles could be completed for the first gas composition and only a total exposure of 100 h was completed in the second gas using two thermal cycles of ~10 and 90 h. After exposure, selected specimens were Cu-plated to protect the surface oxide and metallographically mounted and imaged with light microscopy and a field emission gun, scanning electron microscopy (SEM) equipped with energy dispersive x-ray (EDX) analysis.

Table 1. Composition of the synthetic ash used in Phase 2.

| Constituent | Wt.% |
|---|---|
| $Al_2O_3$ | 16.9 |
| $SiO_2$ | 22.6 |
| CaO | 0.9 |
| $Fe_2O_3$ | 7.8 |
| KOH | 1.0 |
| $TiO_2$ | 0.6 |
| $MgSiO_3$ | 0.3 |
| $Fe_2(SO_4)_3$ | 19.8 |
| $MgSO_4$ | 10.1 |
| $K_2SO_4$ | 4.8 |
| $Na_2SO_4$ | 15.1 |

**Results**

600°C exposures

Figure 1 shows the mass change data for the specimens exposed at 600°C. The specimens were Grades 22 (2.25Cr-1Mo) and 91 (9Cr-1Mo), VM12 (11Cr), 410 (13Cr), 304H (18Cr-8Ni), 310HCbN (25Cr-20Ni), E-Brite (26Cr-1Mo) and Ni-based alloys 625 and 740. Duplicate specimens of Grade 91 were exposed. The highest alloyed materials (310HCbN, E-Brite, 625 and 740) showed very low mass changes in all cases and the lowest alloy specimen, Grade 22, showed high mass gains or losses (spallation) in all cases. For the other alloys there was a recurring pattern, higher mass gains in $O_2$-$H_2O$, a small mass gain with the addition of $SO_2$ at 1 bar and then a much higher (or lower if the reaction product spalled) gain at 17 bar. Figures 2 and 3 illustrate these results for two materials. Figure 2 shows that a typical, duplex oxide [4-7] formed on VM12 after exposure to $O_2$-$H_2O$ at both pressures. The outer layer is an outward-growing mixture of magnetite and hematite and the inner layer is an inward-growing mixed Fe-Cr spinel-type oxide. Consistent with the mass change data, a thin protective Cr-rich scale

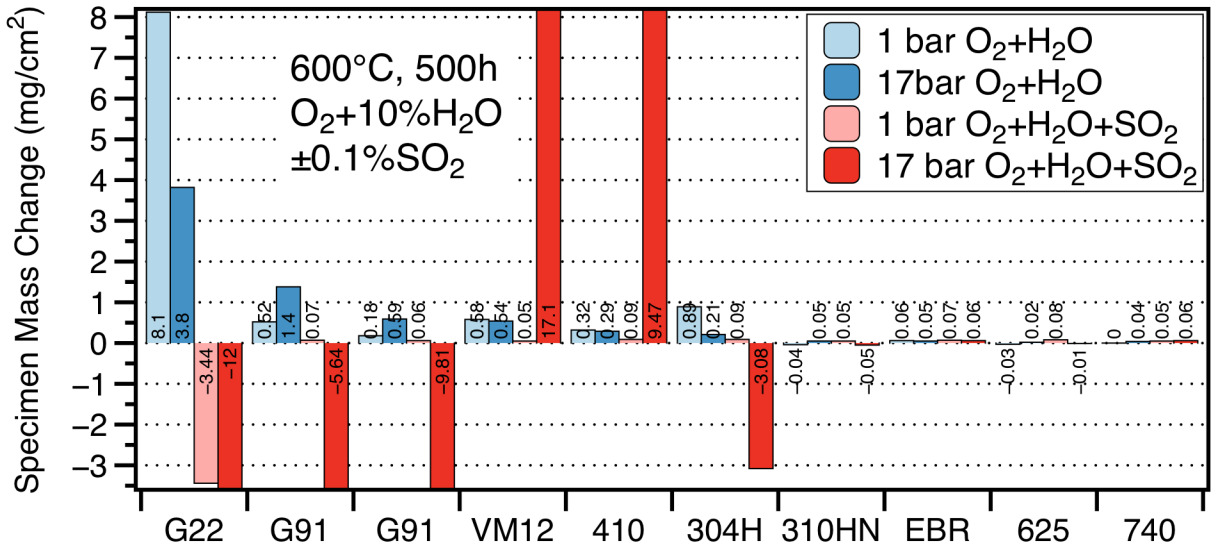


Figure 1. Specimen mass gains after 500 h at 600°C in four conditions.

formed with the addition of $SO_2$ at 1 bar, Figure 2b. However, when the pressure was increased to 17 bar a much thicker oxide formed. Similar results were observed for the 304H specimens in Figure 3. Nominally, the protective behavior for the more highly alloyed specimens shows that there are materials solutions at 600°C for this environment, either one of these more expensive alloys or possibly a high Cr/Ni overlay or coating.

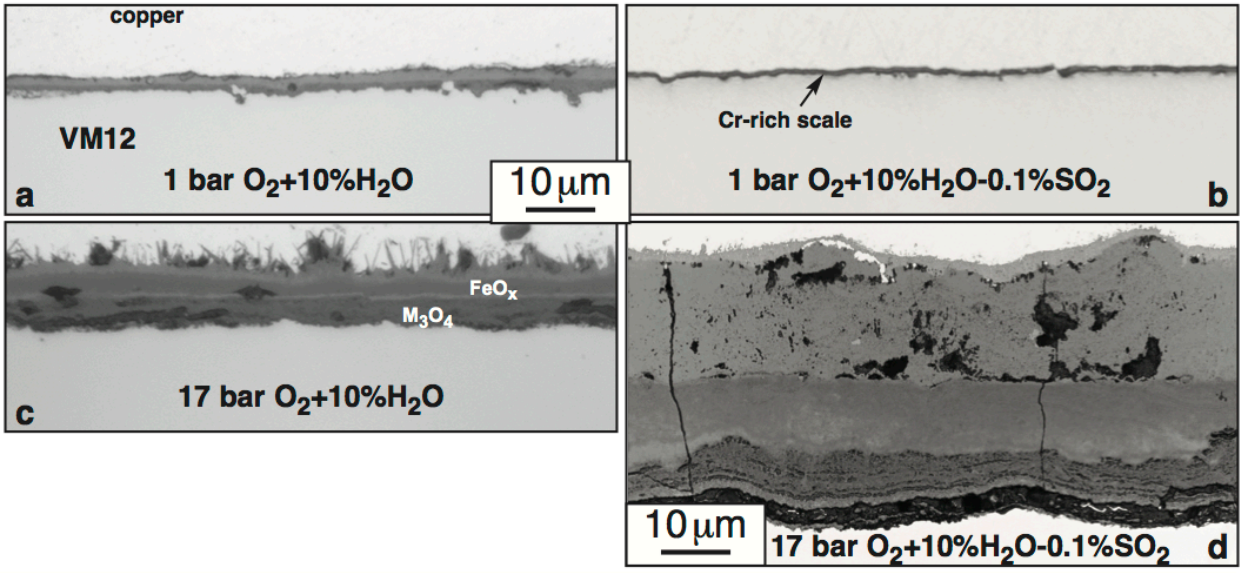


Figure 2. Light microscopy of VM12 specimens exposed at 600°C for 500 h in two environments and two pressures.

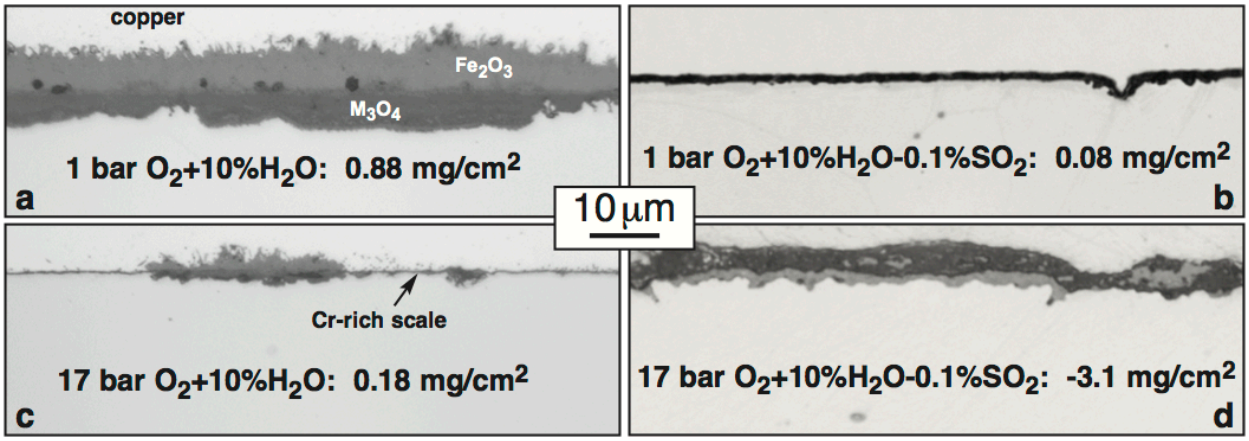


Figure 3. Light microscopy of 304H specimens exposed at 600°C for 500 h in two environments and two pressures.

Figure 4 shows the mass change results after 500 h at 800°C in the four environments for Ni-based alloys 625, CCA617, 282, 740, HR6W, 671 and 214. The alumina-forming alloy 214 showed the lowest mass gains in the four experiments. The rest of the alloys formed Cr-rich oxides and the behavior was somewhat difficult to understand. Without $SO_2$, the mass losses observed for several alloys could be attributed to the evaporation of $CrO_2(OH)_2$ [8]. Generally, there were higher mass gains in 1 bar $O_2$-$H_2O$-$SO_2$. At 17 bar, the behavior varied from small mass changes to large mass losses, which is difficult to explain. Figure 5 and 6 show metallographic cross-sections of the reaction products for two alloys in these experiments. The reaction products are generally consistent with the mass change data in Figure 4. There appeared to be more internal attack in the environments containing $SO_2$. A combination of internal oxidation and sulfidation as well as void formation was observed. More study is needed to further understand these results.

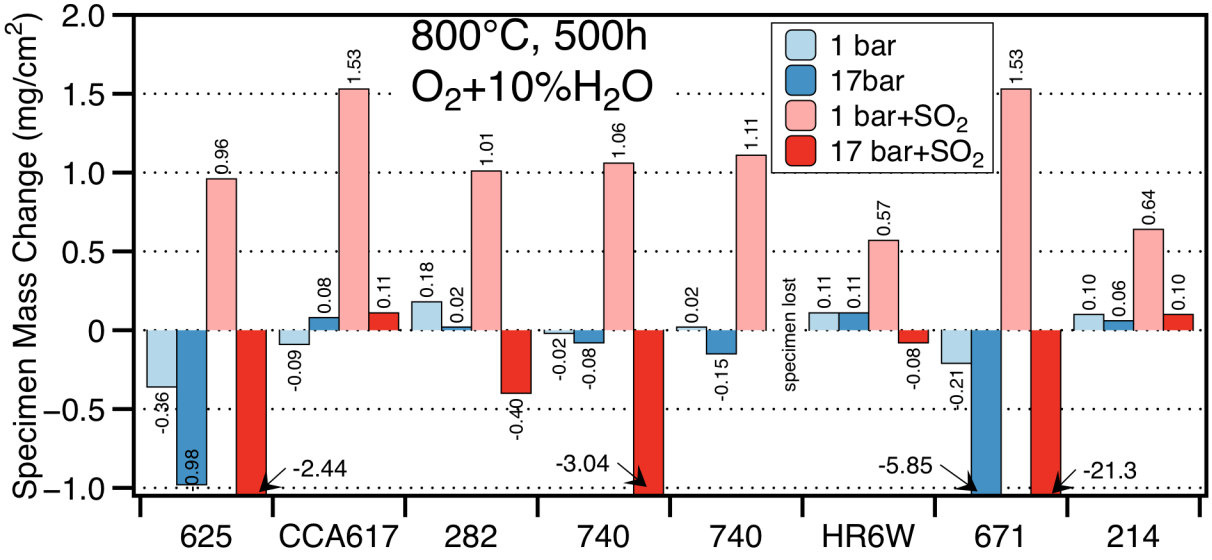


Figure 4. Specimen mass gains after 500 h at 800°C in four conditions.

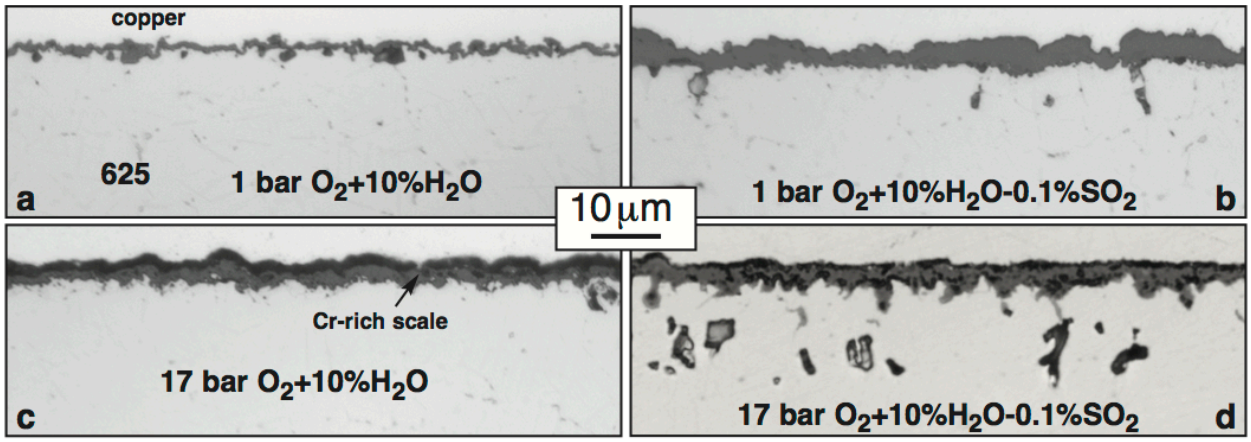


Figure 5. Light microscopy of 625 specimens exposed at 800°C for 500 h in two environments and two pressures.

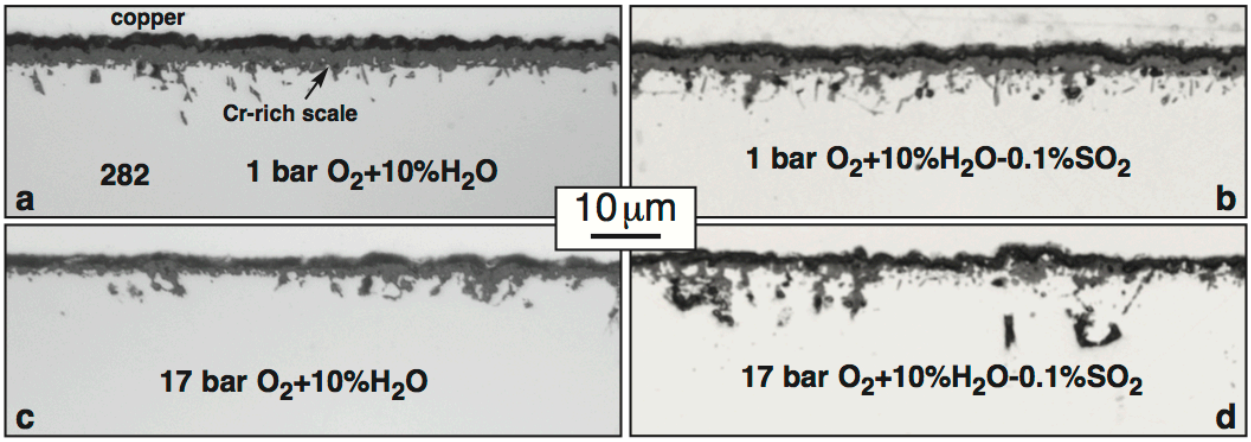


Figure 6. Light microscopy of 282 specimens exposed at 800°C for 500 h in two environments and two pressures.

Phase 2 mass change results are presented in Figures 7 and 8. Duplicate coupons of alloys 304H and 740 were included in this experiment as well as coupons of Grade 91, 347HFG, 310HCbN and 625. As expected, the Grade 91 (9Cr-1Mo) specimens had the lowest Cr content and were readily attacked in both gas mixtures and both pressures with and without synthetic ash. Relatively low mass gains were observed for all of the other bare specimens without ash. However, because of experimental difficulties, the experiment with the higher $SO_2$ content was only conducted for 100 h. With ash, the conventional stainless steels (304H, 347HFG) also were attacked. The higher alloyed specimens (310HCbN, 625 and 740) showed very little attack during these exposures. Figures 9 and 10 show metallographic cross-sections of the 304H specimens in each of the conditions. Note that the micron markers are different in some cases, with much thicker reaction products forming, especially with the ash present. The most significant effect of pressure observed was for the 304H specimens exposed for 400 h in 63.4%$CO_2$-5%$N_2$-1.5%$O_2$-30%$H_2O$-0.1%$SO_2$ with synthetic ash, Figures 9b and 9d. The attack was much higher at 1 bar than at 17 bar. Otherwise there was little effect of pressure observed.

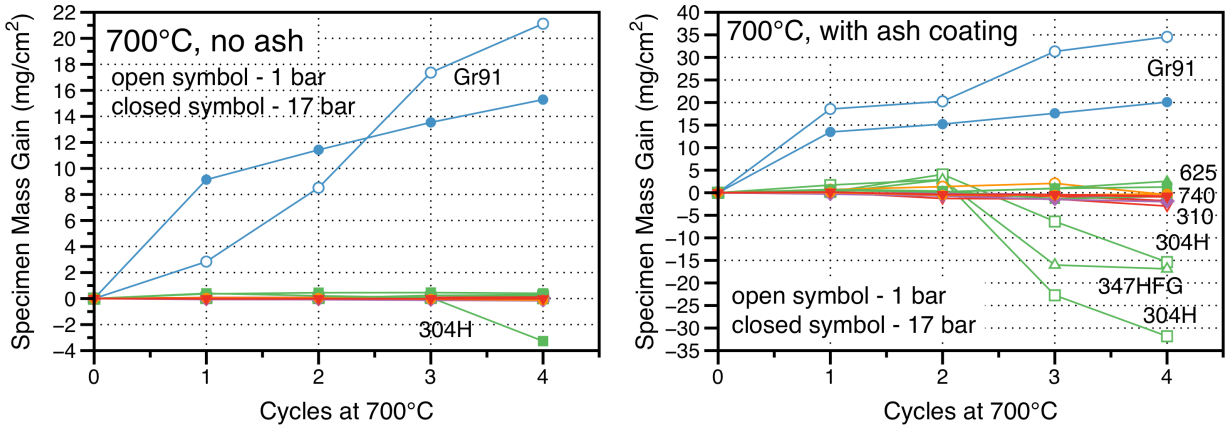


Figure 7. Specimen mass change data during 100-h cycles at 700°C in 63.4%$CO_2$-5%$N_2$-1.5%$O_2$-30%$H_2O$-0.1%$SO_2$ (a) no ash and (b) with ash recoated each cycle.

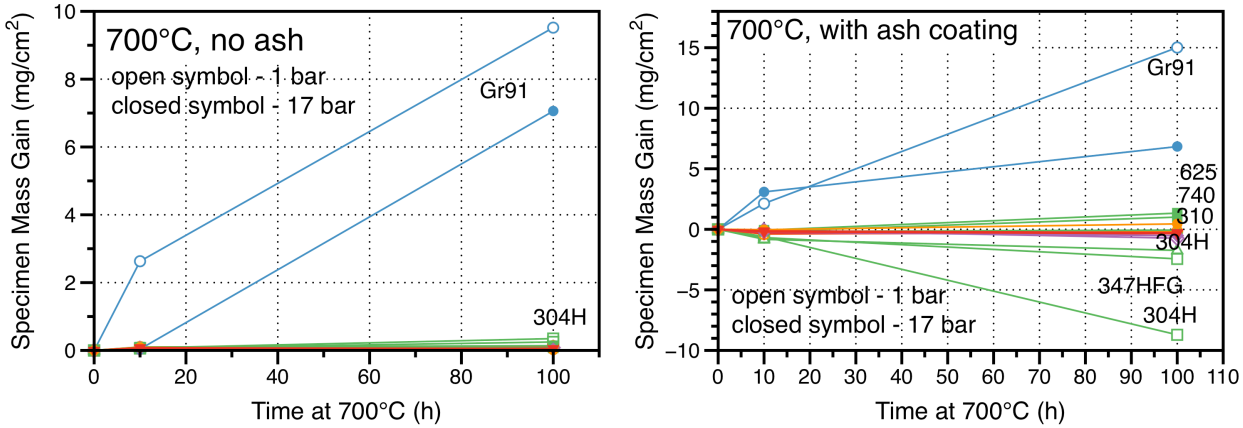


Figure 8. Specimen mass change data at 700°C in 63%$CO_2$-5%$N_2$-1.5%$O_2$-30%$H_2O$-0.5%$SO_2$ (a) no ash and (b) with ash recoated each cycle.

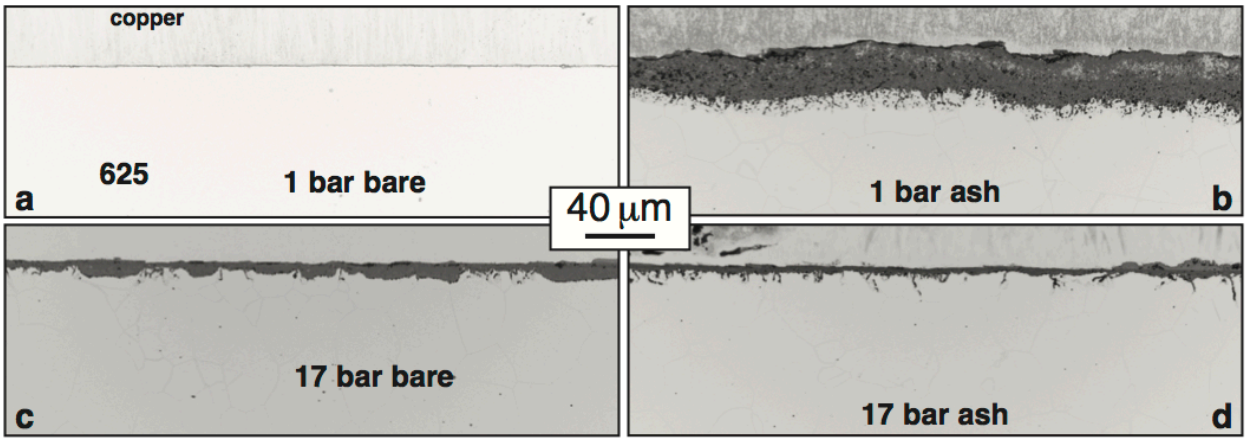


Figure 9. Light microscopy of 304H specimens exposed at 700°C for 400 h in 63.4%$CO_2$-5%$N_2$-1.5%$O_2$-30%$H_2O$-0.1%$SO_2$ at two pressures with and without synthetic ash.

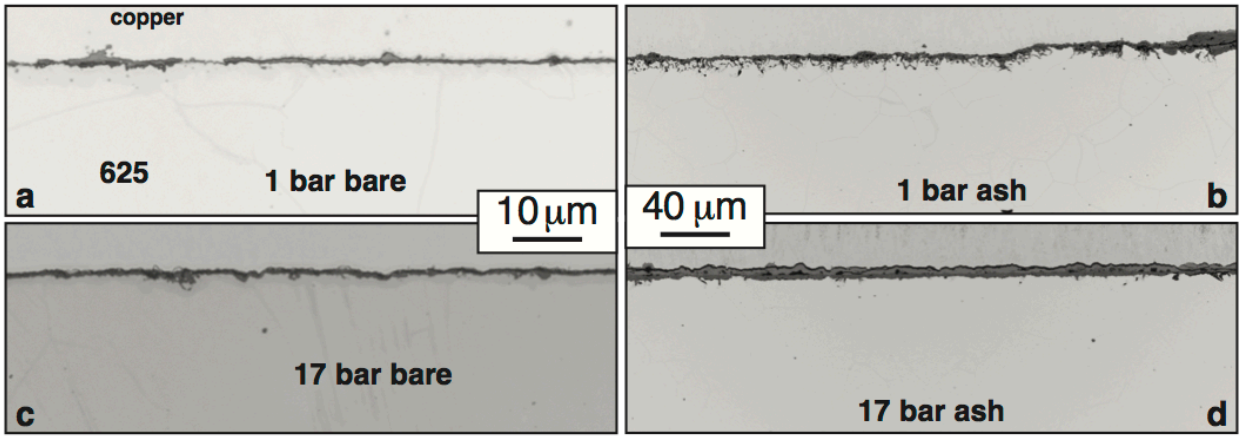


Figure 10. Light microscopy of 304H specimens exposed at 700°C for 100 h in 63%$CO_2$-5%$N_2$-1.5%$O_2$-30%$H_2O$-0.5%$SO_2$ at two pressures with and without synthetic ash.

## Conclusion

The purpose of this research was to determine the feasibility of current commercial alloys with staged pressurized oxy-combustion (SPOC) technology. In Phase 1 without ash, the oxidation behavior of Fe-based alloys at 600°C and Ni-based alloys at 800°C in $O_2$-10%$H_2O$ was similar to prior observations in steam or wet air and there was no obvious detrimental effect of the high $O_2$ environment after 500 h exposures. The addition of $SO_2$ was detrimental, as expected, especially at 17 bar. When synthetic ash was added in Phase 2, no particular effect of pressure was observed for short-term testing at 700°C. Higher alloyed steels (e.g. 310HCbN) and/or Ni-base alloys or overlay coatings on steels appear to be possible solutions for a high S coal SPOC environment. If additional experiments are conducted, particularly at higher pressure, the focus should be on a narrower selection of candidates for longer times. In general, there is limited understanding of the effect of pressure on high temperature oxidation/corrosion and more work is needed in this area.

## Acknowledgements

The experimental work was conducted by M. Howell, M. Stephens, Z. Burns, T. Lowe, K. Adams and T. Jordan. This research was funded by the U.S. Department of Energy, Office of Fossil Energy. The project was conducted to support the SPOC project at Washington University in St. Louis under Profs. R. Axelbaum and B. Kumfer.

## References

1. A. Gopan, B. M. Kumfer, J. Phillips, D. Thimsen, R. Smith and R. L. Axelbaum, “Process design and performance analysis of a Staged, Pressurized Oxy-Combustion (SPOC) power plant for carbon capture,” Applied Energy 125 (2014) 179–188.
2. S. C. Kung, “Measurement of Corrosive Gaseous Species in Staged Coal Combustion,” Oxid. Met. 77 (2012) 289-304.

3. K. A. Terrani, B. A. Pint, C. M. Parish, C. M. Silva, L. L. Snead and Y. Katoh, “Silicon Carbide Oxidation in Steam up to 2 MPa,” J. Am. Ceram. Soc. 97 (2014) 2331-2352.
4. N. Otsuka, Y. Shida and H. Fujikawa, “Internal-External Transition for the Oxidation of Fe-Cr-Ni Austenitic Stainless Steels in Steam” *Oxidation of Metals* 32, 13-45 (1989).
5. H. Nickel, Y. Wouters, M. Thiele and W. J. Quadakkers, "The Effect of Water Vapor on the Oxidation Behavior of 9%Cr Steels in Simulated Combustion Gases," Fresenius J. Anal Chem., 361 (1998) p.540-544.
6. R. Peraldi and B. A. Pint, "Effect of Cr and Ni Contents on the Oxidation Behavior of Ferritic and Austenitic Model Alloys in Air With Water Vapor," *Oxid. Met.,* 61 (2004) 463-483.
7. W. J. Quadakkers, J. Żurek, and M. Hänsel, “Effect of water vapor on high temperature oxidation of FeCr alloys,” JOM 61(7) (2009) 44-50.
8. H. Asteman, J.-E. Svensson, M. Norell and L.-G. Johansson, “Influence of Water Vapor and Flow Rate on the High-Temperature Oxidation of 304L; Effect of Chromium Oxide Hydroxide Evaporation,” *Oxidation of Metals* 54 (2000) 11-26.